Addis Ababa University
አዲስ፡አበባ፡ዩኒቨርሲቲ
SEEK WISDOM, ELEVATE YOUR INTELLECT AND SERVE HUMANITY !

COLLEGE OF NATURAL AND COMPUTATIONAL SCIENCES

SCHOOL OF EARTH SCIENCES

SURFACE WATER AVAILABILITY MAPPING AND ESTIMATING SPATIOTEMPORAL CHANGES BY USING GOOGLE EARTH ENGINE, RIFT VALLEY LAKES BASIN, ETHIOPIA

A THESIS SUBMITTED TO THE SCHOOL OF GRADUATE STUDIES IN PARTIAL FULFILLMENT OF THE REQUIREMENTS FOR A DEGREE OF MASTER OF SCIENCE IN REMOTE SENSING AND GEO-INFORMATICS

BY

Genet Amsalu Yadeta

ID: GSR/9208/15

Advisors

Dr. Binyam Tesfaw

Dr. Behailu Birhanu

Addis Ababa, Ethiopia
May, 2024

ADDIS ABABA UNIVERSITY

COLLEGE OF NATURAL AND COMPUTATIONAL SCIENCES

SCHOOL OF EARTH SCIENCES

Master Stream of Remote Sensing and Geo-Informatics

Mapping Surface water availability and estimating spatiotemporal changes by using Google Earth Engine, Rift Valley lakes basin, Ethiopia

A thesis submitted to the school of graduate studies in partial fulfillment of the requirements for a degree of Master of Science in Remote Sensing and Geo-informatics

By: Genet Amsalu

ID: GSR/9208/15

Addis Ababa, Ethiopia
May, 2024

Declaration

I, Genet Amsalu, hereby declare that this thesis entitled "Surface Water Availability Mapping and Estimating Spatiotemporal Changes by using Google Earth Engine, Rift Valley Lakes Basin, Ethiopia" is the result of my original research work conducted under the guidance of my main advisor, Dr. Binyam Tesfaw, Associate Professor of Remote Sensing and Geo-informatics, and co-advisor, Dr. Behailu Birhanu, Associate Professor of Hydrogeology. I further declare that no part of this thesis has been previously submitted for a degree or diploma to any other university or institution. Any sources of information, ideas, or contributions from other authors have been duly acknowledged and referenced by the established academic conventions and citation style. I take full responsibility for any errors, omissions, or inconsistencies in this thesis. This work is solely the product of my research efforts and intellectual contributions, supported by the guidance and expertise of my advisors.

Addis Ababa University

College of Natural and Computational Science

School of Earth Sciences

Remote sensing and Geo-informatics stream

MSc Thesis on Surface water availability mapping and estimating spatiotemporal changes by using Google Earth Engine, Rift Valley lakes basin, Ethiopia

By Genet Amsalu

School of Earth Sciences

Approved by board examiners:

Prof. K.V. Suryabagahvan	_____	_____
Chairman	Signature	Date
Dr. Binyam Tesfaw	_____	_____
Advisor	Signature	Date
Dr. Behailu Birhanu	_____	_____
Co-Advisor	Signature	Date

Examiners

Acknowledgment

Firstly, I would like to express my heartfelt gratitude to the Almighty God for His blessings and guidance throughout the duration of my study. It is through His grace that I have been able to embark on this journey and bring it to a successful conclusion.

Secondly, I would also like to extend my deepest appreciation to my advisors, Dr. Binyam Tesfaw and Dr. Behailu Birhanu. Dr. Binyam Tesfaw, your mentorship has been a source of strength for me. Your guidance and support have helped me become a stronger researcher and have provided me with the clarity and focus necessary to achieve my objectives. Your constant presence and follow-up have given me the confidence to navigate through challenges and complete my work on time. Dr. Behailu Birhanu, I am truly grateful for the direction and guidance you have provided throughout my research. Your expertise and insights have been invaluable in shaping the trajectory of my study. Your frequent check-ins and feedback have kept me on track and motivated me to give my best. Your unwavering support and presence have made a significant impact on the completion of my research, and I am sincerely thankful for your contributions.

Thirdly, a special mention of gratitude goes to my husband, Bushe, whose unwavering support, understanding, and patience have been my pillar of strength throughout this endeavor. His belief in me and his sacrifices have been a constant source of motivation, and I am truly blessed to have him by my side.

Fourthly, I am also indebted to my friends and classmates, who have contributed directly or indirectly to my thesis work. Their insightful discussions, constructive feedback, and shared resources have enriched the quality of my research and broadened my perspective on the subject matter.

Lastly, I would like to extend my thanks to all those who have supported and encouraged me in various ways during this research journey. Your kind words, motivation, and positive energy have played a significant role in my success, and I am truly grateful for your presence in my life.

Tables of Contents

List of Figures

List of tables

List of acronyms

AVHRR	Advanced Very High-Resolution Radiometer
AVHRR	Advanced Very High-Resolution Radiometer
AWEI	Automated Water Extraction Index
CHIRPS	Climate Hazards Group Infrared Precipitation with Station
CRV	Central Rift Valley
CWB	Climatic Water Balance
ERTS	Earth Resources Technology Satellite
ET	Evapotranspiration
ETM+	Enhanced Thematic Mapper Plus
GCM	General Circulation Model
GEE	Google Earth Engine
GSWD	Global Surface Water Dataset
LULC	Land use land cover
MER	Main Ethiopian Rift
MNDWI	Modified normalized difference water index
MODIS	Moderate Resolution Imaging Spectroradiometer
NDSI	Normalized difference snow index
NDWI	Normalized difference water index
NDWI	Normalized difference water index
NOAA	National Oceanic and Atmospheric Administration's
NWI	Normalized water index

OBIA	Object-based image analysis
OLI	Operational Land Imager
RVL	Rift Valley Lakes
SPOT	Satellite Pour L'observation de la Terre
SR	Surface reflectance
SWA	Surface Water Areas
SWBs	Surface Water Bodies
SWIR	Short Wave Infrared
TM	Thematic Mapper
TOA	Top of atmosphere
USGS	United States Geological survey
WFB	Wonji Fault Belt

Abstract

The surface water availability in Ethiopia is fluctuating spatiotemporally due to natural and anthropogenic stressors. Previously hydrological models were used to estimate surface water availability at small watershed levels. However, data complexity and processing make them unable to assess at a wider basin level and require high performance computing technology. Therefore, in this study, Google Earth Engine (GEE) platform for surface water availability mapping and spatiotemporal surface water change assessment was carried out using Landsat satellite data and global surface water data for the last 4 decades in the Rift Valley Lakes basin. The research also investigates the impact of natural factors such as rainfall and temperature, as well as human-induced factors including land use and land cover changes, on surface water dynamics. The findings revealed that a significant increase in seasonal surface water accounting for a total area of 10 km^2, 48 km^2, and 577 km^2 for year intervals 1984–2000, 2000–2010, and 2010–2020, respectively. The lost surface water body shows an increment of 63 km^2 for the second interval while decrementing of 60 km^2 and 41 km^2 for the rest of the intervals. Lastly, the permanent water shows an increase by 10 km^2, 34 km^2 for intervals 1984-2000 and 2010-2020, respectively while decreasing by 56 km^2 for the year interval 2000-2010. The analysis of stressors revealed notable changes in rainfall and Land use land cover while the temperature shows steady distribution except for two sub-basins. The rainfall distribution shows a decrease in maximum rainfall by 103 mm, and the minimum rainfall by 8 mm for the first year interval. The increment for the next two intervals, by a maximum rainfall of 241 mm, and a minimum rainfall of 232 mm and 10 mm in the maximum, and minimum rainfall 57 mm, respectively. In addition, the Land use land cover shows the spread in the Farmland areas and urban areas and the fluctuation of forest cover extent as well the replacement of bare lands by other land cover classes. The study revealed that fluctuations in surface water availability are primarily caused by variations in rainfall patterns and changes in land use and land cover. Furthermore, the effectiveness of the Google Earth Engine (GEE) platform in visualizing and analyzing large-scale data was demonstrated, suggesting its applicability in different fields. However, to enhance future research, it is crucial to include additional field verification points and incorporate diverse data sources to improve the accuracy of the findings. These measures are essential for advancing understanding in the field and obtaining more reliable and comprehensive results.

Keywords: Surface water availability, spatiotemporal fluctuations, Natural stressors

CHAPTER ONE
INTRODUCTION

1.1 Background

Human survival is dependent on water sources, such as surface water, groundwater, and rainwater (Adugna et al., 2018). Among these sources, surface water, which includes rivers, lakes, wetlands, and streams, are the most critical resource for maintaining the biodiversity of both aquatic and terrestrial ecosystems (Palazzoli et al., 2023; Poff et al., 1997; Vörösmarty et al., 2010). Moreover, water is a vital component of many ecosystems and is essential for the economic prosperity of nations (Granzotti et al., 2018; Poff et al., 1997; Vörösmarty et al., 2010). Therefore Proper management of surface water resources is crucial to ensure the availability of freshwater and to safeguard the integrity of freshwater ecosystems and their functions (Dieter et al., 2018; Granzotti et al., 2018; Jenkins et al., 2010; Poff et al., 1997).

However, surface waters are subject to both natural and human-induced influences that can cause them to shift over time or decline in extent (Granzotti et al., 2018). Consequently, surface water availability and extent are changing globally (Balenzano et al.; Kummu et al., 2016; Rodell et al., 2018). The distribution and dynamics of inland water resources are greatly influenced by changes in land use, land cover, and climate (Palmer et al., 2008; Tulbure et al., 2016; Vörösmarty et al., 2010). In addition, human activities and climate change greatly impact water supplies and the environment. Activities like agriculture and industry strain water resources, while climate change alters availability and quality. Consequently Pollution, habitat loss, and disrupted ecosystems can happen. Sustainable water management and climate adaptation are crucial to solving this problem (Piao et al., 2010; Schewe et al., 2014), Unless the changes in LULC, and climate can lead to increased strain between rural, agriculturally focused regions and urban centers, potentially exacerbating water scarcity issues (Flörke et al., 2018). The shortage of water has emerged as a critical obstacle to sustainable development, as societies struggle to meet the demands for water consumption, while also grappling with the challenges of agriculture and manufacturing (Ejegu & Yegizaw, 2020; Shadeed et al., 2019).

Satellite remote sensing, particularly using Landsat data, has greatly aided in mapping surface water extent. The Thematic Mapper (TM) and Enhanced Thematic Mapper Plus (ETM+) sensors

on Landsat 5,7 and 8 respectively, utilize infrared and visible bands to accurately distinguish surface water from the surrounding land surface (Baker et al., 2006; Potter et al., 2010; Roy et al., 2010; Tulbure & Broich, 2013; Yamazaki et al., 2015). Remote sensing provides significant advantages over traditional methods in monitoring lakes at regional or global scales. It offers wide coverage, allowing for the monitoring of large areas efficiently. Remote sensing enables frequent data collection, providing up-to-date information on lake conditions. It also allows for detecting various lake parameters, such as water quality and extent, using different wavelengths. These advantages make remote sensing an effective instrument for comprehensive and systematic lake monitoring on a larger scale. Its cost-effectiveness, ability to provide high temporal resolution, and consistent observations make it a valuable and efficient tool for comprehensive lake monitoring (Xia et al., 2019).

In the past, optical satellite imagery from sources such as AVHRR (Advanced Very High-Resolution Radiometer), MODIS (Moderate Resolution Imaging Spectroradiometer), SPOT (Satellite Pour Observation de la Terre), Sentinel-2, Landsat series, and GF series were mostly BV employed for extracting Surface Water Areas (SWAs). Among these, Landsat series data is particularly favored due to its medium spatial resolution (30 m), multiple spectral bands, open access, and extensive global observations spanning over 50 years (Wu et al., 2016; Xia et al., 2019; Zhou et al., 2019). A variety of techniques, including the single-band threshold method (Work and Gilmer 1976; White 1978), unsupervised and supervised categorization techniques (Mueller et al., 2016; Ruan et al., 2016; Tulbure et al., 2016; Yang et al., 2015), Water spectral indexes (Ma et al., 2019), as well as machine learning (Miao et al., 2018; Y. Wang et al., 2020). Several water indices, including NDWI(normalized difference water index)(McFeeters,1996), MNDWI(modified normalized difference water index) (Xu, 2006), AWEI(automated water extraction index) (Feyisa et al., 2014), NWI(normalized water index) (Feng, 2012), and WI2015(water index) (Fisher et al., 2016), have been effectively employed to map the SWAs of lakes using Landsat images at a worldwide or regional level due to their comparatively high accuracy, effectiveness, and low implementation costs (Aires et al., 2020; Arvor et al., 2018; Hamunyela et al., 2022; Olthof & Rainville, 2022; Pickens et al., 2020; Worden & de Beurs, 2020).

Wu et al. (2016), for instance, The SWAs of the NYPLs were successfully extracted using Landsat images by employing the MNDWI and object-based image analysis (OBIA) techniques. The

experimental results indicated that the suggested approach yielded satisfactory outcomes compared to visual SWA interpretation. Pekel et al. (2016) analyzed the distribution and changes in the world's surface water during the previous 36 years by utilizing three million Landsat satellite images, creating the 30-m Global Surface Water Dataset (GSWD) from 1984 to 2020. Fisher et al. (2016) examined how popular water indices differed in their ability to autonomously remove surface water. The results of the study underscored that the classification precision of every water index methodology relies on the varied backgrounds and composition of validation pixels. Additionally, it was noted that each water index method has limitations in terms of its suitability for specific geographic areas. The evaluation of various water indices using Landsat OLI images was conducted to detect inland water Bodies.

Several ages temporal series data from remote sensing (including MODIS, Landsat, Sentinel, and GF-1) and scientific datasets are stored in the open cloud computing platform Google Earth Engine (GEE), allowing for concurrent processing and practical big data processing in broad research areas (Liu et al., 2020). GEE has launched recently that serves as a cloud-based platform for geospatial processing. Its primary purpose is to enable planetary-scale analysis of environmental data. With its enormous satellite imagery collection and geospatial datasets, users can easily visualize, manipulate, edit, and generate spatial data. The platform offers a comprehensive set of spatial manipulation tools, empowering scientists, researchers, and developers to identify changes, track trends, and measure variations on the Earth's surface. GEE revolutionizes data analysis by providing a user-friendly and efficient solution for working with large-scale geospatial information. What sets GEE apart from traditional Google Earth is its capability to analyze and manipulate data based on user requirements. Unlike the traditional version, Earth Engine offers access to a vast repository of historical imagery and scientific datasets spanning over thirty years. This collection is regularly updated and expanded on a daily basis. Earth Engine not only organizes and manages these datasets but also makes them suitable for an extensive range of users, including the public, commercial entities, and government administrations. This accessibility allows users to leverage the rich data resources for various purposes, such as research, monitoring, and decision-making processes (Gálvez, 2023).

The GEE has recently been effectively applied for mapping crops and forests (Chen et al., 2017; Q. Duan et al., 2019; Guo et al., 2022; Oliphant et al., 2019; Pan et al., 2021; Phalke et al., 2020),

Dynamics of land use and cover (Hao et al., 2019; Pande, 2022; Xia et al., 2023; Zurqani et al., 2018), as well for mapping of open surface waters (Kandekar et al., 2021; Wang et al., 2019; Zhou et al., 2019). Thus, the long-term dynamics of SWAs can likewise be observed on a broad scale using the GEE.

The RVLB covers an extensive area of over 56,166 km². The region boasts numerous lakes, streams, and marshes, each with its own distinct hydrological and ecological features (Estifanos, 2008). These lakes serve vital socioeconomic purposes, including fishing, grazing, and recreation, Ethiopian Rift Valley, is home to the majority of the country's lakes. However, the majority of these lakes are subject to human pressure, and some are already going to disappear (e.g. Lake Haromaya in 2005) due to excessive use and improper catchment management (Lemma & Desta, 2016; Meshesha et al., 2014). Lake Haramaya, in particular, has been extensively studied, as evidenced by the works of Gebere et al. (2015), Lemma (2011), and Wakgari and Getu (2016). Wakgari and Getu (2016) found that the drying up of Lake Haramaya in 2005 was caused by environmental degradation and land clearing for agricultural purposes. Similarly, Kassawmar et al. (2011) studied the spatiotemporal variability of lakes Abaya and Chamo between 1973, 1986, and 2000, and observed that the lakes had significantly reduced in size by 6.4 km^2 compared to their previous extent. The Rift Valley lakes in Ethiopia are indeed confronted with various challenges arising from human activities, necessitating the implementation of effective catchment management and conservation strategies to safeguard these crucial ecosystems. Among the specific basins within the Ethiopia Rift, the RVLB of Ethiopia stands out as particularly vulnerable to environmental degradation. This area is characterized by lowlands with arid or semiarid conditions, rendering it susceptible to drought events.

The combination of human impacts and the naturally dry climate poses significant risks to the ecological balance of the RVLB. Droughts exacerbate the vulnerability of the region, placing additional stress on the lakes and their associated ecosystems. Consequently, there is a pressing need to adopt sustainable practices and conservation measures that can mitigate the detrimental effects of human activities and improve the resiliency of the RVLB's ecosystems in the face of recurring droughts. Therefore, this study is conducted to map the time series surface water availability and estimate the spatio temporal changes in RVLB then detect the change in

anthropogenic and natural stressors that can cause the change in surface water to make precise decisions of problem mitigation in RVLB.

1.2 Statement of the problem

The term "surface water resources" refers to any body of water above Earth, such as wetlands, glaciers, ice caps, lakes, ponds, streams, and rivers (Huang et al., 2018; Palazzoli et al., 2023). They facilitate rapid civilization, safeguard the diversity of life in both land and marine environments, and ensure economic prosperity by supplying water for industry and agriculture on a local and global scale (Cooley et al., 2021; Huang et al., 2018; Wang et al., 2018; X. Wang et al., 2020; Xiong et al., 2018). Nonetheless, many stresses are spreading across surface water resources due to socioeconomic and technological advancement, water management strategies, and climate unpredictability (Averyt et al., 2013; K. Duan et al., 2019; Erler et al., 2019; Yigzaw & Hossain, 2016).

The extent and position of surface water bodies are subject to changes especially due to both natural and human-induced influences (Hong et al., 2019). The RVLB in Ethiopia run from northwest to southeast, covering a stretch of land from the Dana depressions to Chew Bahir and dividing the Ethiopian highlands into two clear sections. These lakes are home to two unique ecosystems, one with fresh water that supports a wide variety of plant and animal species, and the other being saline-alkaline "soda lakes" that support various flora and fauna, including specialized species as well they play a critical role in a variety of economic and social activities, such as grazing, fishing, and recreation. But, several of these lakes are vulnerable to human impact. As evidenced from the previous studies Kassawmar et al. (2011) studied the spatiotemporal variation of lakes Abaya and Chamo, kedirkan (2019) also studied the water surface changes of lakes Abjata, Shala and Langano. Legesse et al. (2004) investigated the Examination of Lake Abiyata's hydrological reaction as a tropical terminal lake and they investigated as those lakes are Fluctuating through time. Those studies detected only the lake's surface area changing with time. They were focused on a specific goal as Rift Valley is a geologically active region. It is recommended to detect and explore various perspectives to make a confident conclusion and make a wise decision for the problem.

Therefore, this study aims i) to map the surface water availability in the Rift Valley Basin, estimating the spatiotemporal change of major Rift Valley lakes namely, Abaya, Shala,

Chamo,Hawasa,Zeway,Abita, and Langano; ii), Mapping the spatiotemporal change of natural and anthropogenic stressors and correlating with surface water change within the years 1984-2020 in GEE platform.

1.3 The objectives of the study

The general objective of the study is surface water availability mapping and estimating spatiotemporal variations using Google Earth Engine, RVL basin, Ethiopia.

The specific objectives of the study are

- ✓ Mapping the spatiotemporal variations of lakes using satellite images
- ✓ Assessing and quantifying surface water availability within the RVL basin.
- ✓ Evaluating the impact of natural and anthropogenic stressors for the variation in the lake surface water

1.4 Scope of the Study

This research project involves mapping of the spatial and temporal surface water availability of RVL basin, estimating the spatiotemporal variations of the RVLs, as well as an assessment of the influence of natural and human-induced stressors on these lakes.

1.5 Limitations

Regrettably, the study is not without its limitations, which are attributable to the time constraint under which it was conducted. Although particular methods were employed, such as surface water mapping using water indices and supervised classification, it is recommended that a wider range of techniques be utilized to improve the outcomes. Moreover, to effectively address the effect of natural and human-induced stressors, it would be more efficient to incorporate additional evaluation strategies.

1.6 Significance of the study

As mentioned above by-statement of the problem, the RVL basin Lakes are experiencing a gradual fluctuation in both quantity and quality due to both natural and human-induced pressures. This diminishing of water bodies exacerbates the water stress in the region. However, numerous studies have been conducted on the spatiotemporal lake water surface changes of lakes in the study area but the surface water availability in the study area was not estimated. As well from different areas, the surface water availability is estimated by using hydrological models. Even though, those traditional hydrological models have limitations in assessing surface water at the wide basin level due to challenges in accessing and incorporating complex data inputs across the entire basin area.

To address these limitations, a study was conducted using the GEE platform to map and analyze surface water availability. This platform provides a comprehensive and accessible data source recorded by satellite sensors, allowing for detailed analysis and overcoming the complexities of data processing. Therefore, this study aims to map the water availability of the RVL basin, estimating the spatiotemporal variation of the major lakes in the RVL basin, namely Ziway, Shala, Langano, Hawasa, Abita, Abaya, and Chamo Additionally, it evaluates the impact of natural and anthropogenic stressors on the surface water bodies in the RVL basin by using GEE platform. The study intends to contribute an important understanding of the dynamics of surface water availability in the basin, addressing the current limitations in the literature and promoting the utilization of advanced geospatial tools for water resource management.

1.7 Organization of the Thesis

This research study has various contents. From them, **Chapter One provides** the background of the study, including the general and specific objectives, the significance of the research, the statement of the problem, and the scope and limitations. **Chapter two** examines relevant works and concepts related to surface water mapping, as well as previous research on anthropogenic pressures on surface water availability. Related to surface water there is a lot of literature that is to be reviewed. But as its level of significance to my study the topics that were reviewed were surface water mapping, surface water availability, the effect of natural and anthropogenic stressors on surface water availability, and the Landsat image collection for surface water mapping. **Chapter three** describes the study area with location, physiography, soil, drainage, geology, and the methods and data that are utilized in this thesis. **Chapter Four** the results that were obtained within this thesis and the overall analysis of results. **Chapter Five** discusses the result of this study with related literature. **Chapter six** is the last chapter of this thesis which gives the overall conclusions and recommendations for future researchers as this thesis uses it as a benchmark.

CHAPTER TWO

LITERATURE REVIEW

2.7 Surface water availability

Water availability refers to the combined assessment of both the quantity and quality of water that is accessible and suitable for various uses. It takes into account the amount of water physically present in a given area (water quantity) as well as the suitability of that water for specific purposes (water quality). The availability of water can vary across different terrains and can change over time due to various factors (USGS, 2023).

Freshwater resources from surface water bodies are vital in regions with limited access to alternative sources like groundwater. Surface water ecosystems are rich in plant and animal species, serving as biodiversity hotspots (Vörösmarty et al., 2010). There are numerous studies on surface water availability. For instance, Juniati et al. (2019) estimated the availability of surface water by using the SCS-CN model. The model offers a method that is hydrologically sound to more accurately depict capture behavior. His research concentrated on the upper catchments in Indonesia's West Java. Maru et al. (2023) they studied how changes in LULC affect streamflow and the availability of surface water in the sub-watershed of Akaki in Awash Basin. The models utilized were Climatic Water Balance (CWB) and SWAT. Munyaneza et al. (2014) In their research, created a catchment hydrological model that can be utilized to guide Making decisions and organizing water resources to improve the management of the Migina Catchment (257.4 km^2) by utilizing the Hydrologic Engineering Center's (HEC-HMS) semi-distributed hydrological model (version 3.5). In relation to this topic, various studies were done on water availability and affecting factors of it by using hydrological models. However the application of Google Earth Engine was not familiar.

2.1 Surface water mapping

Surface water, comprising lakes, rivers, swamps, and other aquatic bodies, is vital for Earth's water resources. It is critical in supporting industrial production, agriculture, and climate management. Additionally, surface water is an essential indicator of environmental and climatic changes in terrestrial ecosystems (Zhang et al., 2019). A significant portion of the planet's surface freshwater, accounting for 87%, is stored in natural lakes and artificial reservoirs, collectively known as Surface Water Bodies (SWBs) (Gleick and Heberger, 2014).

Accurate forecasting of lake levels is of paramount importance for the efficient operation of hydropower plants, commercial navigation, residential, agricultural, and industrial activities, as well as water resource planning and management in many countries (Huang et al., 2018). The primary factors influencing fluctuations in lake levels include evaporation, groundwater harvesting, precipitation within the basin, and incoming and outgoing water flows (Talebizadeh and Moridnejad, 2011).

Moreover, the lake level forecast is heavily influenced by complicated hydrometeorological and human-caused factors, therefore using these elements for this purpose could lead to low prediction accuracy (Godwin et al., 2019; Haghighi & Kløve, 2015; Khan & Coulibaly, 2006). That is difficult to evaluate quickly and readily (Haghighi & Kløve, 2015). Hence to allocate water in a just and equitable manner to various sectors, and ecological services, as well as a greater awareness of the implications of climate change, accurate and regular observation of fluctuations in the water level in lakes and reservoirs is essential (Yuan et al., 2015).

The prompt and precise collection of surface water spatial distribution data is crucial for managing and monitoring water resources as well as preventing flood and drought disasters (Huang et al., 2018; Vörösmarty et al., 2010). In recent decades, the detection and extraction of surface water and its alterations have made great use of the vast amounts of data that remote sensing satellites at various geographical, spectral, and temporal resolutions provide. These satellites have become major sources (Alesheikh et al., 2007; Du et al., 2012; El-Asmar & Hereher, 2011; Huiping et al., 2011). As additional evidence, many studies conducted in the last few decades have concentrated on surface water mapping techniques using remote sensing imagery (Brisco, 2015; Yamazaki et al., 2015).

2.2 Anthropogenic impact on surface water resources

The pressure on hydrological resources is significant and ongoing due to humanity's capacity to manage and utilize water resources throughout history (Bierkens, 2015; Ceola et al., 2015; Wada et al., 2017). In particular, Human actions, including land cover change and temperature modification have had an indirect impact on the terrestrial water cycle, as well as direct actions such as water withdrawals and diversions (Rost et al., 2008). Additionally, population growth, urbanization, economic development, and food security policies have a noticeable influence on the world's water demand.

Currently, the annual growth rate of water consumption is 1% (Water, 2020). However, six months of the year, two-thirds of people on the planet have water scarcity (Mekonnen & Hoekstra, 2016). By 2050, domestic use, thermal electricity production, and manufacturing are projected to result in a 55% increase in water demand (Connor, 2015). In this regard, rivers and lakes are particularly vulnerable to overuse and depletion as they are the principal supply of water for human use, along with groundwater (Gleick, 1993).

2.2.1 Population growth and urbanization

Urbanization is a human-induced shift in land utilization as a result of the interplay of various physical and socioeconomic factors. It refers to the increasing percentage of people living in urban regions in a nation, resulting in a decrease in the rural population share (Satterthwaite et al., 2010). When formerly natural landscapes are transformed into urban water-impervious lands, urbanization increases the strain on freshwater resources by concentrating people in one place and reducing the amount of freshwater that is accessible (Sun et al., 2013).

Urban uses currently make up 10%–20% of all water withdrawals in developing world basins, and demand is growing quickly due to urban population expansion (Srinivasan et al., 2013). That's because the majority of the increase in this. Among the primary human-caused variables that alter water flow patterns and river morphology and severely strain river systems are demographic growth and the urbanization process (Ceola et al., 2019; Grizzetti et al., 2017; Paterson et al., 2015). Furthermore, the global share of anthropogenic freshwater usage that is caused by the industrial and household sectors is 19% and 11%, respectively (Flörke et al., 2013).

Freshwater is a limited resource; it makes up only 2.5% of the water on Earth, most of which is submerged (Ranjan et al., 2006). Jevon's paradox, which holds that contrary to expectations, increased (rather than decreased) water use efficiency does not necessarily lead to decreased consumption (Polimeni & Polimeni, 2006), illustrates how the Freshwater consumption is growing as a result of many factors like population growth, water pollution, economic development, and technological advancement (Schleich & Hillenbrand, 2009).

2.3 Impacts of climate change on surface water resources

One of the main causes of water stress is a warming climate, which results in temporal and spatial changes in temperature, precipitation, and evapotranspiration (ET). These variations have an impact on river runoff and groundwater recharge, endangering water security (K. Duan et al., 2019;

Kundzewicz, 2008). Specifically, the frequency of hydrologic severe events, including drought and flood, is increased by climate change, leading to a reduction in water supply and an increase in water demand (Brown et al., 2019; Zhuang et al., 2018).

Furthermore, there is an interaction and influence among the alterations in climatic factors (Fig 1**)**. At the watershed level, the quantity of locally available water is, in fact, determined by the difference between precipitation and ET. On the other hand, ET intensifies with temperature, drying surfaces, decreasing soil moisture, and decreasing surface waters (K. Duan et al., 2019). Water management is being significantly impacted by climate change, which is also having an effect on the hydrological cycle. Human progress and security will thus be significantly impacted by this (Parry et al., 2009).

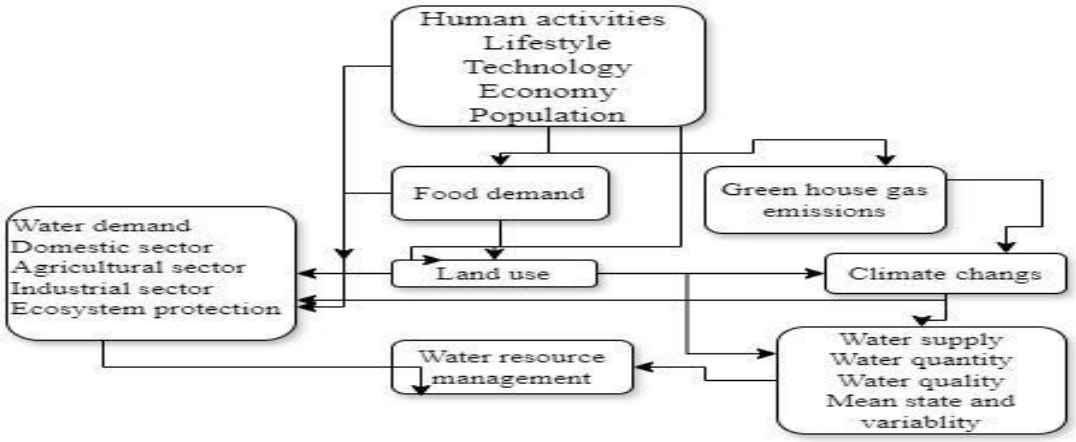

Figure 1 The interdependence of human activities, climate change, and water supply and demand

2.3.1 Precipitation change

The primary means of land-based water bodies is precipitation, as stated by Kundzewicz (2008). Therefore, surface water, in addition to the entire hydrologic cycle, is highly susceptible to fluctuations in precipitation and severe weather conditions brought on by climate change, such as droughts and floods (Arsiso et al., 2017; Brunner et al., 2021; McKinnon and Deser, 2021; Pendergrass et al., 2017). Changes in precipitation patterns have an influnce on the availability of surface water, which in turn affects ecosystems and human populations (Konapala et al., 2020; Paucar-Caceres et al., 2017).

2.3.2 Temperature change

Temperature influences each and every element of the water cycle. River flow, soil moisture, ET, and precipitation are only a few of the systems that are impacted by climate change. Temperature changes the availability of water by regulating the evapotranspiration demand, which includes the evaporation from soils, plants, and trees, as well as the transpiration process, which is connected to the use and release of water from plants (Gupta et al., 2022). According to Kundzewicz (2008) and Balling and Goodrich (2011), rising temperatures lead to a rise in the potential ET rates and the amount of water stored in the atmosphere, which in turn causes more intense precipitation.

2.4 Remote sensing for surface water

Remote sensing technologies offer highly efficient techniques for ongoing, multi-scale monitoring of the Earth's surface that enable spatially explicit and temporally frequent observations to accurately map and track the dynamics of surface water bodies on regional and global scales, providing greater efficiency and detail compared to traditional in-situ measurement methods (Donchyts et al., 2016).

Two primary types of sensors commonly used for measuring surface water are optical sensors and microwave sensors. Optical sensors rely on capturing and analyzing light reflected from the Earth's surface. They are sensitive to various wavelengths of light and provide high-resolution imagery. However, their effectiveness can be limited in cloudy or vegetation-covered areas due to the obstruction of light. On the other hand, microwave sensors utilize longer wavelengths that can penetrate through clouds and certain types of vegetation. This allows them to operate effectively day and night, regardless of weather conditions or solar radiation. Microwave sensors can provide valuable information about surface water, even in challenging environments.

2.4.1 Surface water detection with satellite sensors

Since the launch of the first Earth Resources Technology Satellite (ERTS-1) in 1972, optical sensors on satellites have proven effective in monitoring significant changes in land cover on the Earth's surface (Deutsch & Ruggles, 1974). Surface water dynamics, a significant aspect of land cover change, have been a prominent focus of Earth observation (Schaffer-Smith et al., 2017). Optical sensors are categorized into three groups based on spatial resolution, which determines the level of detail captured within a pixel. These categories include coarse (>200 m), medium (5-200

m), and high (<5 m) resolution. The choice of sensor for detecting surface water is directly influenced by spatial resolution.

2.4.1.1 Coarse spatial resolution sensors

Coarse-resolution remote sensors, such as the National Oceanic and Atmospheric Administration's Advanced Very High-Resolution Radiometer (NOAA/AVHRR), offer high information generalization and temporal resolution but have inherent limitations in accuracy. Despite being primarily designed for atmospheric and oceanic monitoring, the NOAA/AVHRR sensor has proven capable of detecting large-scale flood events (Barton & Bathols, 1989). Following its initial detection of large-scale flood events, several studies have further investigated the capability of the NOAA/AVHRR sensor to identify flood inundation (Domenikiotis et al., 2003; Islam & Sado, 2000).

The Moderate Resolution Imaging Spectroradiometer (MODIS) sensor, installed on the National Aeronautics and Space Administration's Terra and Aqua satellites, is another prominent member of the coarse-resolution category. Since its launch in 2000, MODIS data have found extensive applications in atmospheric monitoring, land cover analysis, and land use change studies. Additionally, MODIS sensors have proven effective in identifying surface water (Brakenridge & Anderson, 2006; Chen et al., 2013).

MODIS, like other coarse spatial resolution sensors, has gained widespread usage due to its rapid revisit time and wide coverage capabilities. With over a decade of continuous Earth surface monitoring, MODIS sensors have generated a significant dataset that is well-suited for investigating spatiotemporal dynamics of surface water. Consequently, MODIS time series data have been utilized to identify changes in lake water (Cai et al., 2016).

2.4.1.2 Medium spatial resolution sensors

The Landsat satellite series has been highly successful, providing consistent medium-resolution imagery for over four decades since its establishment in 1972. The Multispectral Scanner (MSS) sensor was later replaced by the Thematic Mapper (TM) and Enhanced Thematic Mapper Plus (ETM+) sensors on Landsat-4, Landsat-5, and Landsat-7. Landsat-8 introduced the Operational Land Imager (OLI) sensor, offering spatial resolutions ranging from 80 to 30 meters, with a 15-meter resolution in the panchromatic band. These resolutions enable precise detection of surface water dynamics.

Landsat TM images played a crucial role in early mapping efforts in the US (Deutsch & Ruggles, 1974; McGinnis & Rango, 1975). The widespread applications of surface water detection using Landsat TM images have increased significantly, particularly since Landsat-5 exceeded its expected service life (Chen et al., 2014; Pardo-Pascual et al., 2012). Despite being launched in 2013, Landsat-8 with its OLI sensor has already found extensive use in surface water detection (Acharya et al., 2016; Gao et al., 2016; Yang et al., 2015).

The SPOT satellite series, equipped with Systeme Probatoire d'Observation de la Terre (SPOT) sensors, offers resolutions of around 10 meters, surpassing the capabilities of Landsat images. While SPOT data is not freely accessible like Landsat data, several studies have successfully utilized SPOT imagery to detect surface water or identify flood eve (Davranche et al., 2010; Fisher & Danaher, 2013).

2.4.1.3 High spatial resolution sensors

Advancements in remote sensing research have focused on improving the spatial resolution of sensors, a key objective in the field. Recent sensors such as GF-1/2, ZY-3, Quickbird, RapidEye, Worldview, IKONOS, and Quickbird have achieved spatial resolutions ranging from meters to submeters. This level of detail allows for the successful detection of small water bodies. However, these sensors do have limitations. They often have limited scene coverage, making it challenging to effectively map large bodies of water. Additionally, the presence of shadows in their images can pose difficulties (Sawaya et al., 2003). Particularly in mountainous or metropolitan environments, which might have a negative impact on water detection. Furthermore, there are significant limitations on the availability of the majority of these sensors' photos as well as their revisit frequency.

2.5 Surface water extraction techniques

The extraction of surface water from optical images is based on the noticeable decreased reflection of water in infrared channels relative to other land cover types. Various techniques for removing water regions from optical remote sensing images have been developed as a result. One simple method for creating a water map is to density slice a single infrared band (Frazier and Page, 2000). Water maps can also be derived from land cover maps created using supervised or unsupervised classification techniques (Manavalan et al., 1993; Ozesmi & Bauer, 2002).

Decision trees have been constructed to distinguish one type of water coverage from another using multispectral bands (Acharya et al., 2016; Olthof, 2017; Sun et al., 2011). However, the classification rules for these approaches are often difficult to construct and may not be reliable enough for use in all situations. Water indices are a useful tool for distinguishing between areas with and without water by utilizing multiple bands to calculate differences. These indices have been created to extract surface water extent or to assess the extent of flood inundation.

Two commonly used indices for this purpose are the (NDWI) and the MNDWI. The NDWI was first introduced by McFeeters in 1996 and was widely used in the early 21st century by researchers such as Chowdary et al. (2008) and Hui et al. (2008). However, Xu (2006) improved upon the NDWI by changing the Near Infrared (NIR) band to the SWIR band resulting in the mNDWI. This modification allows the SWIR band to capture minor features of water that were not previously visible. Additionally, the mNDWI is more stable and reliable than the NDWI because the NIR band is more sensitive to sediments and other optically active substances in water. As a result, the mNDWI has been widely utilized in recent studies by researchers such as Chen et al. (2014) and Mohammadi et al. (2017).

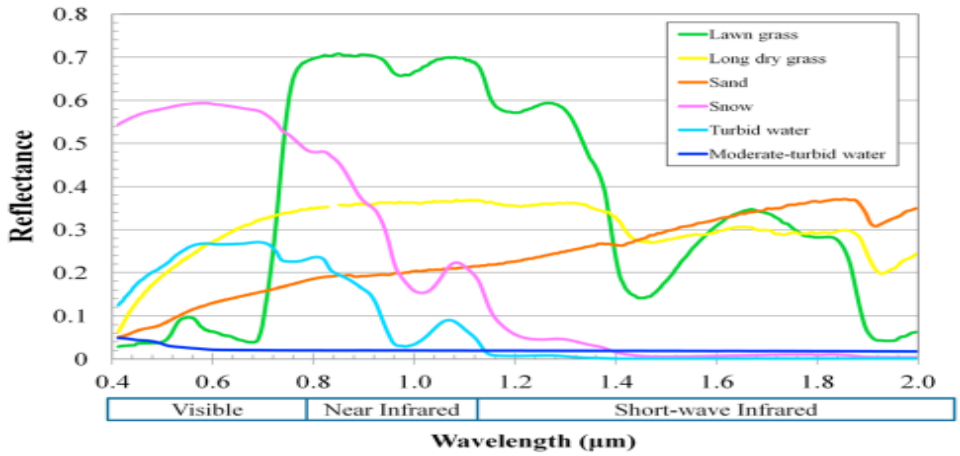

Figure 2 the spectral signature of land cover types from the United States Geological Survey (USGS) spectral library.

One limitation of the mNDWI is its inability to effectively differentiate between water and snow, as snow typically exhibits higher reflectance values in all visible and infrared channels compared to water (Fig 2**)**. Despite this, the normalized difference between the Green band and the Shortwave

Infrared (SWIR) band of snow is equal to that of water, making it challenging to distinguish between the two. To address this issue, the normalized difference snow index (NDSI), which shares the same formula as mNDWI, has been utilized in numerous studies to extract snow cover (e.g., Choi and Bindschadler, 2004; Salomonson and Appel, 2004).

Therefore, when using mNDWI to identify water bodies in areas with snow cover, it is critical to exercise caution, as snow and water may be easily distinguished using a single visible or NIR band. It is recommended to use mNDWI in conjunction with a visible or NIR band for more accurate results. When utilizing water indices to identify water bodies, one of the most critical considerations is thresholding. Typically, the NDWI and mNDWI readings are higher than 0 based on the reflectance properties of the water. As a result, a threshold of 0 is commonly employed for extraction of water from index images. However, adjusting the threshold value can often improve the extraction results, as proposed by Ji et al. (2009) and Xu (2006).

2.6 Spatiotemporal monitoring

Due to numerous human-made and natural variables, surface water bodies are inherently dynamic and may undergo changes in size over time. These fluctuations in water bodies have a significant impact on human resources, other natural resources, and the environment (Karpatne et al., 2016). Hence, the spatiotemporal monitoring of these dynamics is necessary to comprehend the global or regional availability of water resources and gain insights into the natural processes that influence water storage. Multi-temporal remote sensing images are often used for this purpose (Heimhuber et al., 2016; Schaffer-Smith et al., 2017; Thito et al., 2016). One notable application is the monitoring of lake water body dynamics. Several studies have utilized MODIS data and Landsat images to extract spatiotemporal information about changes in lake water surfaces.

For instance, Feng et al. (2012) used a time series of MODIS data to evaluate the surface water area of Poyang Lake from 2000 to 2010 and found that the lake's extent had fluctuated greatly during this Period. Using Landsat time series data, Kassawmar et al. (2011) examined the spatiotemporal variability of Abaya and Chamo lakes between 1973, 1986, and 2000, and found that the lakes' area had degraded by 6.4 km^2 compared to previous years. Deoli et al. (2022) utilized multiband rationing index from Landsat satellite bands to study the dynamic changes in the water spread area of Nainital Lake between 2001 and 2018 and discovered that the lake's water spread area significantly reduced between March and June and July and October at a 5% significance

level. The greatest reduction occurred between March and June (7.7%), followed by July to October (4.67%) and November to February (2.79%). Sarp and Ozcelik (2017) used Multi-temporal images to assess the time series changes in Lake Burdur from 1987 to 2011 and found that the lake's surface area sharply declined between 1987 and 2011, particularly between 1987 and 2000 when it lost almost one-fifth of its 1987 size. Xu et al. (2020) employed an automatic approach to extract open water from Taihu Lake using Landsat imagery, and the results indicated that this approach has significant potential for automatically extracting continuous open surface water. Ahmed et al. (2021) through the analysis of time series Landsat images from 2001, 2011, and 2019, a geospatial study was conducted on Deepor Beel Lake. The findings revealed a significant decrease in the lake's water storage capacity over the last two decades. Specifically, the storage capacity of the lake decreased from 20.95 million m^3 in 2001 to 16.73 million m^3 in 2011 and further declined to 15.35 million m^3 in 2019. This decline poses a major challenge to the lake's long-term sustainability.

CHAPTER THREE

MATERIALS AND METHODS

3.1 Description of the study area

The study was conducted within the Ethiopian portion of the Rift Valley Lake basin, which is situated between 36°35'45"–39°23'31" E longitude and 4°24'29"–8°26'38" N latitude covering a total area of 56166 km^2 (Fig 3). The Ethiopian Rift, formed by volcanic and faulting activities, has given rise to a series of volcano-tectonic depressions that have transformed into lakes.

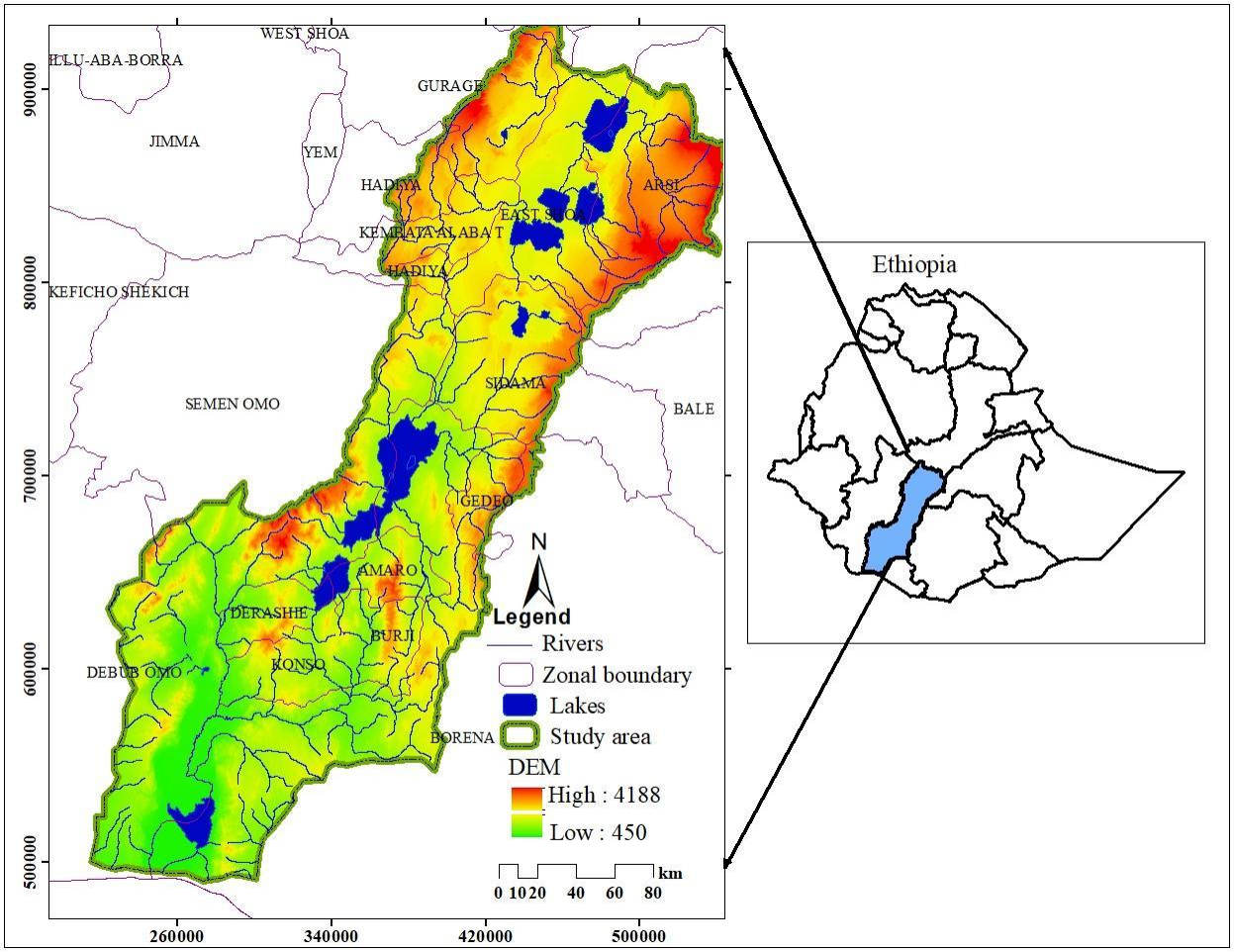

Figure 3 Location map of the study area

(This study area is rich of Lakes. The major lakes are lake zeway, lake chamo lake abaya, lake shala ,lake langano ,lake Abijata ,Lake Hawasa and lake chew bahier . Those lakes shows fluctuation from time to time due to different natural and anthropogenic stressors).

This geological phenomenon is a portion of the Great Rift Valley in east Africa known as the Afro-Arabian rift, which stretches from Jordan in the Middle East to Mozambique in southern Africa Within the Ethiopian highlands, the Ethiopian rift valley divides the region into a northern and southern section, extending from the border with Kenya to the Red Sea. The Rift Valley runs in a northeast to southwest direction and consists of three distinct subsystems, Chew Bahir (Lake Stephanie), the Central Rift Valley (CRV), and the Afar triangle. The Ethiopian Rift widens as it moves northward and gradually narrows as it crosses the boundary between Ethiopia and Kenya in the south. This region spans from the northern Afar depression to Kenya in the south, encompassing the wide basins of Abijata-Ziway, Abaya-Chamo.

3.1.3 Physiography and Landform

Volcanic and faulting activity caused a variety of depressions caused by volcano tectonics in the rift floor, which eventually developed into lakes, forming the Ethiopian Rift. Part of the Great east African Rift Valley, often known as the Afro-Arabian rift, the Ethiopian Rift stretches from Jordan in the Middle East through Eastern Africa to Mozambique in the southern region of the continent. The Ethiopian Rift Valley divides the country from its border with Kenya to the Red Sea, and the Ethiopian highlands are divided into two halves, one in the north and one in the south.

The Rift Valley floor is home to three main bodies of water, which span from the northeast to the southwest, as noted by (Alemayehu et al., 2006). In the East Shewa Zone of the Oromiya region, Lake Ziway is located within the Adami Tullu-Jiddo Kombolcha Woreda district. Addis Ababa, the capital of the nation, is approximately 150 kilometers to the north of Lake Ziway. Ziway, a settlement on the western side of the lake, sits at an elevation of approximately 1636 meters above mean sea level. About 30 kilometers southwest of Lake Ziway lies Lake Abijata, which is part of the Southern Nations, Nationalities, and Peoples region. The valley containing the lakes is surrounded by mountains to the east and west. Mount Kaka, situated to the east of the lakes, rises to an elevation of 4245 m above msl, or approximately 2000 m msl (Fig 4).

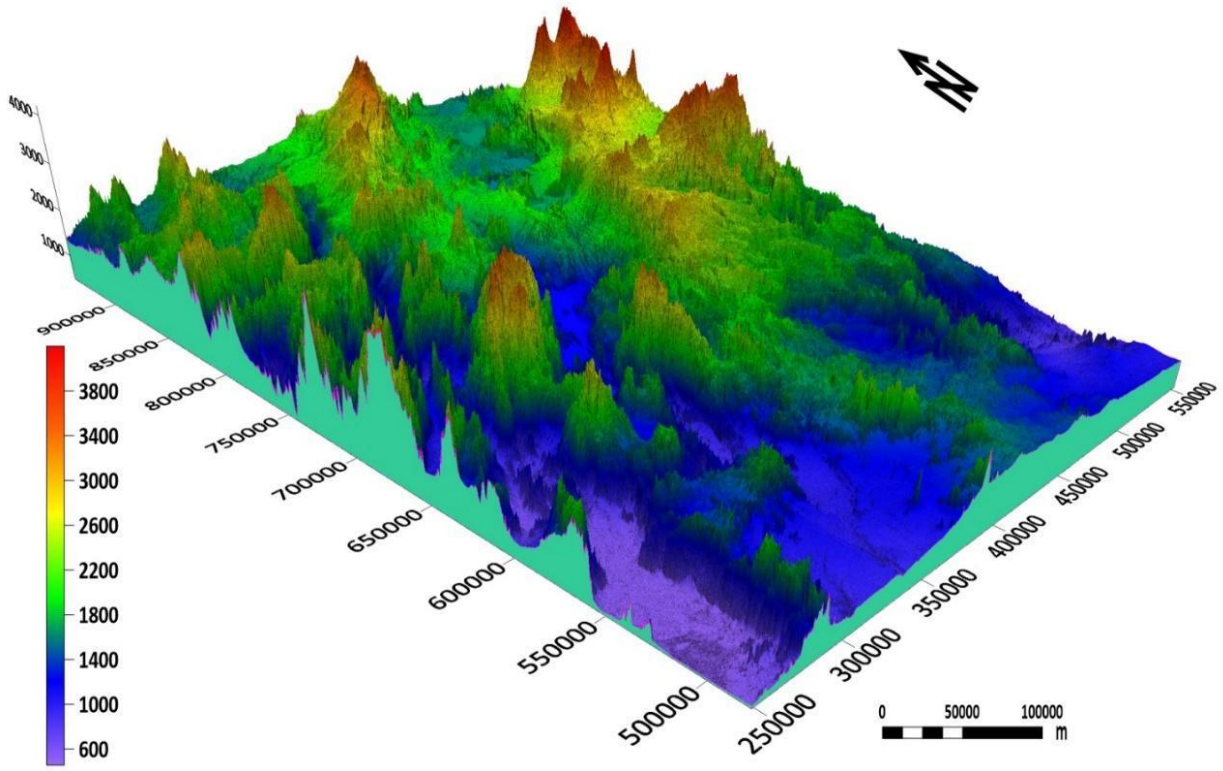

Figure 4 the physiography map of the study area

The majority of rivers and lakes in the CER valley are located at an elevation of around 1500 m. The lakes area is characterized by hills, ridges, and volcano-tectonic depressions. The study area is part of the African Rift, which extends from the Aden Junction and traverses the eastern African countries of Djibouti, Eritrea, Ethiopia, Kenya, Uganda, and Tanzania in a southwest to south-southwest direction. The valley is geologically characterized by active faults, active volcanoes, and hot springs, indicating its status as a geothermal zone. Petrological and geophysical data indicate that the lithosphere beneath the valley has been thinned due to a hot mantle. The valley is considered to be a separating boundary of the African Plate, with the Nubian Plate located to the west and the Somalian Plate to the east. Both plates are moving apart at a rate of approximately 5 mm per year (Stamps et al., 2008).

3.1.4 Regional geology and tectonic setting

MER has been the subject of geological studies since the early 1970s. In the 1970s and 1980s, basic geological research was carried out to investigate natural resources such minerals and geothermal areas. In particular, the presence and evolution of MER in the context of "Plate

Tectonics" were examined in the 1990s by WoldeGabriel et al. (1990), Le Turdu et al. (1999), and WoldeGabriel et al. (2000).

Numerous geological and archeological investigations have been carried out as MER is important from the perspective of Quaternary geology for the genesis and evolution of Hominidae. Due to structural characteristics, the Ethiopian Rift Valley is separated into three geologic zones: the northern, center, and southern rift valley sections. Ethiopia's Northern Rift System stretches from Afar to Adama, with the Afar triangle extending up to Lake Beseka. The tectonically regulated endorheic basin features that make up the Central Rift Valley (CRV) system, which stretches from Adama to Hawassa, are comprised of a chain of four hydrologically related lakes: Lake Ziway, Lake Abijata, Lake Langano, and Lake Shala. The Southern Rift System, which includes the Hawassa, Abaya, Chamo, and Chew-Bahir Lakes, stretches from Hawassa to Chew Bahir. The rift valley lakes basin is located in the Main Ethiopian Rift's central-southern region (MER). From the Oligocene to the Quaternary, MER evolved. Major volcanic episodes in the Oligocene, middle Miocene, late Miocene, early-middle Pleistocene, and Holocene are known to have occurred at that time (Woldegabriel et al., 1990). The earliest known volcanic activity was the Oligocene basalt and rhyolite flows, which built lava plateaus in the vicinity of the rift borders (such as the Blue Nile Gorge). Some sections of the rift generated confinement basaltic flows by the middle Miocene. The northern portion of the study region was covered by a massive pyroclastic flow during the Pliocene (Fig 5). Geothermal well observations of this distinctive pyroclastic flow deposit, which is presently found at a depth of about 2100 m in the basin floor, show that the rift basin has had at least 2 km of downslope since its eruption (Woldegabriel et al., 1990; WoldeGabriel et al., 2000). The Wonji Fault Belt (WFB), the primary spreading axis of the Middle East Rift (MER), is developed at the rift floor in the Pleistocene, and along its length, floor basalt and rhyolite Erupt.

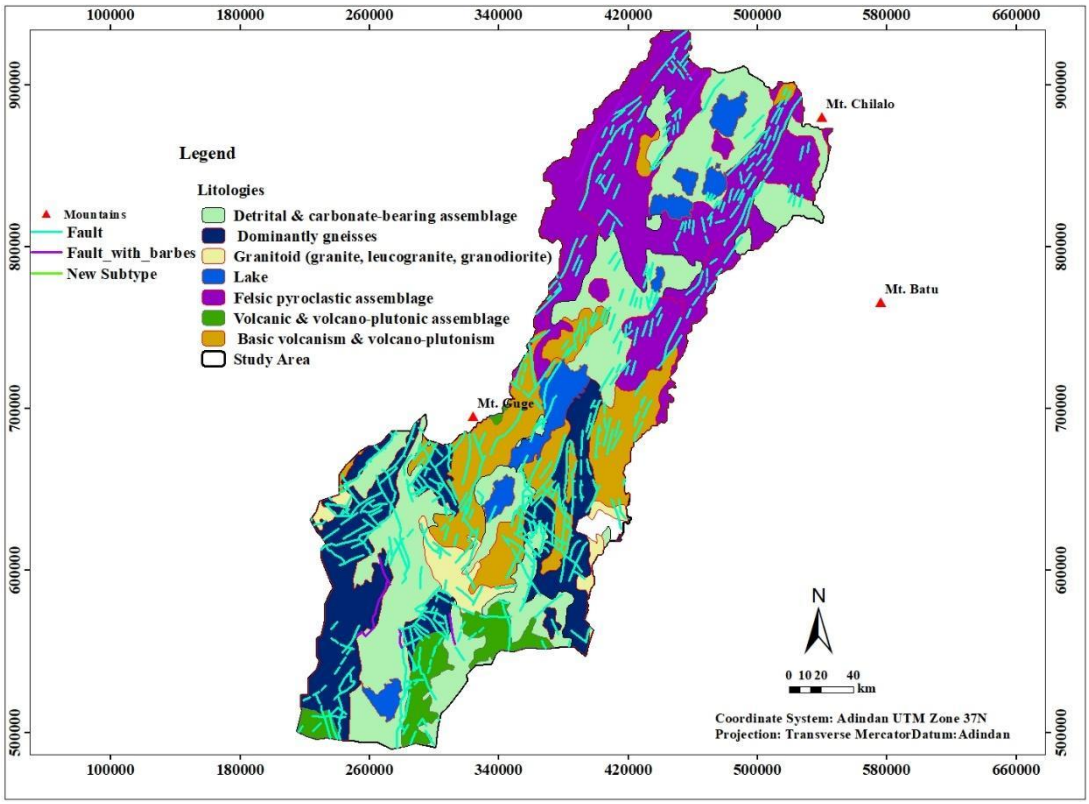

Figure 5 Geological map (source: Ethiopian geology)

(The Rift Valley Lakes basin is geologically active region which consists of many geological structures. This basin around the upper part is highly composed of felsic pyroclastic assemblage around the Lake areas the geologies are detrital and carbonate-bearing assemblage, and around the bottom consists of varieties of geological units such as Granitoid, basic volcanism, and volcanic plutonism and genesis).

The rhyolitic and peralkaline fissure basaltic eruptions that form volcanoes and calderas are the hallmarks of volcanic activity. MER developed during this time as a symmetrical depression zone, and several lakes arose and vanished as a result of volcanic deposit obstruction and/or climate change. A sequence of tensional faults traveling NE-SW generated the MER, while the Wonji Fault Belt, a more recent system of NNE-SSW trending faults, sliced through it as shown below Table 1. The Afar depression is where the rift begins in the north, and it continues as symmetrical grabens in the middle Near the Ethiopian border, the rift continues peculiarly.

Table 1 Geological units

Period	Quaternary	Neogene	Paleogene
Geological units	Wonji Group	Chilalo Trachytes	Kella Basalts
		Nazareth Group	A laji Formation
		Butajira Ignimbrites	
		Nazret Group/Afar Group	
		Guraghe Basalts	
		Shebele Trachytes	
		"Ancher Basalts", "Arba	
		Guracha Silicics"	
Age(Ma)	0.0117	5.33	33.9
Source	WoldeGabriel et al. (1990)	WoldeGabriel et al. (1990)	WoldeGabriel et al. (1990)
	EWTEC (2008)	Halcrow (2008)	Halcrow (2008)
	Halcrow (2008)	EWTEC (2008)	

Kenya, where little asymmetrical basins emerge in its place, and the Rift eventually connects to the N-S direction of the Kenya Rift. Both of the MER's rift escarpments' structural and stratigraphic relationships with volcanic rocks point to a two-stage rift formation. The early phase was characterized by a succession of alternating and opposite half grabens and began in the late Oligocene–early Miocene. In late Miocene times, the half-grabens became a symmetrical fissure. Active rifting during the Plio-Pleistocene was another feature of the region; an estimated 2000 meters of subsidence occurred there (Woldegabriel et al., 1990).

3.1.5 Drainage pattern

The Rift Valley drainage systems exhibit diverse flow directions, with streams coursing through the region in various ways (Fig 6). The Awash River, for instance, flows northeasterly before converging into a network of small lakes and marshy areas. The southern part of the Rift Valley sub-basin is known for its multitude of lakes and small streams, earning it the nickname of the "lakes region." This area comprises fault depressions that are filled with water from streams that flow down from the surrounding mountain slopes.

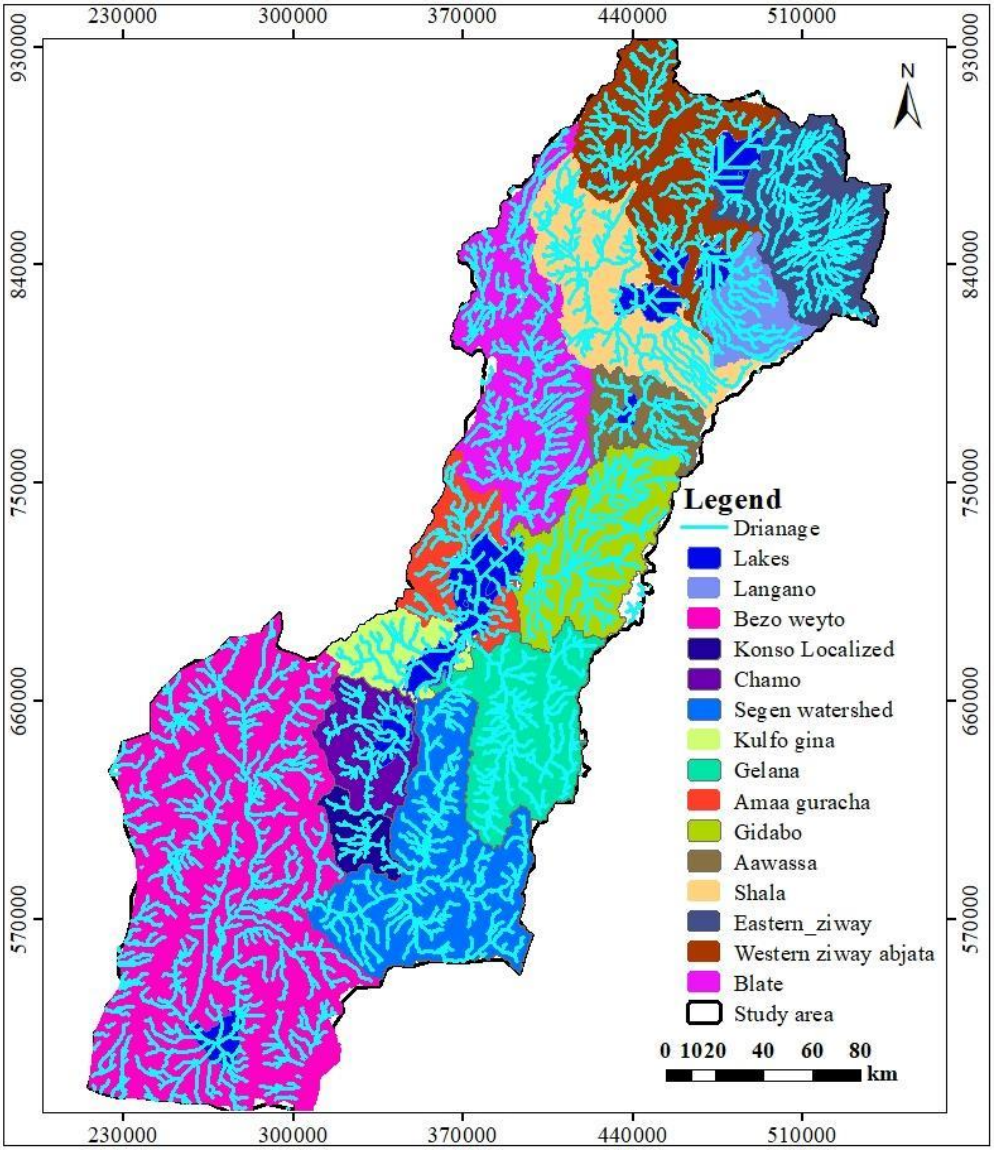

Figure 6 Drainage map of the study area (source: from Hydro sheds)

3.1.6 Soil

Numerous factors, including location, height, climate, and geological history, can affect the soil composition in the RVLB. This area often has a somewhat varied range of soil types. Because of their volcanic beginnings, some parts of the Rift Valley may have very fertile, mineral-rich soil. Rich soils fit for farming can be produced by volcanic ash deposits. Alluvial soil is created in basins where sediments carried by rivers and streams deposit. Many crops can thrive in this kind of soil due to its fertility.

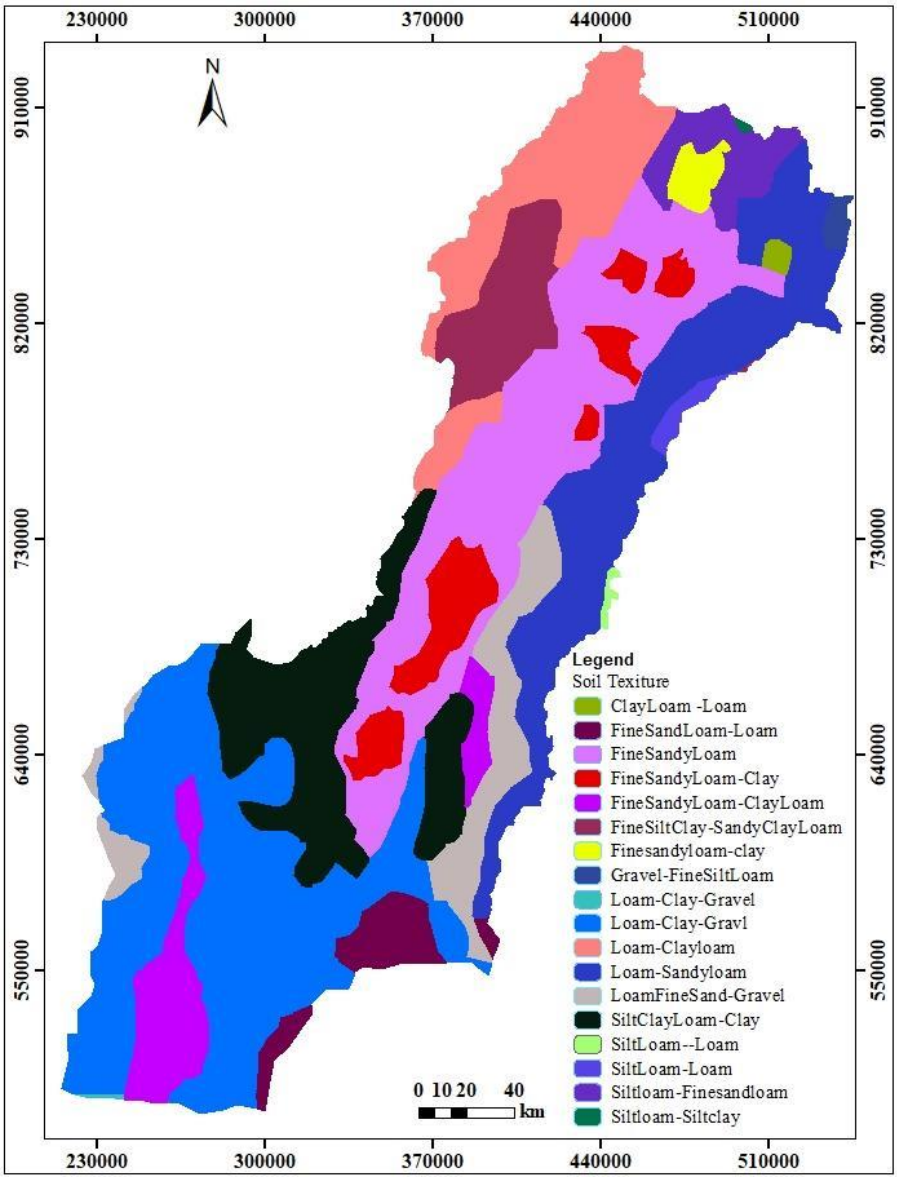

Figure 7 the soil map (source from FAO)

The composition of the clay or sandy soils may vary across the basin. However clay soils can be less permeable, they retain moisture better than sandy soils and often have good drainage, but they may need more regular irrigation. The evaporation and concentration of salts in certain areas may result in greater salinity levels in the soil. It may be necessary to treat the soil or choose particular crops as a result of this in agriculture.

3.2 Geospatial data

This research study has used primarily a Global surface water dataset in the Google Earth Engine platform (https://earthengine.google.com). Pekel et al. (2016), extracted the dataset of changes in global surface water over the past 32 years were quantified using three million Landsat satellite images at a 30-meter resolution. The research recorded the months and years when water was present, identified areas where occurrence changed, and characterized the nature of these changes in terms of seasonality and persistence. The findings revealed that between 1984 and 2020, approximately 90,000 square kilometers of permanent surface water disappeared, which is roughly equivalent to the area of Lake Superior. However, during the same period, new permanent bodies of surface water covering 184,000 square kilometers were formed in other locations.

This dataset used the complete collection of orthorectified top-of-atmosphere reflectance and brightness temperature images (L1T) from the Landsat 5 Thematic Mapper (TM), Landsat 7 Enhanced Thematic Mapper-plus (ETM^{+}), and Landsat 8 Operational Land Imager (OLI) (Pekel et al., 2016), acquired between 16 March 1984 and 10 October 2015 was used (Woodcock et al., 2008; Wulder et al., 2012). It consists of the surface water occurrence data from 1984–2020, surface water transition data, and also yearly surface water data. Surface water availability yearly in GEE has the data yearly from 1984 to 2020. For this study, the intended data were the years 1984, 2000, 2010, and 2020. For this data preprocessing and post-processing steps were made and exported to the drive by using a code in GEE after this displaying the layout is done in ArcGIS 10.7.

Landsat time series data of Landsat 5TM, 7ETM, and 8OLI satellite data series of years 1990-2020 Which is used for land use land cover mapping and extraction of the major lakes of the RVLB. Those Landsat time series data are cloud-masked, georeferenced, and clipped with the study area boundary for the purpose of processing of data in the GEE platform (https://earthengine.google.com/). Those Landsat images for 1990, 2000, and 2010 are Top of atmosphere (TOA) images and for recent years it is surface reflectance (SR) images the reason is that those earlier years don't have access to surface reflectance images for those years with study area boundaries. For Land use land cover mapping sentinel images due to their higher resolution, they were highly necessary but in case this study it uses years 1990-2020 earlier than the year when sentinel satellites were launched in case it becomes mandatory to use Landsat satellite images. Landsat data description presented Table 2.

Table 2 Landsat image data

Landsat 5 TM			
Bands	Wavelength(micrometer)	Resolution(m)	Data accusation
Band 1 – Blue	0.45-0.52	30	Feb 01/01/1990
Band 2 – Green	0.52-0.60	30	
Band 3 – Red	0.63-0.69	30	
Band 4 - NIR)	0.76-0.90	30	
Band 5 -SWIR 1	1.55-1.75	30	
Band 6 – Thermal	10.40-12.50	30	
Band 7 -SWIR 2	2.08-2.35	60(30)	

Landsat 7 ETM			
Bands	Wavelength (micrometer)	Resolution (m)	Date of acquisition
Band 1 – Blue	0.45-0.52	30	Jan 15/01/2000 Jan 01/01/2010
Band 2 – Green	0.52-0.60	30	
Band 3 – Red	0.63-0.69	30	
Band 4 – NIR	0.77-0.90	30	
Band 5 - SWIR 1	1.55-1.75	30	
Band 6 – Thermal	10.40-12.50	30	
Band 7 - SWIR 2	2.09-2.35	60 (30)	
Band 8 – Panchromatic	.52-.90	15	

Landsat 8 OLI			
Bands	Wavelength (micro meter)	Resolution (m)	Date of acquisition
Band 1 - Coastal aerosol	0.43-0.45	30	March 01/12/2020
Band 2 – Blue	0.45-0.51	30	
Band 3 – Green	0.53-0.59	30	
Band 4 – Red	0.64-0.67	30	
Band 5 – NIR	0.85-0.88	30	
Band 6 - SWIR 1	1.57-1.65	30	
Band 7 - SWIR 2	2.11-2.29	60(30)	
Band 8 – Panchromatic	0.50-0.68	15	
Band 9 – Cirrus	1.36-1.38	30	
Band 10 - TIRS 1	10.6-11.19	100	
Band 11 – TIRS	11.50-12.51	100	

3.2.1 Rainfall data

Climate Hazards Group Infrared Precipitation with Station data (CHIRPS) is a 35+ year quasi-global rainfall data set. This research study has used the spatiotemporal CHIRPS rainfall data of the years 1990, 2000, 2010, and 2020 in the Google Earth engine platform. In GEE this dataset is extracted by the study area by code for processing the data.

3.2.2 Temperature data

The NEX-GDDP-CMIP6 dataset provides downscaled global climate change projections derived from the climate model runs conducted as part of the Coupled Model Intercomparison Project Phase 6 (CMIP6). This dataset covers all four of the "Tier 1" greenhouse gas emissions scenarios, known as the Shared Socioeconomic Pathways (SSPs) that were developed to support the Intergovernmental Panel on Climate Change's Sixth Assessment Report (IPCC AR6).

The dataset includes daily, bias-corrected climate change projections at a high spatial resolution, which accounts for the effects of local topography. This high-resolution climate data is valuable for assessing the impacts of climate change on processes that are sensitive to fine-scale climate variations. For the purposes of this research study, the spatiotemporal temperature data from the NEX-GDDP-CMIP6 dataset is available within the Google Earth Engine (GEE) platform and will be downloaded for analysis within the study area.

3.3 Method

Remote sensing technology has emerged as a valuable tool for water extraction due to its advantages over traditional monitoring methods. Traditional methods are often labor-intensive, time-consuming, and lack real-time capabilities. In contrast, remote sensing offers large-scale coverage, high precision, and real-time imaging, making it extensively used in the extraction of water. This technology enables efficient and accurate monitoring of water resources, facilitating timely decision-making and effective resource management (Jia et al., 2018; Lan et al., 2022)

Techniques for extracting water using data from remote sensing can be categorized into thresholding, machine learning (classifier), and deep learning techniques. Thresholding sets a specific threshold for water presence, machine learning employs algorithms to classify water and non-water pixels, and deep learning uses neural networks to automatically learn features for accurate classification. The choice of method depends on data availability, accuracy requirements, and computational resources (Frazier & Page, 2000).

3.3.1 Water indices

To identify water bodies, a variety of satellite remote sensing techniques are available, including image classification, linear unmixing, single-band thresholding, and water index (Gürsoy & Atun, 2019; Gürsoy et al., 2015). Water indices that can generate more accurate, faster, and easier information than others are better at recognizing water bodies since linear unmixing and image classification rely on human skill, involve high computation, and use single-band thresholding based on limited information (Du et al., 2014). One of the most often utilized water indices for identifying open surface water bodies is the normalized difference water index (NDWI), which was developed by McFeeters (1996). It was initially produced by Landsat's green and near-infrared (NIR) spectral bands.

In the literature, the most frequently preferred water indices are NDWI and MNDWI derived from Landsat imagery (Du et al., 2014; Liu et al., 2016; Xu, 2006). Although NDWI gains from vegetation and soil characteristics' strong NIR reflectance (Ko et al., 2015). MNDWI is better at differentiating between water and built-up areas (Du et al., 2014). Numerous studies have concluded that NDWI(Green, SWIR) is preferable to NDWI(Green, NIR) (Du et al., 2014; Ji et al., 2009), however some studies have shown the contrary (Acharya et al., 2016; Liu et al., 2016) their result showed the performance of NDWI (Green, NIR) is comparatively superior in terms of the lake expansion effect, and that as the lake size grows, the NIR region's ability to discriminate between different classes of water improves. The rationale behind this is that the quality of a water body might differ based on its color, composition, and depth (Fisher et al., 2016). This study uses NDWI methods of water body extraction method. This index determines the amount of moisture storage in vegetation that interacts with incoming solar radiation.

$$NDWI = (Green - NIR) / (Green + NIR) \qquad (McFeeters, 1996)\ (1)$$

In band format

$NDWI = (B2 - B4)/(B2 + B4)$ For Landsat 5TM and 7ETM image

$NDWI = (B3 - B5) / (B3 + B5)$ For Landsat 8OLI image

3.3.2 Thresholding

Otsu's thresholding, a global threshold selection technique, is popular due to its ease of use and efficiency. This approach assumes that an image has two classes they are background and

foreground, and that it is possible to use an ideal threshold to distinguish between the two classes. To determine the ideal threshold, an image's gray-level histogram was used (Otsu, 1979). This study used this method with NDWI for extraction of only water bodies the values of NDWI are between -1 and 1, which means positive for water bodies and negative for non-water.

Therefore this thresholding only extracts the image with an attribute value greater than or equal to 0. Thresholding is a crucial consideration to be made when using water indices to locate bodies of water. Because of the reflectance characteristics of the water, the NDWI and mNDWI measurements are usually greater than 0. Because of this, extracting water from the index image usually involves using a threshold of 0. On the other hand, Ji et al. (2009) and Xu (2006) suggest that changing the threshold value can frequently enhance the extraction outcomes.

3.3.3 Supervised classification

Supervised classification is a common method used to classify data according to established standards input features. It involves training a model on labeled data and then using that model to predict the class of new, unseen data. A collection of observations for which the categorization has already been determined is referred to as training data, or "supervised" data.

Algorithms that "learn" patterns in data to forecast a corresponding discrete class are known as supervised classification approaches. These are adaptable statistical prediction methods that are referred to as machine learning methods all together. "Computing computers to optimize a performance criterion using example data or past experience" is the definition of machine learning (Alpaydin, 2020). These methods have been effectively used for optical data by terrestrial remote sensing for a number of years, and they are increasingly being used for acoustic data seabed mapping.

Using a classification technique, all of the pixels in a satellite image can be put into a class related to the kind of land cover. To extract information based on application, a satellite image must be classified (Abburu & Golla, 2015). Thematic maps are produced by image categorization using remotely sensed images. Different elements of the earth's surface, such as vegetation, buildings, and highways, are depicted on generated maps. Not the same different image quality is produced by satellite sensors. The quality of satellite images determines classification accuracy. The process of classifying images involves four steps: preprocessing the image, choosing a feature based on

specific criteria to define the pattern, choosing a classifier, and finally evaluating the accuracy of the classification (Mahmon et al., 2015).

This study utilized the supervised classification technique of the Random Forest Classifier within the GEE platform. The Random Forest algorithm, developed by Leo Breiman and Adele Cutler, is a popular machine learning method that combines the outputs of multiple decision trees to yield a single, more robust result. The approach is widely adopted due to its ease of implementation and ability to handle both classification and regression problems effectively. The strength of Random Forest lies in its capacity to improve accuracy and manage complex datasets by leveraging the collective predictions of the ensemble of decision trees. The versatility and effectiveness of the Random Forest algorithm have contributed to its widespread adoption across various domains. For the land use/land cover mapping task in this study, the researchers collected training samples for five broad land cover class water, urban, forest, cropland, and bare land.

3.3.4 Evaluation of the impact of stressors

3.3.4.1 Land use land cover change assessment

LULC is the use of land for a variety of purposes such as agriculture, conservation, development, recreation, wildlife habitats, urban areas, or any other activity. It also encompasses the consequences of human-environment interaction in a given area, which are impacted by socioeconomic dynamics and climate change processes (Prakasam, 2010; Rawat & Kumar, 2015; Reis, 2008). LULC identification has become an essential component of sustainability research (Zhang et al., 2014) and is critical for assessing global, regional, and local environmental change (Vivekananda et al., 2021). Human population and influence on land have grown significantly over the past century (Hasan et al., 2022) and the process of changing over time is dynamic and ongoing. For good planning, sustainable development, environmental monitoring, global change, and the assessment of forest degradation, accurate and up-to-date LULC maps are crucial (Dewan & Yamaguchi, 2009; Shapla et al., 2015).

This study detects changes in LULC from different spatiotemporal land use and land cover maps which are processed by using satellite images in GEE (https://earthengine.google.com/). This work has employed the well-established supervised classification method. This classification technique aids in the grouping of LULC detected by satellite imagery. This technique involves an image

analyst using a specific algorithm to supervise the pixels; the scene's many land cover categories are explained numerically. Training locations are considered to be a typical sample of the recognized cover type. After this, the training sites are combined to create a key that can be used to interpret the numerical values of various land cover types as stated by spectral properties for a certain kind of interest (Ramachandran & Reddy, 2017). Finally, for mapping purposes, the image is exported to the drive and mapped by using the software Arc GIS 10.8.

3.3.4.2 Temperature Change Assessment

From the processed spatiotemporal temperature data interpolation is made and change is detected statically from the interpolated map to detect its influence on surface water availability. Then it is exported to drive and then the data is converted to annual temperature then the data is imported to ArcGIS 10.7.1 by x and y data then interpolation is made to categorize the areas with similar temperature distribution. Then statistically the change overall in temperature is detected. Finally detecting the change in temperature for those years and correlating it with surface water change.

3.3.4.3 Precipitation change assessment

The 30-year+ quasi-global rainfall dataset is called Climate Hazards Group InfraRed Precipitation with Station data (CHIRPS). CHIRPS generates gridded rainfall time series for trend analysis and seasonal drought monitoring by combining in-situ station data with satellite imagery with a resolution of 0.05°. The monthly mean rainfall for each year is downloaded by using this asset Id "UCSB-CHG/CHIRPS/PENTAD. Then it is exported to drive and then the data is converted to annual rainfall then the data is imported to ArcGIS 10.7.1 by x and y data then interpolation is made to categorize the areas with similar rainfall distribution then statistically the change overall in rainfall is detected. Finally detecting the change in rainfall for those years and correlating it with surface water change drastically from the interpolated rainfall map.

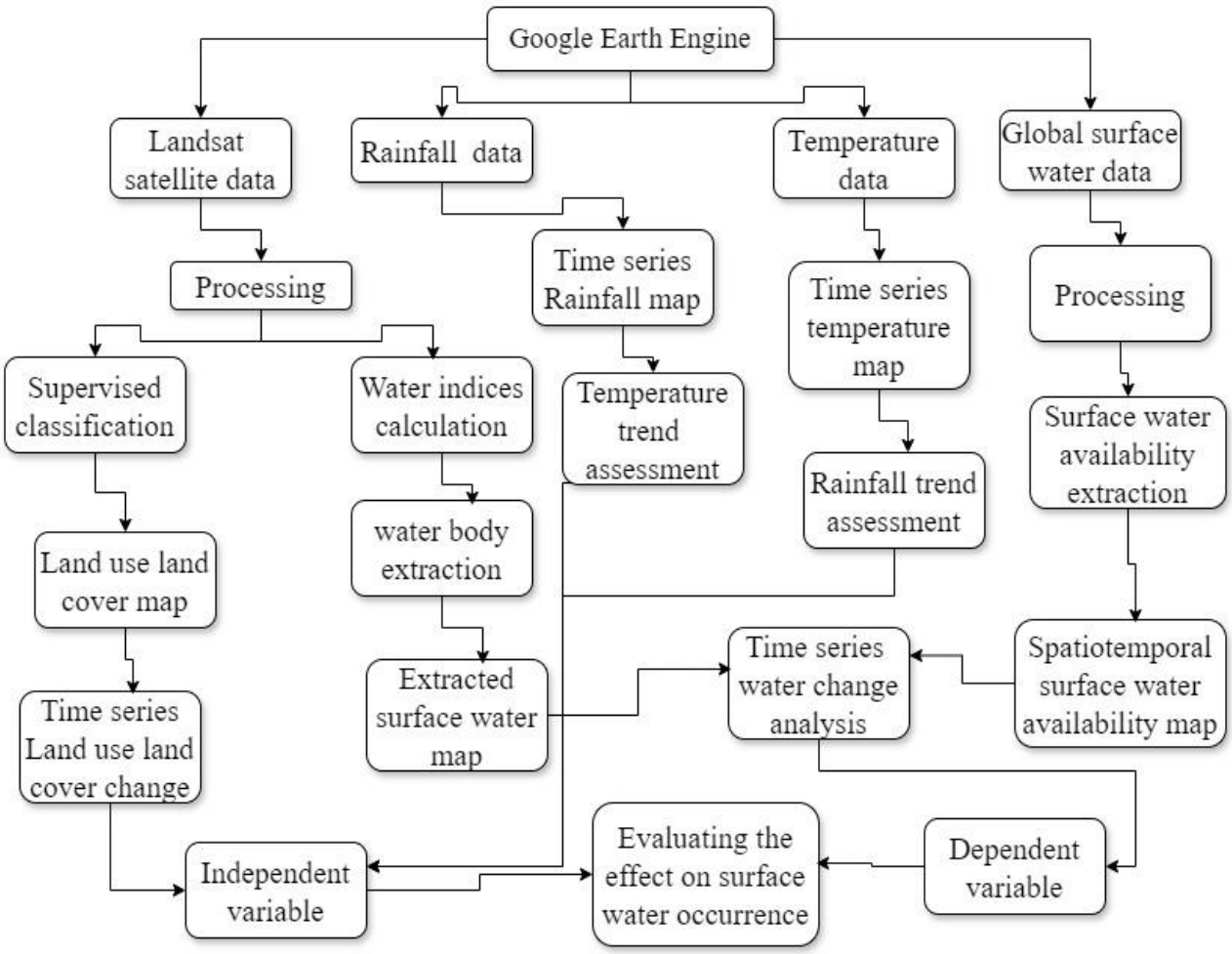

Figure 8 the methodology flow chart

CHAPTER FOUR

RESULTS

4.1 Spatiotemporal Surface Water Availability

The spatiotemporal surface water availability map of the RVL basin presents a representation of the presence and changes of surface water bodies over time. The map classifies the water availability into four distinct categories they are No observation, and these areas lack surface water data, indicating a lack of recorded water presence for the year. No Water/Lost Water Bodies, these areas previously contained surface water bodies but have experienced a decline or loss of water over the studied period. Seasonal Water Bodies are newly formed surface water bodies that emerge periodically, typically during the rainy season or other specific times of the year. Permanent Water Bodies, these areas consist of surface water bodies that are consistently present throughout the entire year, indicating a permanent source of water. By categorizing surface water into these classes, the map provides insights into the spatiotemporal variations in surface water availability for the years 1984, 2000, 2010, and 2020 in RVLB.

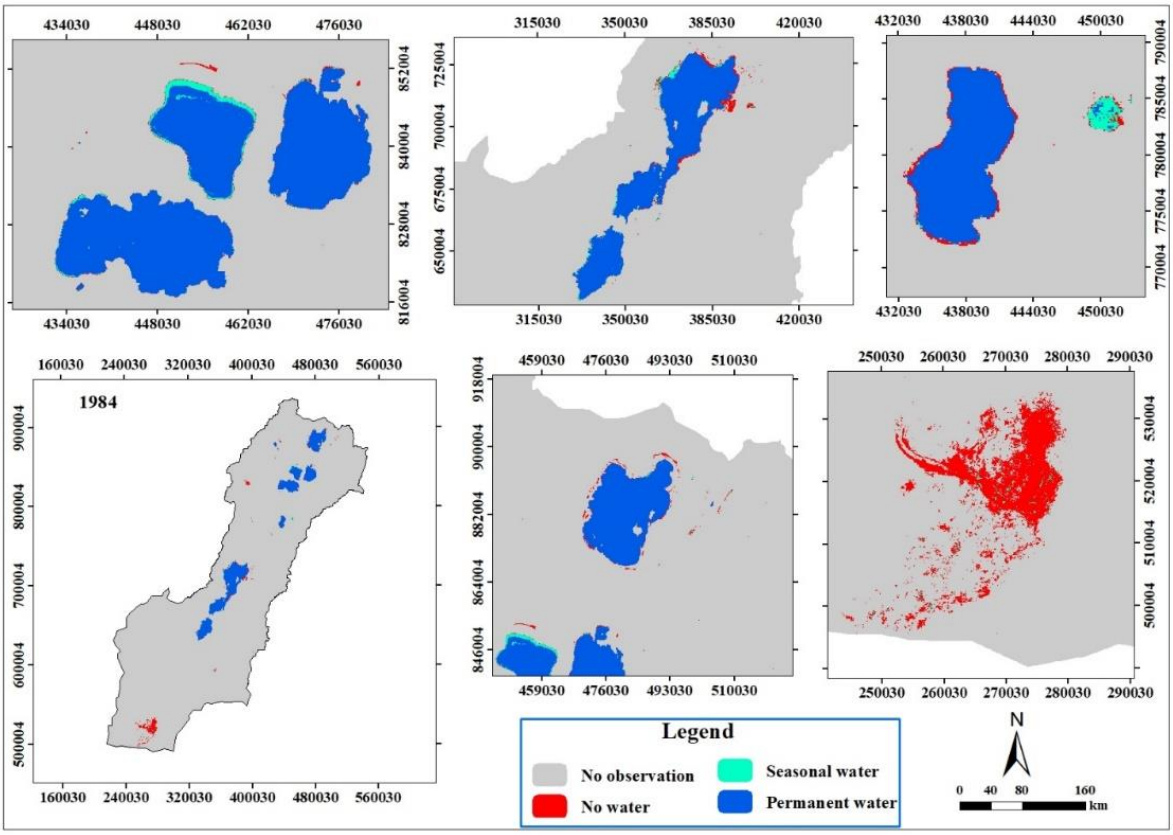

Figure 9 the surface water availability in 1984

The surface water availability assessment for the year 1984 indicates that the no observation area covers 53098 km^2, the lost water body occupies 381 km^2, the aerial extent of seasonal water bodies was 90 km^2, and the permanent water body spans 2598 km^2.

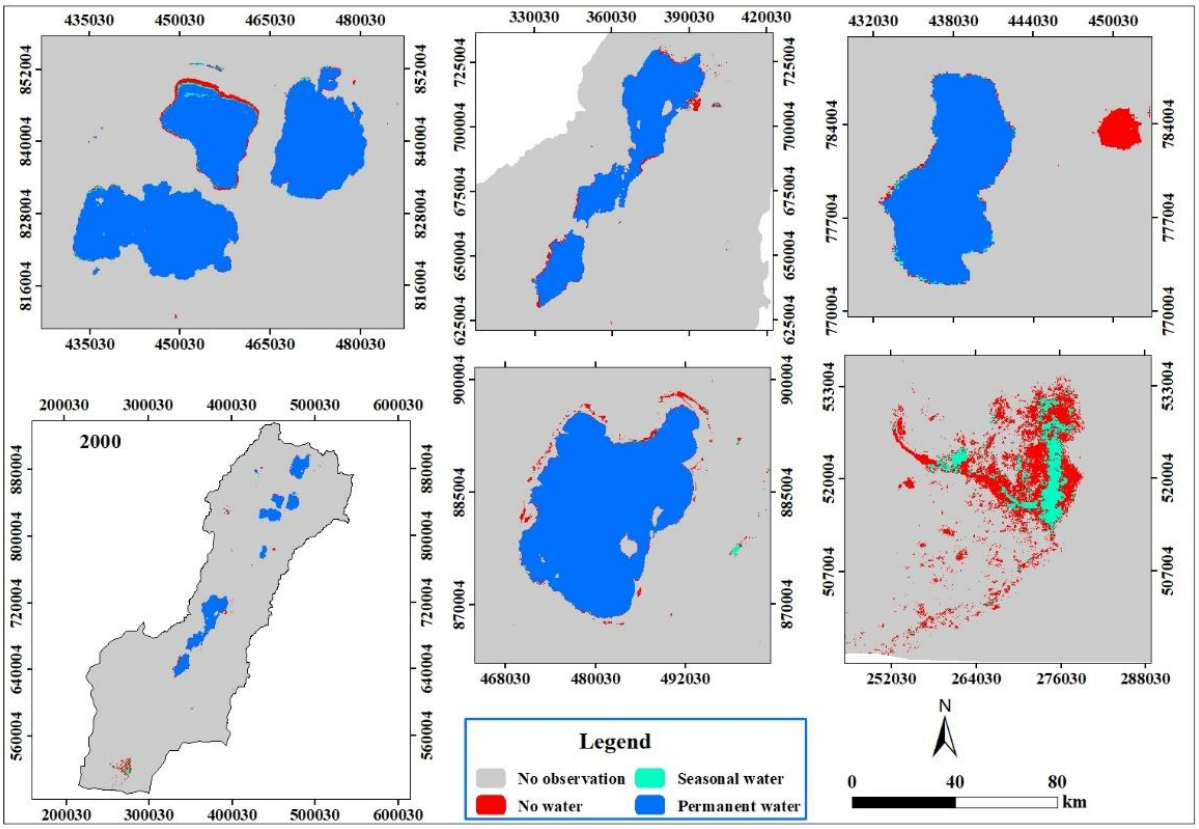

Figure 10 the surface water availability in 2000

Moving to the year 2000, the no-observation area expands to 53138 km^2, the lost water body decreases to 321 km^2, the area of seasonal water bodies remains at 100 km^2, and the permanent water body remains similar at 2608 km^2 (Fig10). In 2010, the no-observation area covered 53082 km^2, the lost water body increased to 384 km^2, the area of seasonal water bodies increased to 148 km^2, and the permanent water body decreased slightly to 2552 km^2 (Fig 11).

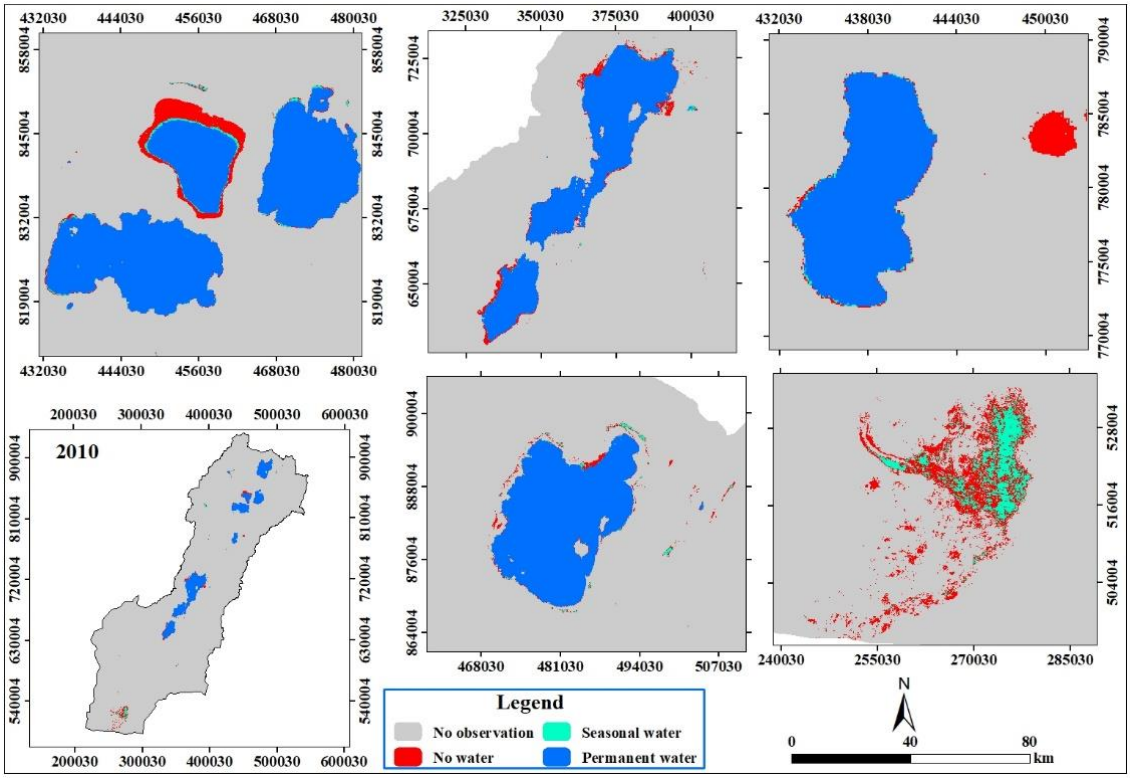

Figure 11 the surface water availability in 2010

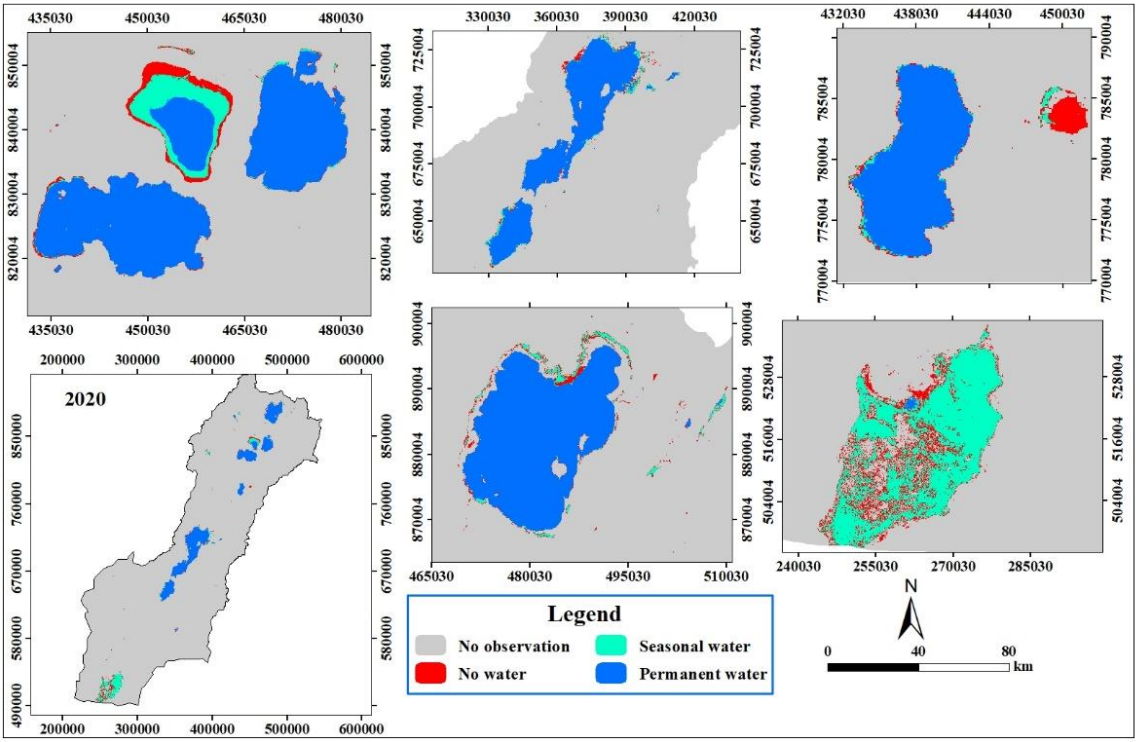

Figure 12 the surface water availability in 2020

Finally, in 2020, the no-observation area contracts to 52513 km^2, the lost water body reduced to 343 km^2, the area of seasonal water bodies significantly expanded to 725 km^2, and the permanent water body remained relatively stable at 2586 km^2 (Fig 12). Surface water availability in the RVL basin experiences varying fluctuations from year to year. Analyzing the changes in surface water from 1984 to 2000 reveals a combination of positive and negative trends. During this period the No observation which, is the area with no recorded surface water expanded by 40 km^2, No Water/Lost Water Bodies the area of no water decreased by 60 km^2, with a 58 km^2 increase in the area of seasonal water bodies, suggesting the formation of additional surface water bodies during specific seasons. The area of permanent water bodies also increased by 10 km^2.

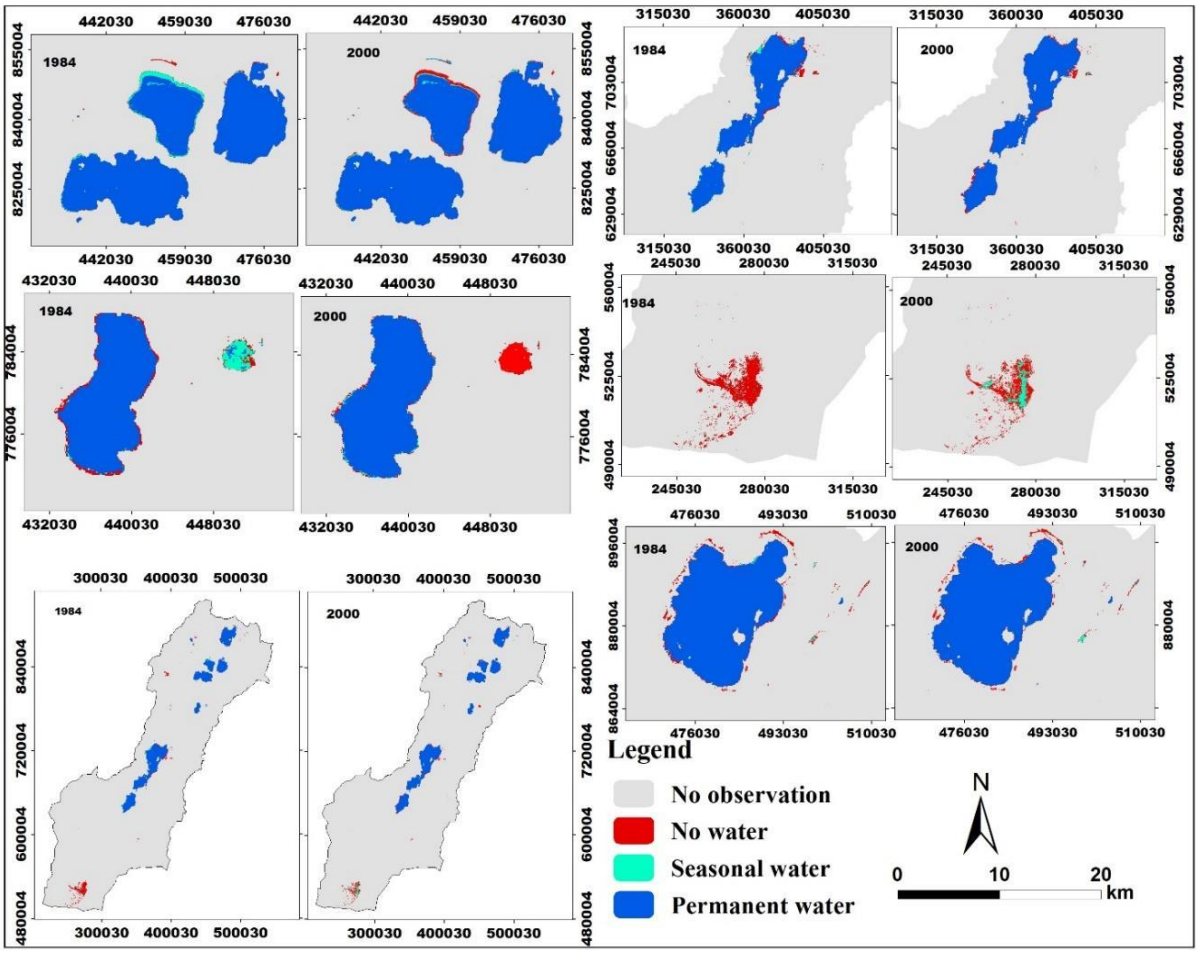

Figure 13 the visual change of surface water between years 1984 and 2000

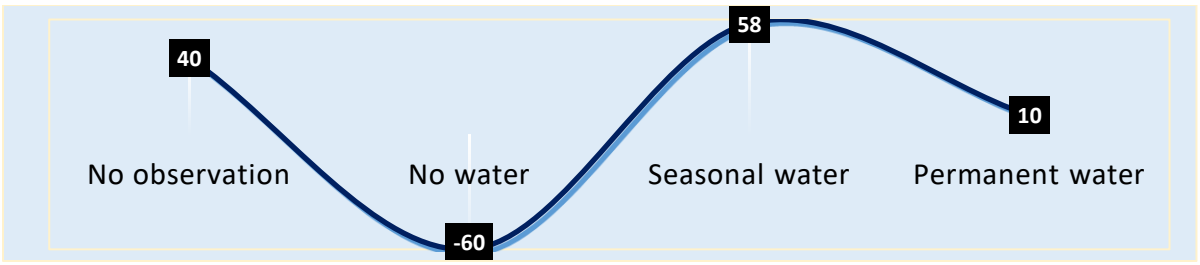

Figure 14 the change of surface water availability between 1984 to 2000

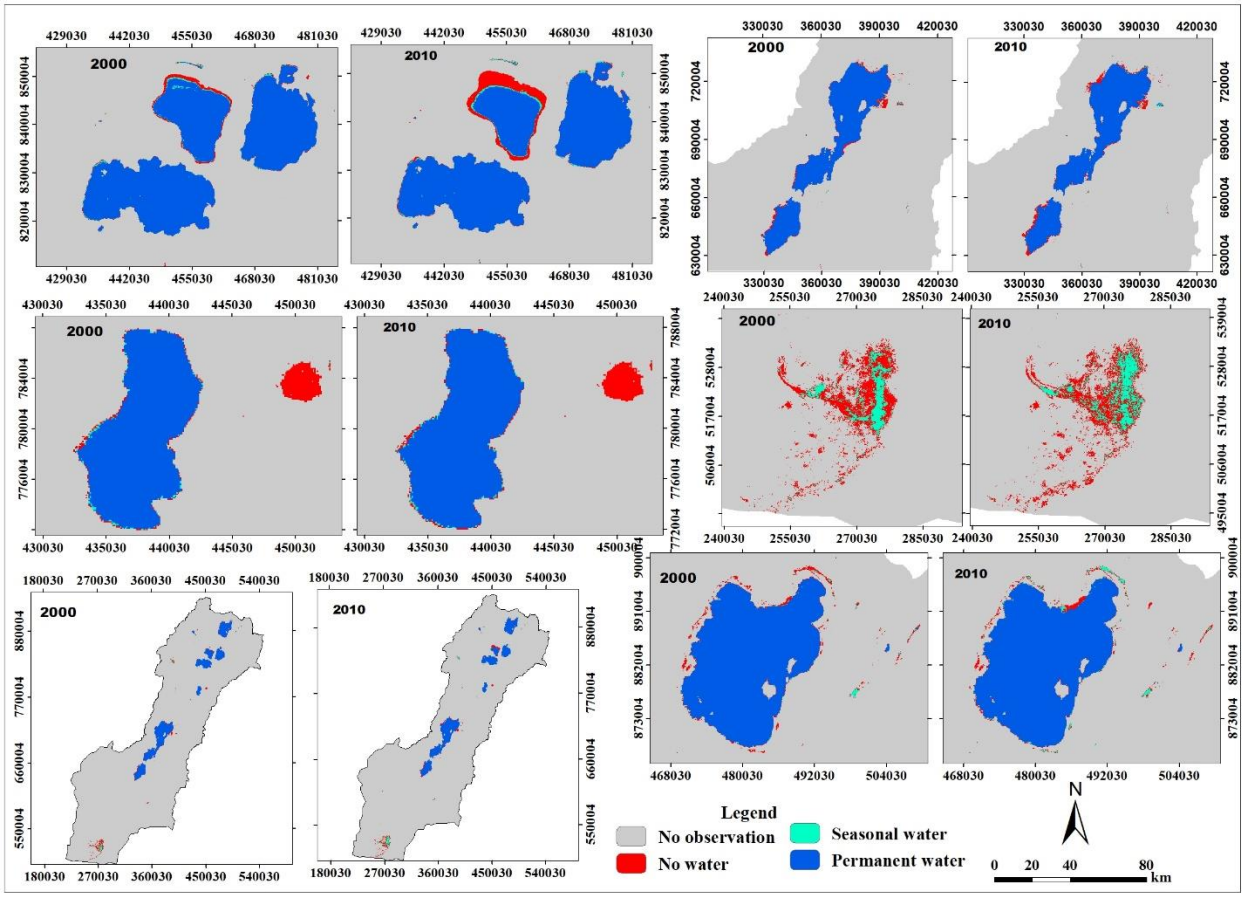

Figure 15 the surface water availability change between 2000 to 2010

The surface water availability between year 2000 to 2010 shows that the decrement of the No observation by 56 km^2 ,the expansion of No water areas by 63 km^2 , the expansion of seasonal water by 48 km^2 and the decrement of permanent water by 56 km^2 (Fig 15).

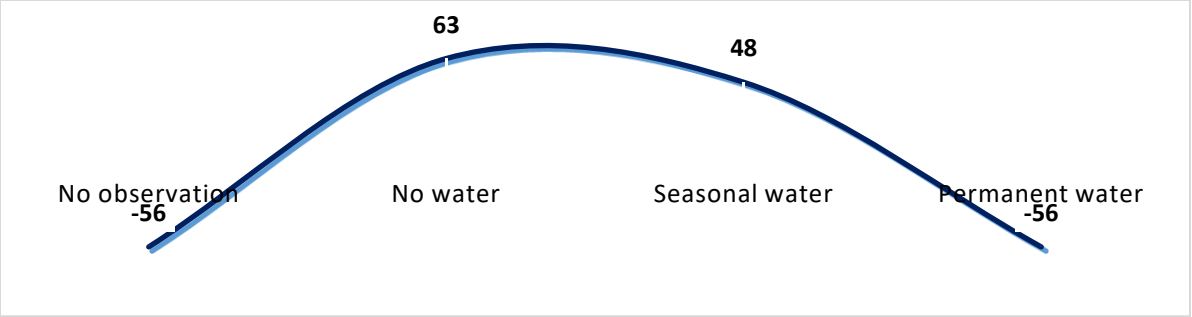

Figure 16 the surface water availability change of 2000-2010

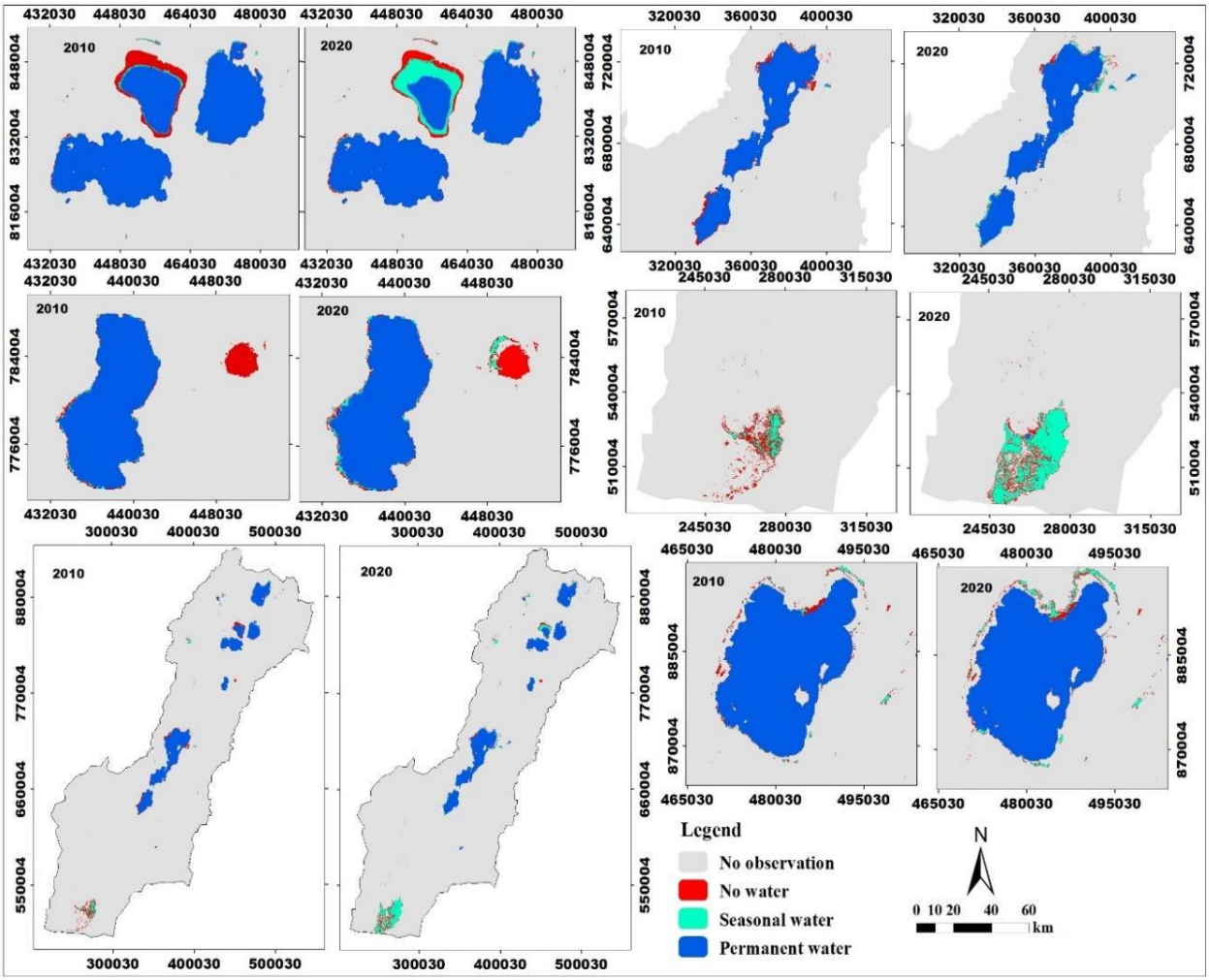

Figure 17 the visual change of surface water between years 2010 and 2020

Between 2010 and 2020, an analysis of surface water availability reveals several changes. The replacement of lost water bodies by new seasonal waters resulted in a significant increase of 577 km^2 in seasonal waters. Additionally, the negative change in the no observation areas indicates a

decrease of 569 km^2, suggesting improved monitoring and observation of surface water. There was also a decrease of 41 km^2 in lost water bodies, On the other hand, the positive change in permanent water classes shows an increment of 34 km^2 in water bodies that persist throughout the year. These changes reflect the dynamic nature of surface water availability during the specified time period

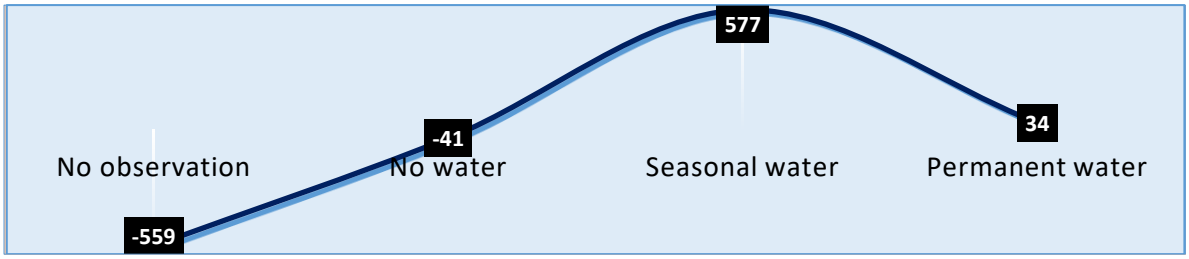

Figure 18 Surface water availability change from 2010 to 2020

Table 3 the surface water availability spatiotemporally

	Year				
Surface water availability	1984 area (km^2)	2000 area (km^2)	2010 area (km^2)	2020 area (km^2)	Description of the classes
No observation	53098	53138	53082	52513	this class shows the areas that have no surface water data record in the year
No water	381	321	384	343	no water is the surface water record that has the surface water before but now those water bodies are lost
Seasonal water	90	100	148	725	seasonal water is the surface water that has new surface water bodies that emerge seasonally, especially during the rainy season
Permanent water	2598	2608	2552	2586	permanent water is the surface water record that shows the surface water bodies that stay permanently for a year days

4.2 The spatiotemporal change in lakes

Lake Abijata

Abijata Lake, located within the RVLB, has experienced a consistent decline in its aerial extent over the years. However, in 2023, there was a significant increase in its size, indicating a positive change. Analyzing the lake's aerial extent for individual years, it was found that in 1984, the lake covered an area of 183.46 km^2. By 1990, the extent had reduced to 120.49 km^2. In 2000, it expanded to 163.26 km^2, followed by a decrease to 119.95 km^2 in 2010. The extent further declined to 76.22 km^2 at an unspecified point in 2020. However, in the current year, 2023, the lake experienced a substantial increase in its aerial extent, reaching 154.67 km^2 (Fig 17).

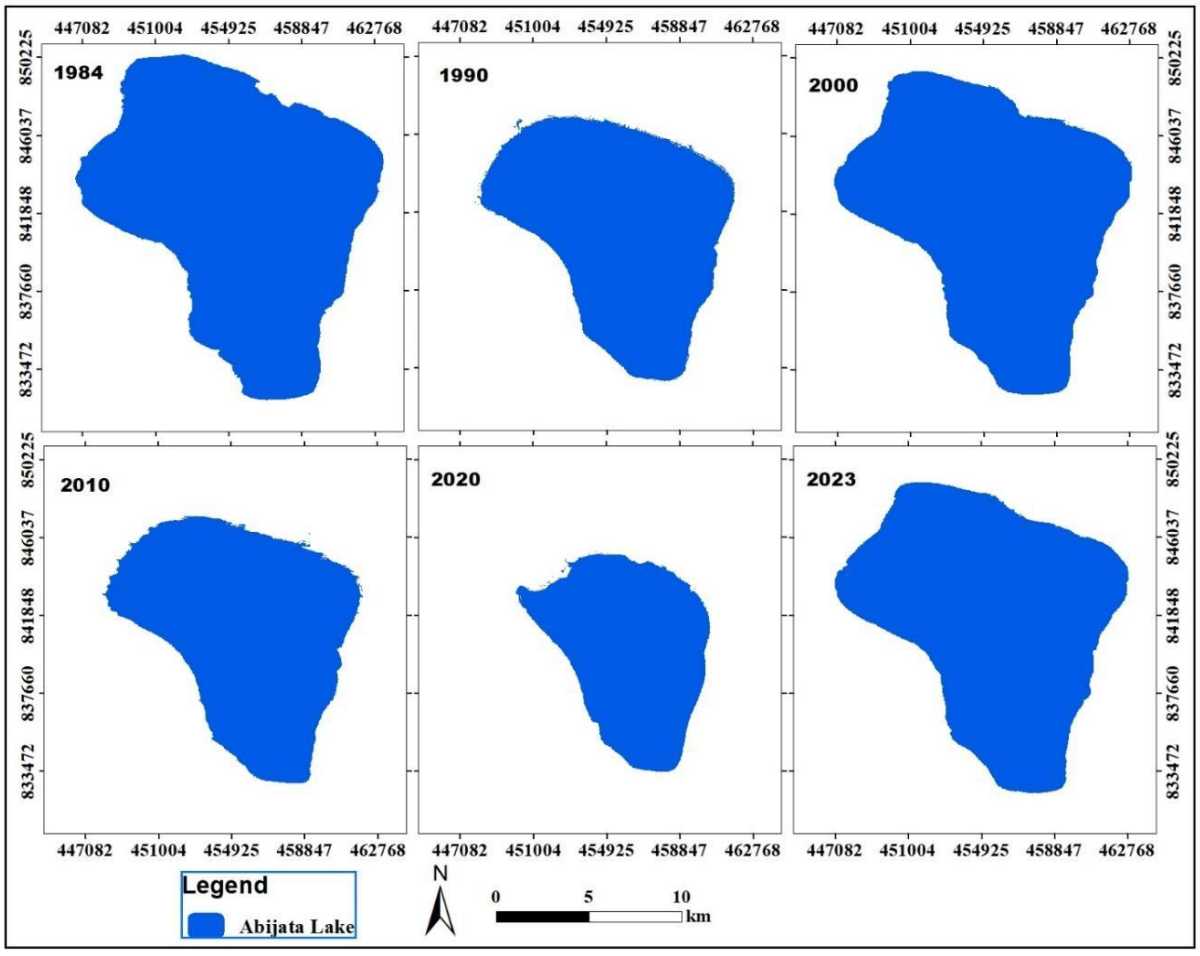

Figure 19 Spatiotemporal Abijata lake fluctuation during 1984–2023

Lake Langano

Lake Langano ranked as the fourth largest lake in the RVLB, has exhibited relatively consistent areal extent over the years. Based on the assessment results, in 1984, the lake covered an area of 229.70 km^2. By 1990, the extent slightly increased to 229.89 km^2. In 2000, the area of the lake measured 229.38 km^2. A slight decrease was observed in 2010, with the lake's area measuring 227.10 km^2. By 2020, the area expanded to 228.34 km^2. Finally, in the year 2023, the aerial extent of Lake Langano decreased to 226.75 km^2 (Fig18).

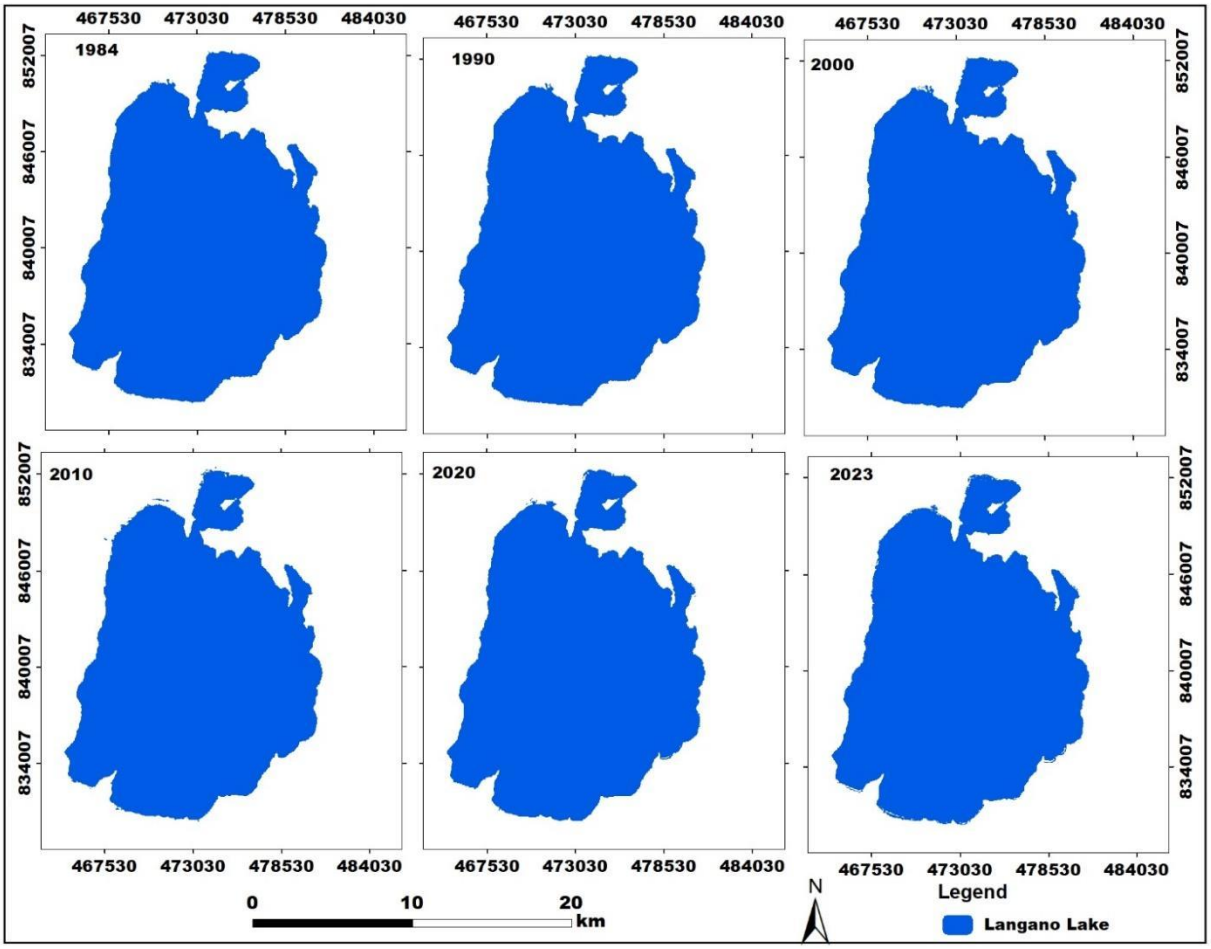

Figure 20 Spatiotemporal Langano lake fluctuation during 1984–2023

Lake Ziway

Ziway, the second largest lake in the RVLB, has exhibited fluctuating areal extent from 1984 to 2023. Analyzing the lake's area individually, in 1984, Ziway covered an extent of 409.30 km^2. By the following year, 1990, the areal extent of the lake increased slightly to 411.33 km^2. In 2000, the area expanded further to 414.21 km^2. However, in 2010, there was a slight decrease, with the lake's

area measuring 413.66 km^2. By 2020, the area of Ziway Lake reached 414.07 km^2. Finally, in the year 2023, the lake's overall extent increased to 415.68 km^2 (Fig 19). These findings highlight the fluctuating nature of Ziway Lake's size over time, with both increases and decreases in its areal extent observed during the assessed period.

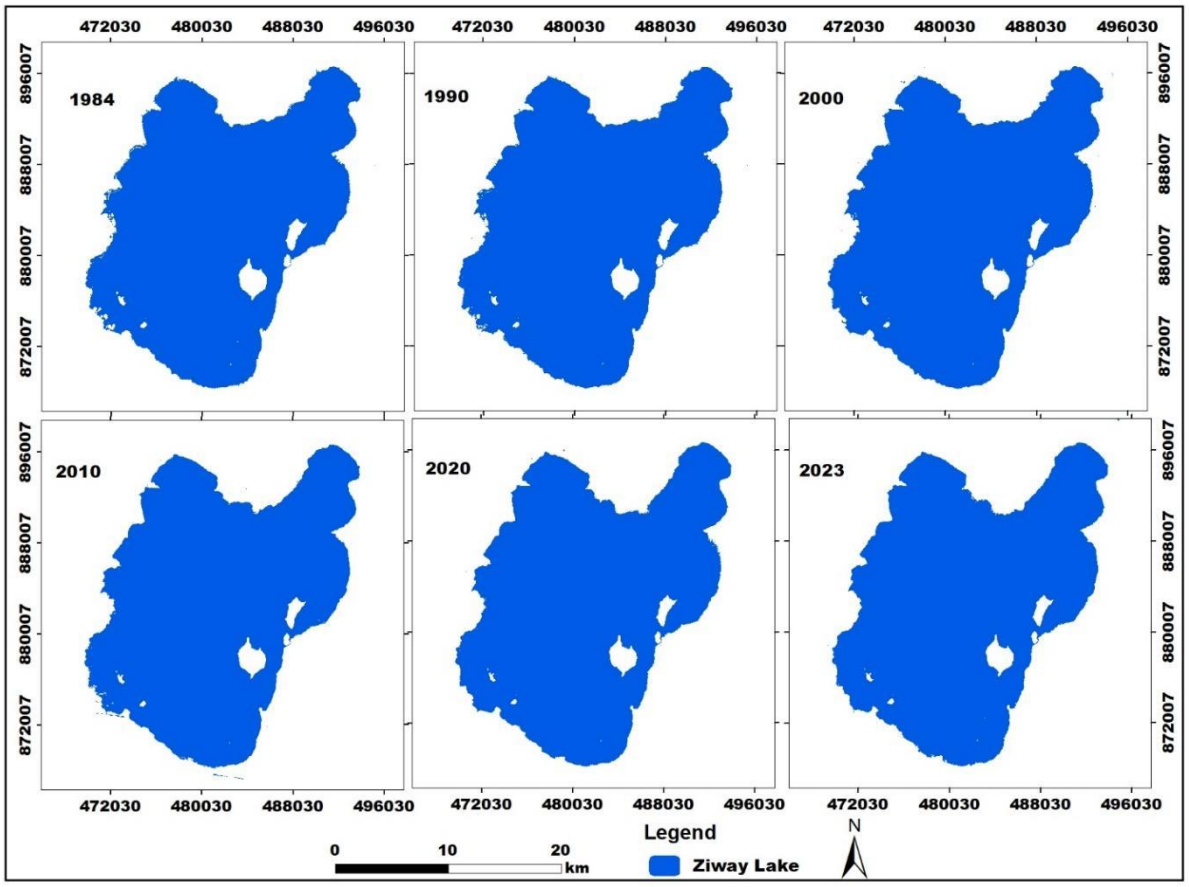

Figure 21 spatiotemporal Ziway Lake fluctuation from 1984 to 2023

Lake Shala

Lake Shala, located in the RVLB, has experienced fluctuations in its aerial extent over the years. Analyzing individual years, in 1984, the lake covered an area of 307.16 km^2. By 1990, the aerial extent slightly increased to 307.27 km^2. However, in 2000, there was a decline, with the lake's area measuring 305.94 km^2. In 2010, the aerial extent further decreased to 303.09 km^2. By 2020, the area of Lake Shala reduced to 300.27 km^2. Finally, in 2023, the lake's area decreased to 292.10 km^2 (Fig 20).

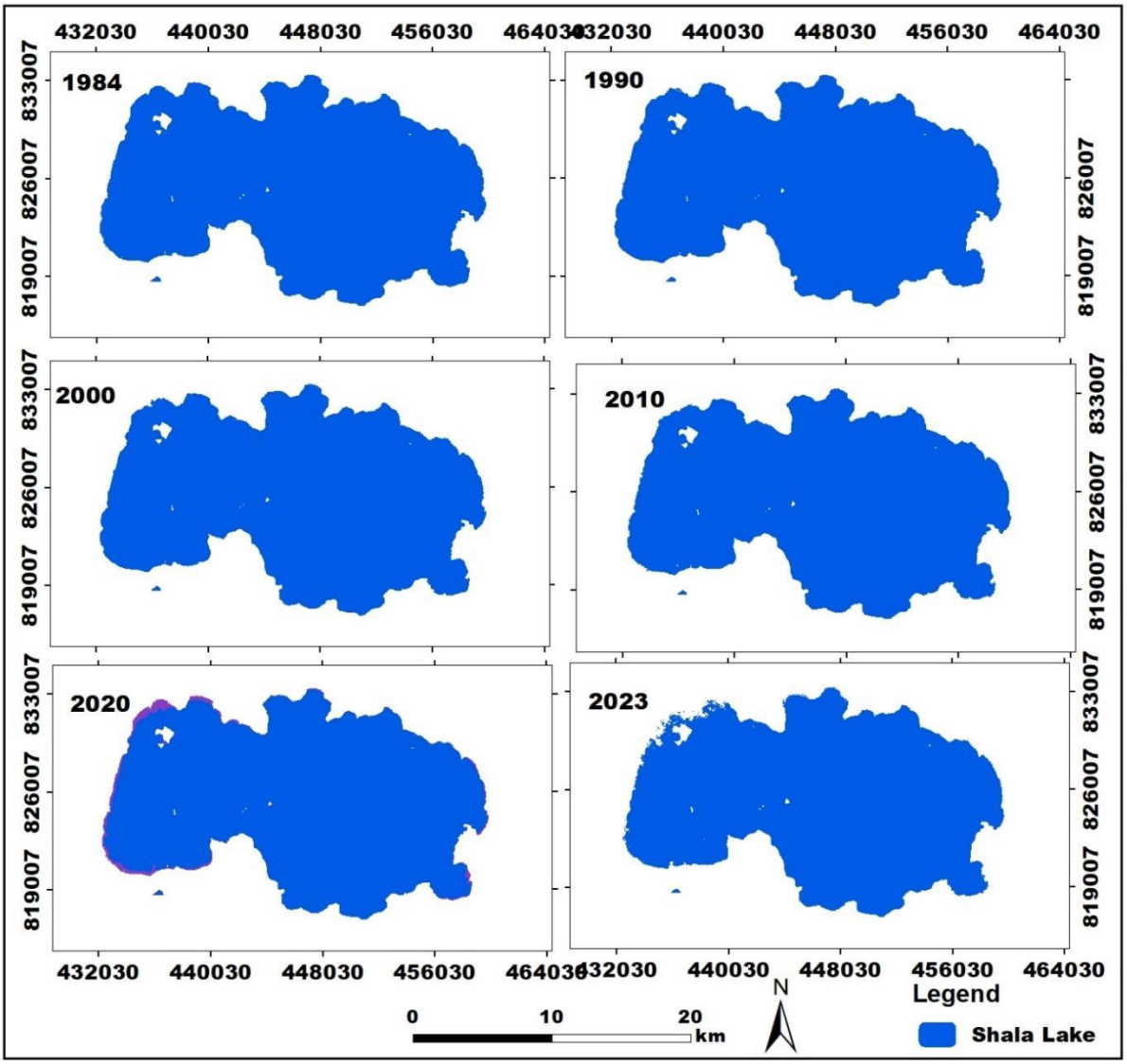

Figure 22 Spatiotemporal Langano lake fluctuation from 1984 to 2023

Lake Hawassa

Hawassa Lake, located near Hawassa town, has exhibited spatiotemporal fluctuations in its areal extent from 1984 to 2023. In 1984, the lake covered an area of 87.06 km^2. By 1990, the areal extent increased to 88.26 km^2. In 2000, the lake's area expanded further to 92.58 km^2. However, in 2010, there was a slight decrease, and the lake's area measured 91.74 km^2. By 2020, the lake's area remained relatively stable at 91.89 km^2. Finally, in 2023, the areal extent of Hawassa Lake decreased to 90.69 km^2 (Fig 21).

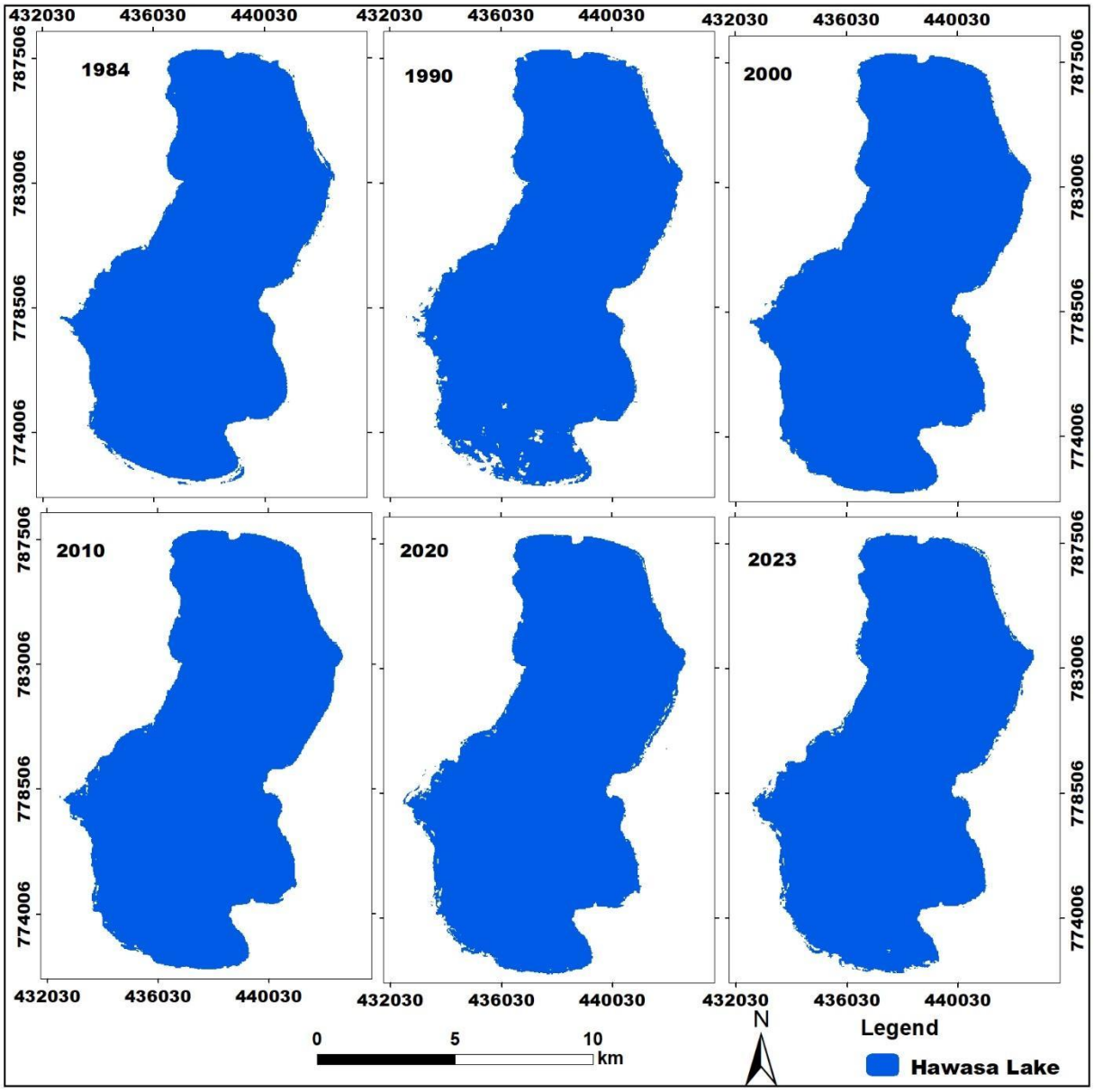

Figure 23 Spatiotemporal Hawassa lake fluctuation from 1984 to 2023

Lake Chamo

Lake Chamo, the third largest lake in the RVLB, has displayed fluctuations in its areal extent from 1984 to 2023.In 1984, the lake covered an area of 280.64 km^2. By 1990, the areal extent expanded significantly to 322.82 km^2. However, in 2000, there was a decrease, and the lake's area measured 313.99 km^2. In 2010, the aerial extent further decreased to 299.48 km^2. By 2020, the lake's area

experienced a recovery and expanded to 313.14 km^2. Finally, in 2023, the areal extent of Lake Chamo reached its highest point at 332.64 km^2 (Fig 22).

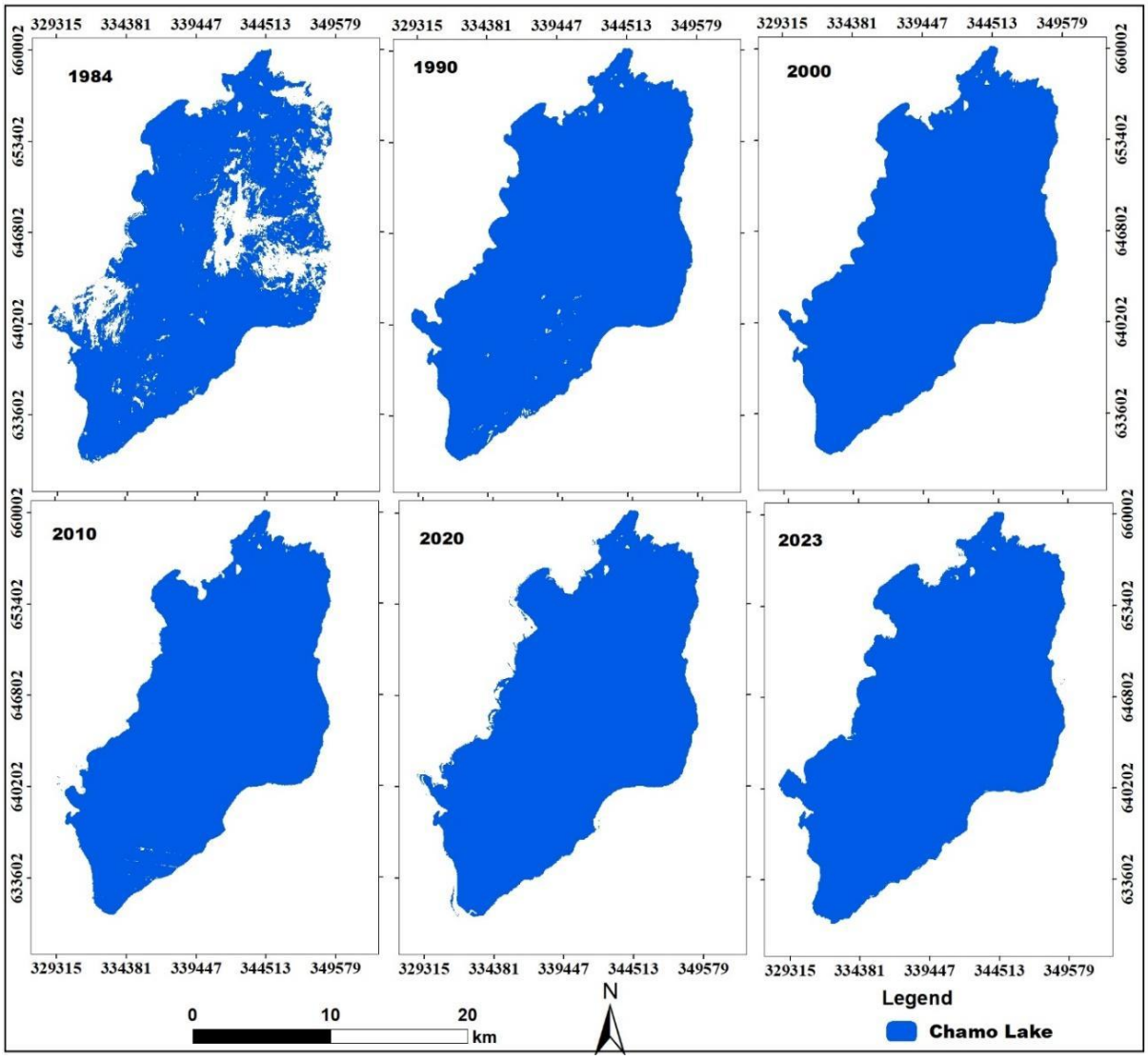

Figure 24 Spatiotemporal Chamo lake fluctuation from 1984 to 2023

Lake Abaya

Lake Abaya, the largest lake in the RVLB in terms of extent, has exhibited fluctuations in its areal extent from 1984 to 2023. In 1984, the lake had a relatively small areal extent of 786.64 km^2. However, by 1990, it significantly increased to 1058.31 km^2. In 2000, the areal extent further expanded to 1084.83 km^2. In 2010, there was a slight decrement, and the lake's area measured

1078.52 km^2. By 2020, the areal extent decreased to 1184.83 km^2. Finally, in 2023, it showed some increment and reached 1170.30 km^2 (Fig 23).

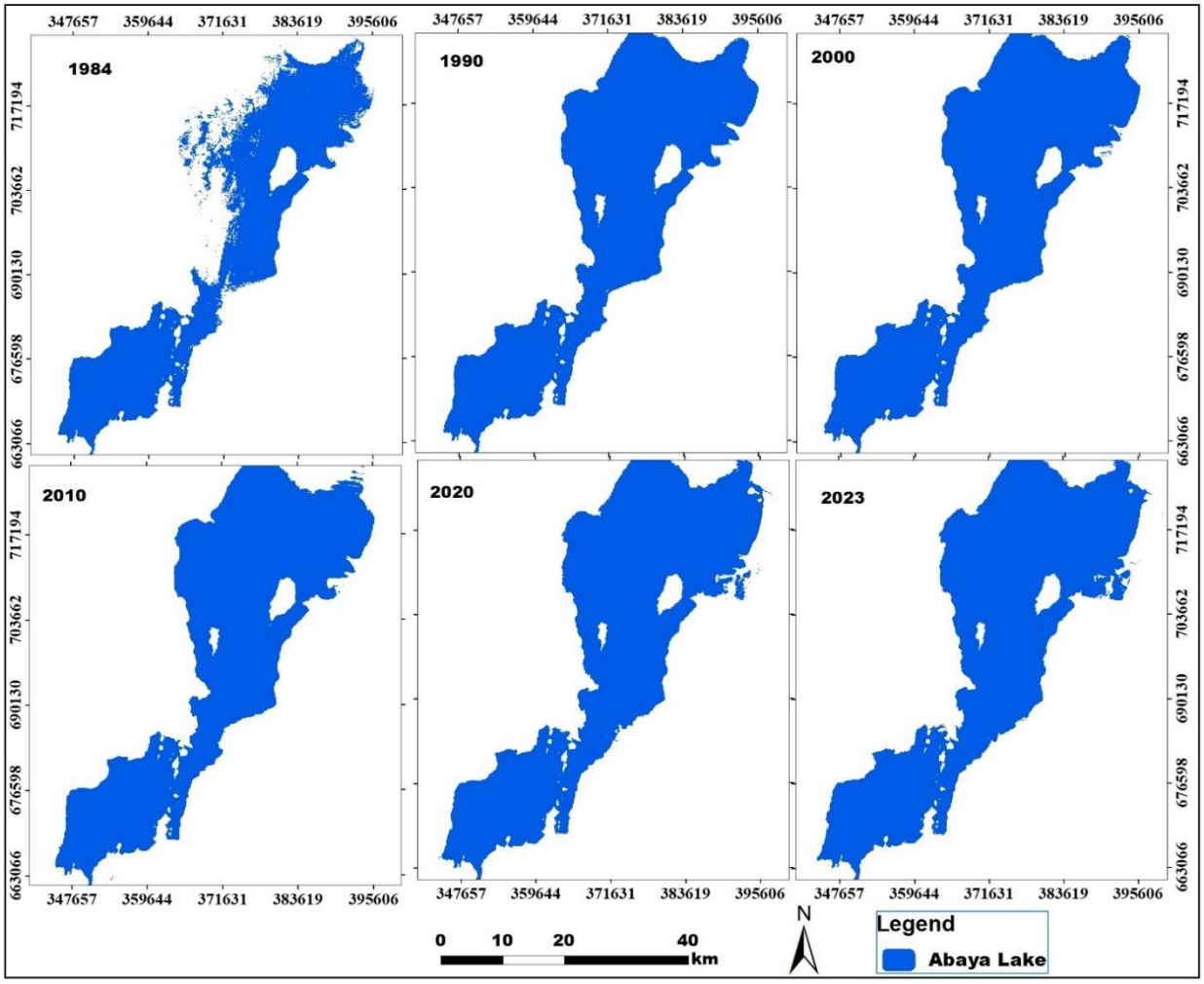

Figure 25 Spatiotemporal Abaya lake fluctuation from 1984 to 2023

The Lakes in the RVLB exhibit varying degrees of fluctuation over time. To assess the specific fluctuations observed in each lake, Lake Abijata shows fluctuations in its areal extent over the mentioned time periods From 1984 to 1990, the lake experienced a decrease of 62.97 km^2, Between 1990 and 2000, there was an increase of 42.77 km^2 in the lake's area, From 2000 to 2010, the lake's areal extent decreased by 43.31 km^2, Between 2010 and 2020, there was a further decrease of 43.73 km^2 in the lake's area, From 2020 to 2023, Lake Abijata exhibited an expansion, with its areal extent increasing by 78.45 km^2.

Lake Chamo experienced fluctuations in its areal extent during the specified time periods: From 1984 to 1990, the lake's area increased by 42.18 km^2, Between 1990 and 2000, there was a decrease of 8.83 km^2 in the lake's area, From 2000 to 2010, the lake's areal extent decreased by 14.51 km^2, Between 2010 and 2020, there was an increase of 13.66 km^2 in the lake's area, From 2020 to 2023, Lake Chamo further expanded, with its areal extent increasing by 19.50 km^2.

Lake Abaya experienced significant variations in its surface area throughout the specified periods. Between 1984 and 1990, the lake experienced a significant increment of 271.67 km^2, From 1990 to 2000, there was a further increase of 26.52 km^2 in the lake's area, Between 2000 and 2010, the lake's areal extent decreased by 6.31 km^2, From 2010 to 2020, there was a substantial increase of 106.31 km^2 in the lake's area, Between 2020 and 2023, Lake Abaya showed a decrement once again, with its areal extent by 14.53 km^2.

Lake Hawassa exhibited notable changes in its surface area during the specified periods: From 1984 to 1990, there was an increase of 1.20 km^2 in the lake's area, between 1990 and 2000, there was a further increase of 4.32 km^2 in the lake's area, from 2000 to 2010, and there was a decrease of 0.84 km^2 in the lake's area, Between 2010 and 2020, there was a modest increase of 0.15 km^2 in the lake's area, From 2020 to 2023, there was a subsequent decrease of 1.20 km^2 in the lake's area.

Lake Shala experienced notable fluctuations in its surface area over the mentioned time periods: From 1984 to 1990, there was a decrease of 0.11 km^2 in the lake's area, Between 1990 and 2000, there was a further decrease of 1.33 km^2 in the lake's area, From 2000 to 2010, there was a decrease of 2.85 km^2 in the lake's area, Between 2010 and 2020, there was a decrease of 2.82 km^2 in the lake's area. From 2020 to 2023, there was a subsequent decrease of 8.17 km^2 in the lake's area.

Lake Ziway exhibited notable fluctuations in its surface area during the specified time periods: From 1984 to 1990, there was an increment of 2.03 km^2 in the lake's area. Between 1990 and 2000, there was a further increment of 2.88 km^2 in the lake's area, From 2000 to 2010, there was a decrease of 0.55 km^2 in the lake's area, Between 2010 and 2020, there was an increment of 0.41 km^2 in the lake's area, From 2020 to 2023, there was a subsequent increment of 1.61 km^2 in the lake's area.

Overall, the lakes in the Rift Valley Lakes basin demonstrate varying levels of fluctuation, with some experiencing significant changes in their areal extent over the examined time periods.

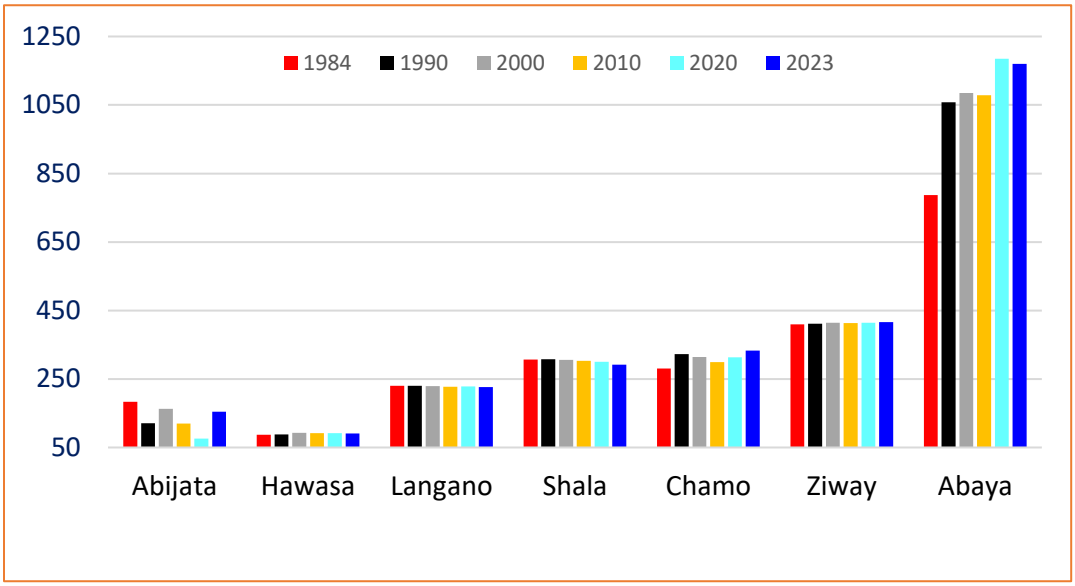

Figure 26 the change in the major lakes from 1984 to 2023

Table 4 the overall lake area in km2

Lake area (km^2)							
Year	Ziway	Abaya	Chamo	Langano	Shala	Abijata	Hawasa
1984	409.30	786.64	280.64	229.70	307.16	183.46	87.06
1990	411.33	1058.31	322.82	229.89	307.27	120.49	88.26
2000	414.21	1084.83	313.99	229.38	305.94	163.26	92.58
2010	413.66	1078.52	299.48	227.10	303.09	119.95	91.74
2020	414.07	1184.83	313.14	228.34	300.27	76.22	91.89
2023	415.68	1170.30	332.64	226.75	292.10	154.67	90.69

4.1.3 The spatiotemporal rainfall change

The rainfall map in this study provides a description of the distribution of rainfall across different sub-basins within the Rift Valley Lakes basin. It serves as a valuable tool for understanding the variations in rainfall patterns over a decade. In 1990, the study recorded the minimum amount of rainfall at 801mm in the Amaa Guracha sub basin. On the other hand, the Gidabo sub basin experienced the highest rainfall distribution of 1099mm. The rainfall amounts in the remaining

sub basins fell within this range. This information highlights the spatial variability in rainfall across the basin during that year. Moving forward to the year 2000, there was a slight decrease in rainfall compared to 1990. The Segen watershed sub basin recorded the lowest rainfall distribution at 698mm, while the hawassa sub basin experienced the highest rainfall amount at 1091mm. These values indicate the changes in rainfall patterns over the decade, with some sub basins experiencing reduced rainfall and others maintaining relatively higher amounts (Fig 25).

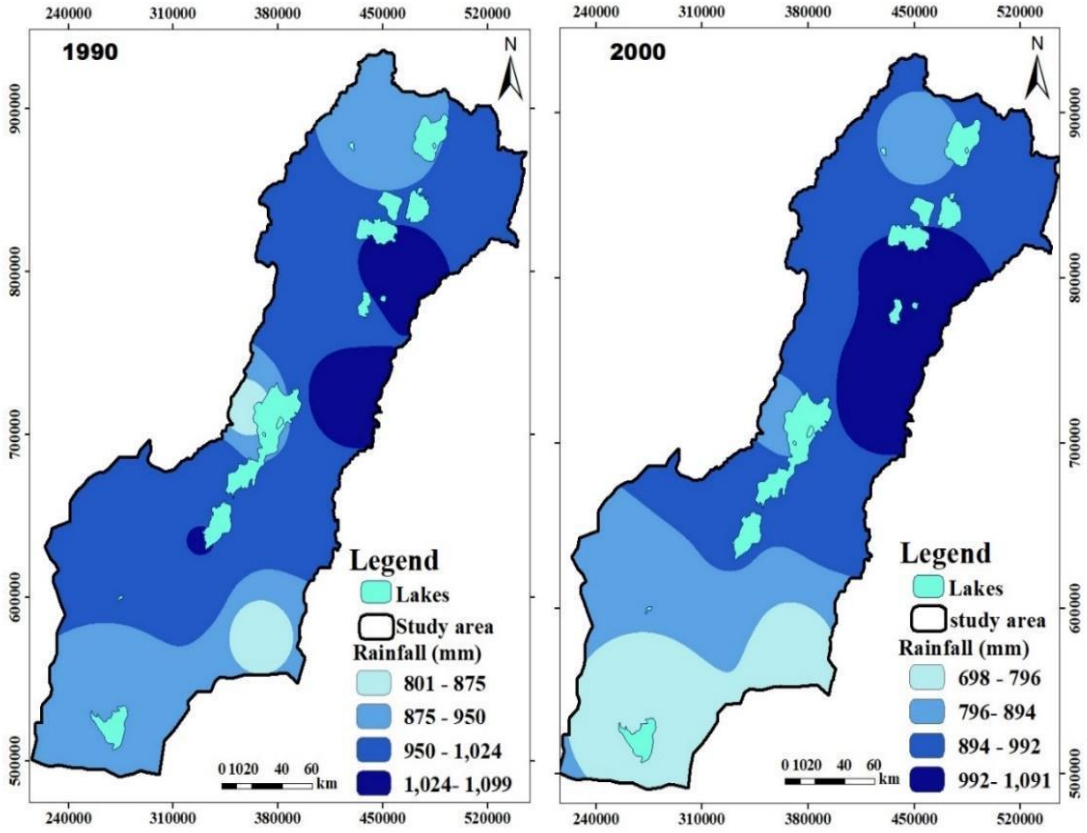

Figure 27 Rainfall map of 1990 and 2000

In comparison to previous years, the rainfall distribution in 2010 and 2020 showed an increase. In 2010, the Gidabo sub-basin had the highest recorded rainfall distribution, measuring 1332 mm. Conversely, the Segen watershed sub-basin experienced lower rainfall amounts, with a reading of 948 mm. This indicates the spatial variability in rainfall across the basin during that year. Similarly, in 2020, the Gidabo sub-basin maintained its position with the highest rainfall distribution, recording 1342 mm. On the other hand, the Segen watershed sub-basin had the lowest rainfall distribution, measuring 987 mm. These values suggest that the rainfall patterns in 2020 were higher compared to previous years, although there were still variations among the sub-basins (Fig 26).

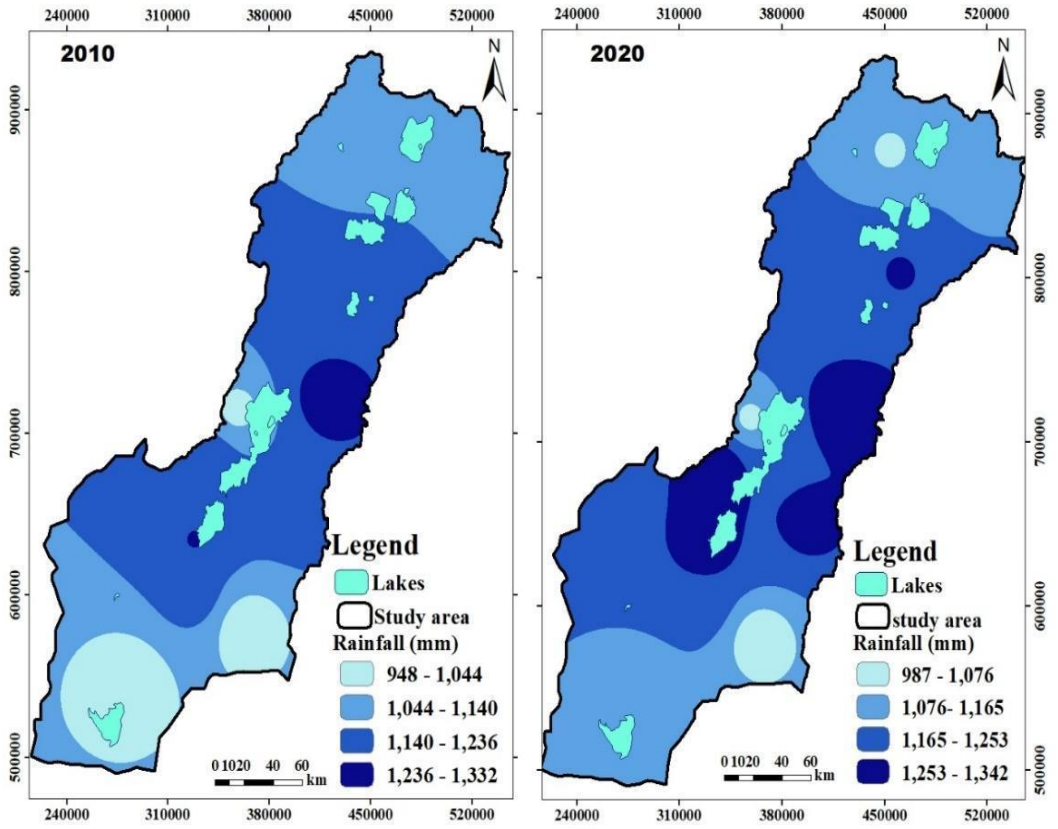

Figure 28 the rainfall map of 2010 and 2020

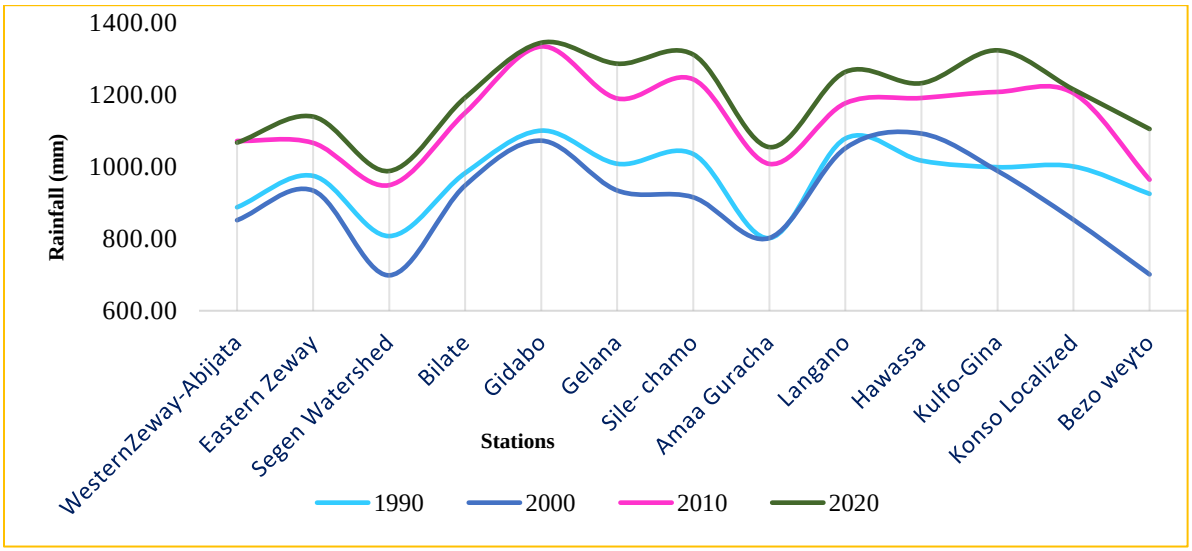

Figure 29 Rainfall distribution for each year around the stations

4.1.4 Temperature change

The time series temperature map in this study provides a visual representation of temperature distribution across different sub-basins within the Rift Valley Lakes basin. In 1990, the Eastern Ziway sub-basin recorded the highest annual temperature of 23°C. On the other hand, the Bezo Weyto sub-basin had the lowest annual temperature reading of 16°C. Moving to the year 2000, the Eastern Ziway sub-basin experienced the lowest temperature reading of 16°C, while the Bezo Weyto sub-basin recorded the highest annual temperature of 23°C. Interestingly, the temperature variation between 1990 and 2000 was relatively small, and the sub-basins with both the lowest and highest temperature readings remained the same (Figure 28).

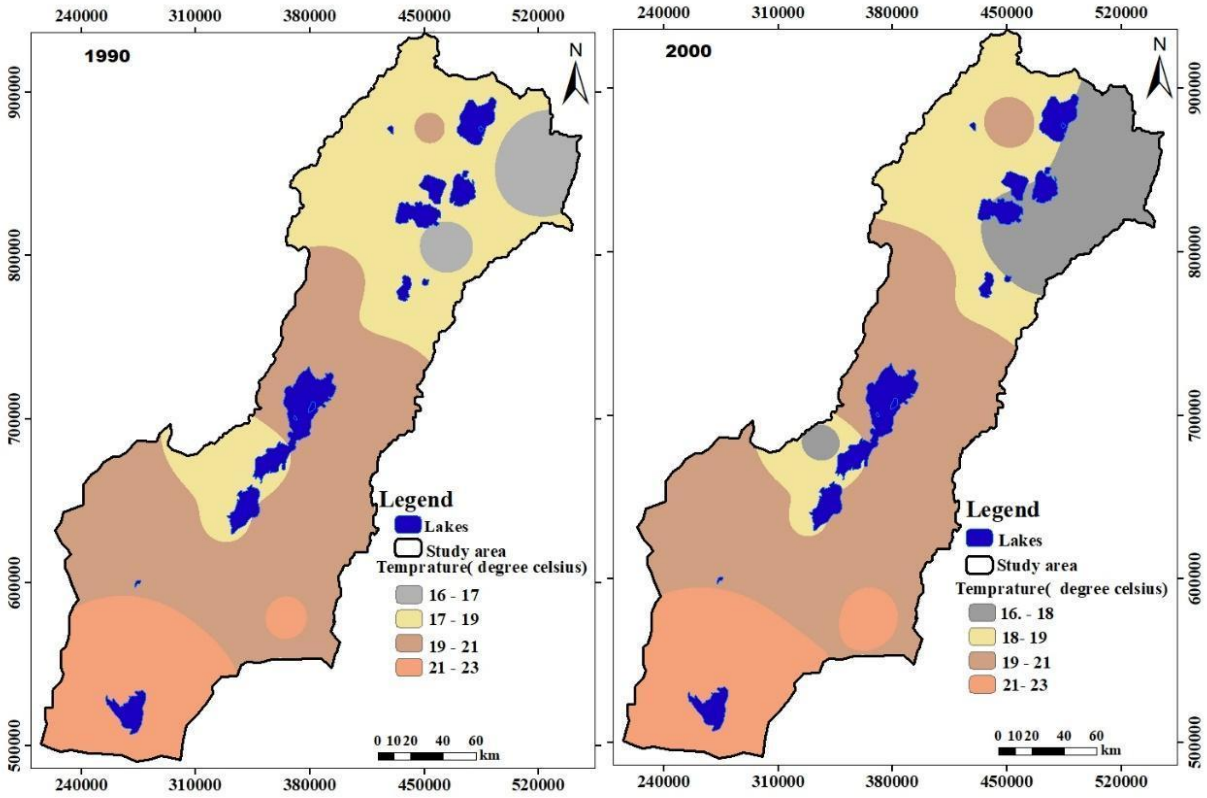

Figure 30 the temperature map of year 1990 and 2000

In 2010, the Bezo Weyto sub basin recorded the highest annual temperature of 23°C, while the western Ziway sub basin had the lowest temperature reading of 16°C. Similarly, in 2020, both the Bezo Weyto and western Ziway sub basins registered the highest temperature readings. The lowest temperature reading of 16°C was recorded in the Kulfo Gina sub basin. It is worth noting that,

apart from the eastern Ziway and western Ziway sub basins, the remaining sub-basins exhibited relatively similar temperature readings during both 2010 and 2020 (Figure 29).

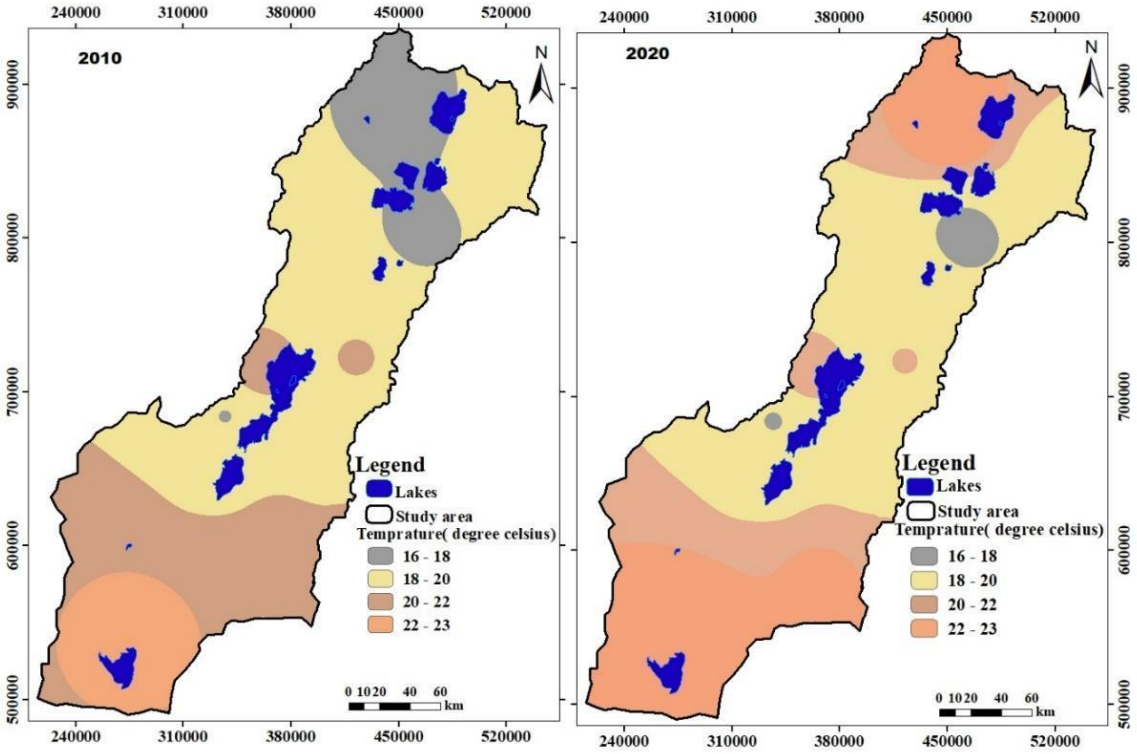

Figure 31 the temperature map of year 2010 and 2020

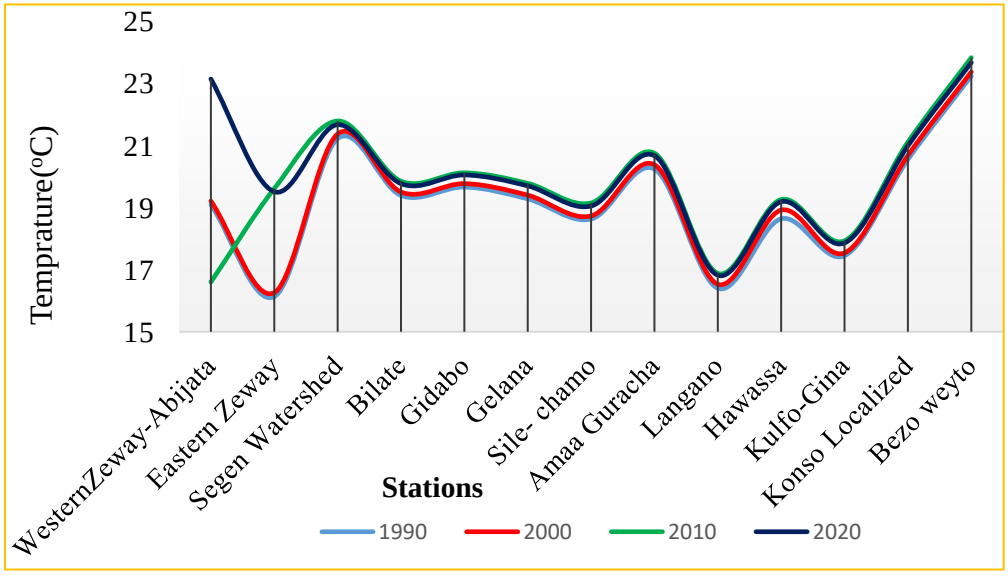

Figure 32 the temperature spatiotemporal change around all stations

4.1.5 Land-use and land-cover change status

The LULC mapping was conducted using the Random Forest classifier within the Google Earth Engine platform. The classification system assigned specific values to different land cover classes: 0 for water, 1 for forest, 2 for cropland, and 3 for bare land. The Random Forest classifier was trained using training samples derived from Landsat images captured in the years 1990, 2000, 2010, and 2020. Each class was represented by 50 training samples. The overall accuracy of the land use land cover classification was calculated using a code. The classification achieved an overall accuracy of 0.95 for the year 1990, 0.96 for 2000, 0.95 for 2010, and 0.95 for 2020. This indicates a high level of accuracy in classifying the land cover within the study area.

The spatiotemporal analysis of LULC changes for the years 1990, 2000, 2010, and 2020 reveals variations in the extent of different land cover features, including water, urban areas, cropland, bare land, and forest. In 1990, the water bodies covered an extent of approximately 2603 km^2. The forested areas measured approximately 13589 km^2, while cropland covered an area of about 32972 km^2. The remaining land cover class, bare land, occupied an extent of around 7310 km^2. Moving to the year 2000, the water bodies expanded slightly, covering an area of about 2673 km^2. The forested areas decreased to approximately 6767 km^2. Cropland expanded to cover an area of about 38487 km^2, and the extent of bare land increased to around 8548 km^2.

Table 5 Land use land cover area

	Land cover classes(km^2)				Over all accuracy
year	Water	Forest	Cropland	Bare land	
1990	2603	13589	32972	7310	0.95
2000	2673	6767	38487	8548	0.96
2010	2732	10474	39102	4167	0.95
2020	3518	10454	41806	697	0.95

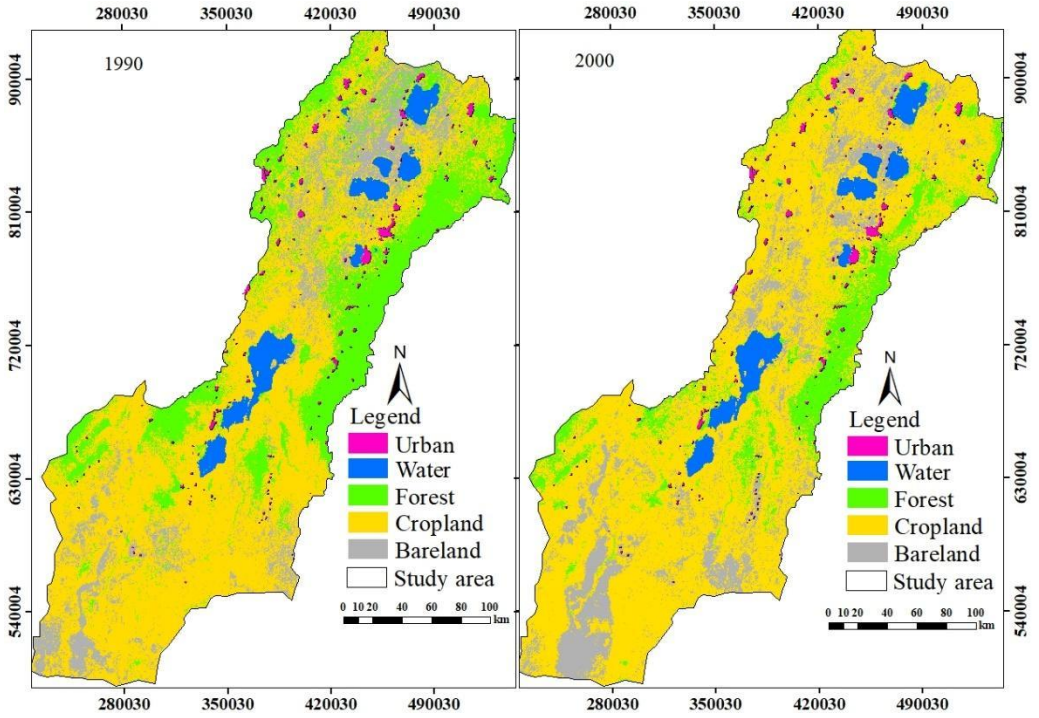

Figure 33 Land use and land cover map of years 1990, 2000

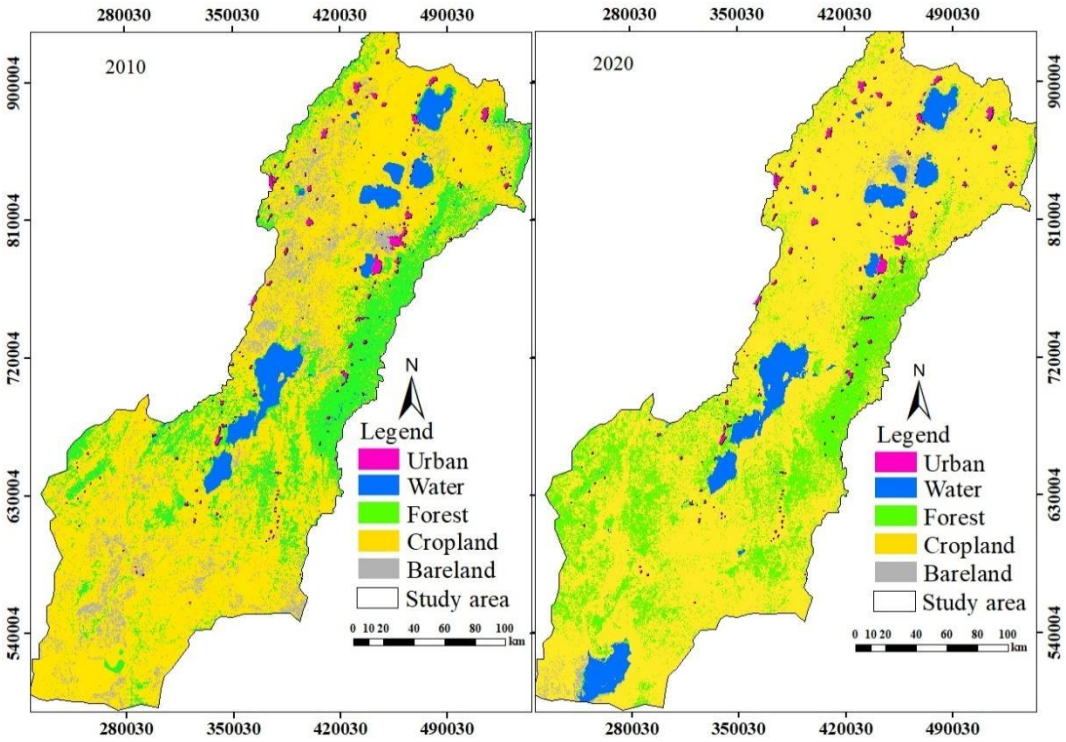

Figure 34 Land use and land cover map of years 2010 and, 2020

In 2010, the water extent expanded to approximately 2732 km^2. The forest cover decreased to around 10474 km^2 compared to the previous year. Cropland expanded significantly and covered an area of approximately 39102 km^2. The extent of bare land was measured at around 4167 km^2. Moving to the year 2020, the water extent further increased to about 3518 km^2. The forest cover remained relatively stable at approximately 10454 km^2. Cropland continued to expand, covering an area of around 41806 km^2. The extent of bare land decreased significantly and was recorded at approximately 697 km^2.

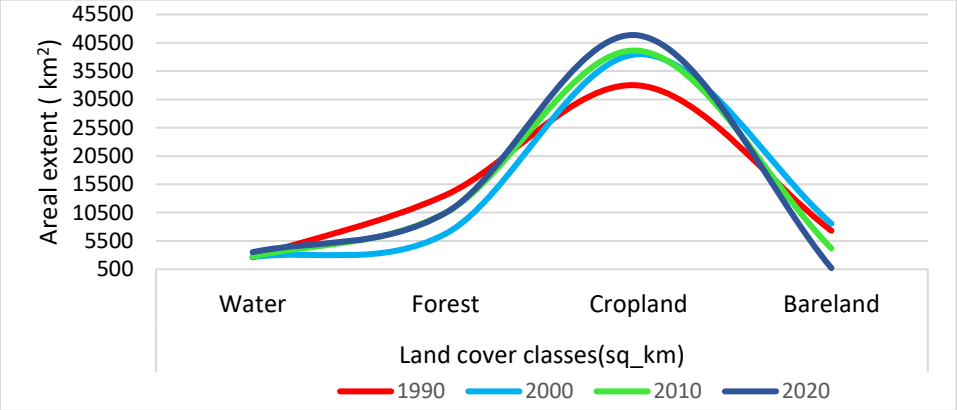

Figure 35 the overall land use land cover change

LULC transition	1990-2000 km^2	2000-2010 km^2	2010-2020 km^2
water to water	2557	2582	2545
water to forest	8	28	35
Water to cropland	15	39	66
Water to bare land	0	1	38
Forest to water	28	70	118
Forest to forest	5638	3341	3479
Forest to cropland	7105	1130	2412
Forest to bare land	483	14	3
Cropland to water	40	51	27
Cropland to forest	939	2325	2138
Cropland to cropland	26731	16341	7070
Cropland to bare land	4888	2041	356
Bare land to water	22	0	5
Bare land to forest	2	97	14
Bare land to cropland	4113	6910	1555
Bare land to bare land	3033	1396	19

CHAPTER FIVE

DISCUSSION

Landsat satellite data is indeed widely used in various research studies, particularly for extracting surface water bodies and conducting land use and land cover mapping. For example, in a study conducted by Shemilese Girma in 2016, Landsat images from 1970 to 2010 were utilized to extract and analyze lakes in Ethiopia. The study aimed to identify the most endangered lakes and investigate the causes of their degradation. By analyzing the Landsat data, the researcher was able to assess the spatiotemporal changes in the lakes and understand the factors contributing to their decline. Similarly, Dr Binyam and Shimelse conducted a study in 2019 focusing on Lake Abijata in Ethiopia. Landsat images spanning from 1972 to 2015 were used to extract and analyze the lake. The researchers investigated the fluctuation of Lake Abijata over time, using the Landsat data to understand the changes in its extent and characteristics. Furthermore, Kassawmar et al. (2011) employed Landsat data to extract and analyze the spatiotemporal fluctuation of Lake Chamo and Abaya. The study aimed to assess the changes in water levels and surface area of the lakes over a specific time period.

Landsat satellite data is extensively utilized for mapping land use and land cover, in addition to its water body extraction capabilities. The multispectral and multitemporal characteristics of Landsat images enable researchers to classify and analyze different types of land cover, such as forests, croplands, urban areas, and bare land. Notably, studies conducted by Muttitanon and Tripathi (2005) and Dwivedi et al. (2005) exemplify the effectiveness of Landsat satellite imagery in land use and land cover mapping. In their research, Muttitanon and Tripathi (2005) employed Landsat 5 TM (Thematic Mapper) color composites from 1990, 1993, 1996, and 1999 to conduct land use and land cover mapping in Ban Don Bay, Surat Thani, Thailand. The researchers utilized supervised classification techniques to locate training samples and extract valuable land use and land cover information. This approach facilitated the identification and analysis of the spatial distribution of different land cover classes within the study area. Similarly, Dwivedi et al. (2005) employed Landsat Thematic Mapper data to analyze land use and land cover changes in specific regions of Ethiopia. By leveraging Landsat images, the researchers were able to identify and quantify changes in land cover over time. This analysis provided valuable insights into the

dynamics of land use patterns and the associated environmental changes in the study area. The studies highlight the significant contributions of Landsat satellite data in land use and land cover mapping. The rich multispectral and multitemporal information provided by Landsat images enables researchers to effectively classify and monitor land cover types, aiding in land management, environmental planning, and resource assessment.

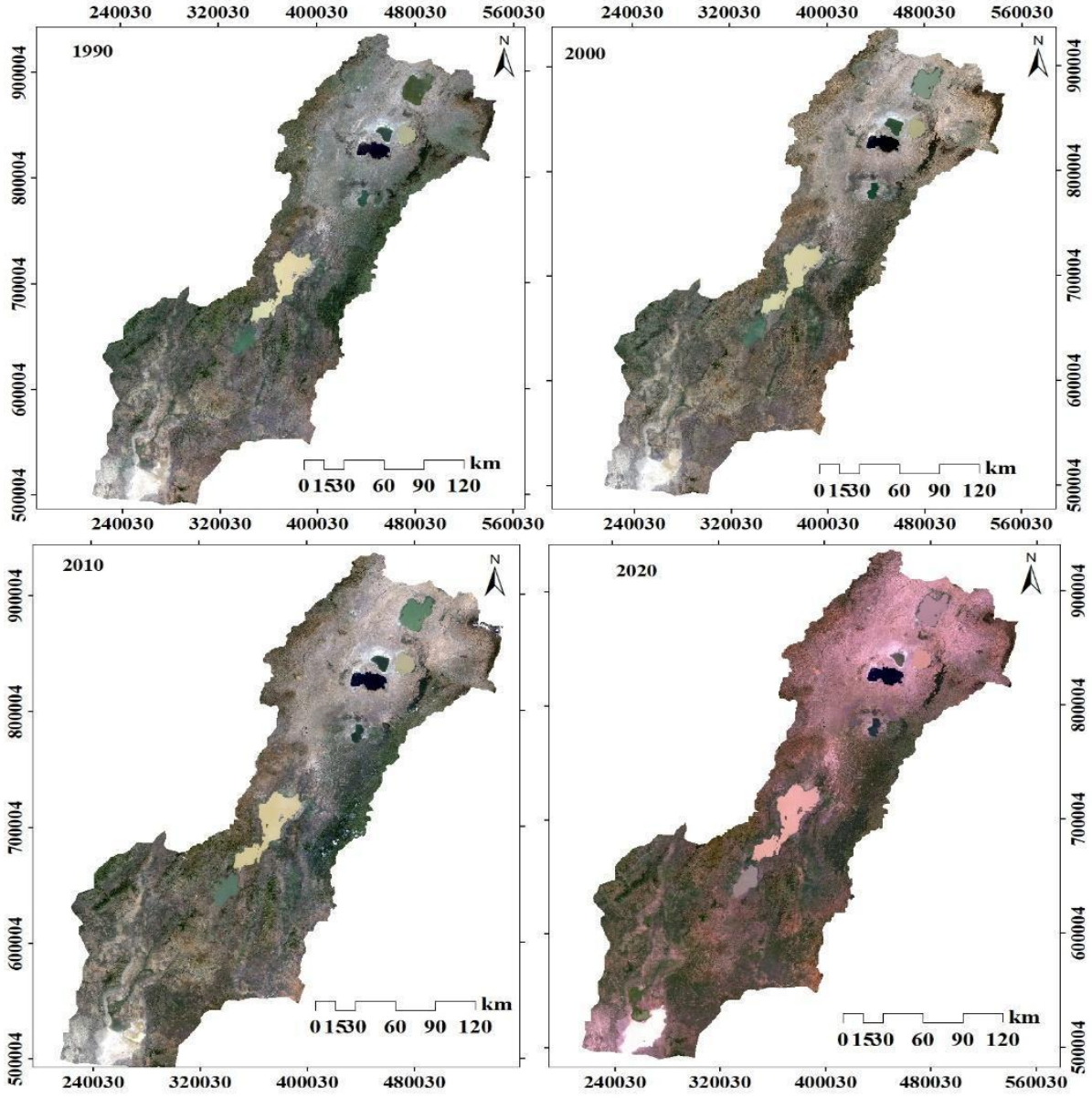

Figure 36 Landsat images

By having the applicability this study utilized Landsat satellite images from 1990 to 2020 to extract land use land cover mapping and detect spatiotemporal transitions in land cover. In addition to mapping land use and land cover, the study also employed Landsat satellite imagery to assess surface water availability and extract major lakes within the Rift Valley lakes basin.

The findings of the study indicate that surface water availability exhibits seasonal variations, with the emergence and disappearance of water bodies. This aligns with previous literature, which highlights that surface water bodies are influenced by both natural and human factors, leading to changes in their extent over time (Granzotti et al., 2018). It is important to recognize that surface water availability is subject to global changes, as documented in studies by Balenzano et al., Kummu et al. (2016), and Rodell et al. (2018). These global changes further emphasize the need to monitor and understand the dynamics of surface water resources in order to effectively manage and sustain them.

The distribution and dynamics of inland water resources are indeed strongly influenced by changes in land use, land cover, and climate. In this particular study, it was observed that the temperature distribution remained relatively consistent over time and space. However, the fluctuations in surface water were primarily driven by two factors they are rainfall patterns and changes in land use and land cover. The study employed a surface water transition map to classify the changes in surface water into 12 distinct classes. These classes include No water which is the areas where no surface water is present. Permanent water are the areas with consistent and permanent surface water bodies. New water which are the newly formed surface water bodies. Seasonal water: Surface water bodies that appear and disappear with seasonal changes. New seasonal water are the Seasonal water bodies that have recently formed. Lost seasonal water are the Seasonal water bodies that have disappeared. Seasonal to permanent indicates the transition from seasonal water to permanent water, permanent to seasonal: which shows transition from permanent water to seasonal water. Ephemeral permanent shows the temporary surface water bodies that persist for a certain duration. Ephemeral seasonal are the temporary surface water bodies that appear and disappear with seasonal changes. No data are the areas where data is unavailable (Fig 35).

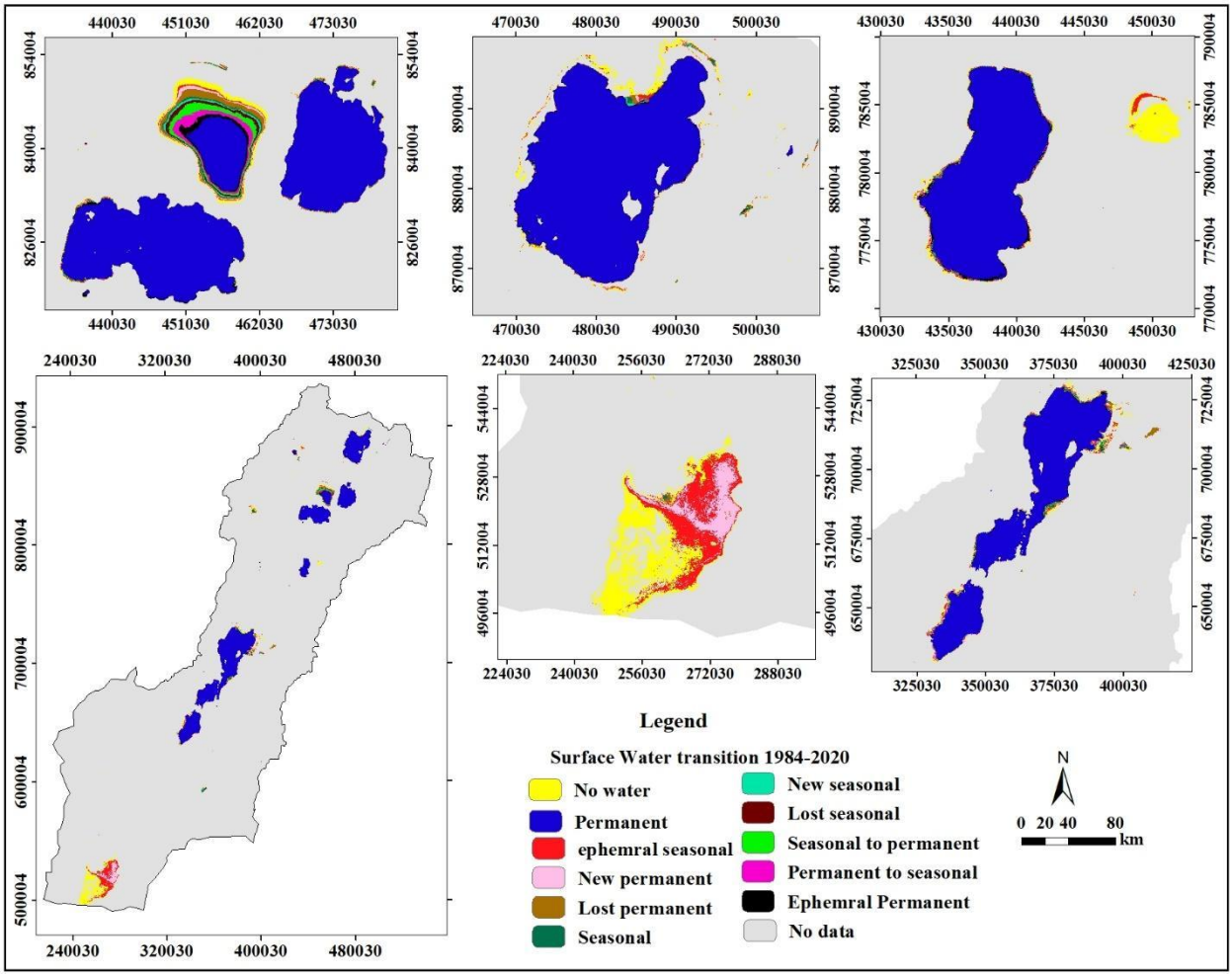

Figure 37 the overall surface water transition from 1984 to 2020

The current status of Abaya Lake has almost expanded in its Extent as shown in the extracted lakes of the year 2023 and also in the field photo **Fig** 36(b). The area around Abaya is surrounded by Forests. This is one case of the expansion of Abaya and Chamo Lake. The Lake Abaya-Chamo wetland has faced increasing threats over the period of 1990-2019 due to predominantly anthropogenic factors, which have induced land use and land cover dynamics (LULC). Settlements, agriculture, water bodies, and forest cover in the lake-wetland area have shown overall net increases during this three-decade period (Zekarias et al., 2021).

On the plain western shores of Lake Abaya-Chamo wetland, agroforestry and livestock rearing are the primary activities. Crop farming, utilizing both rain-fed and irrigation methods, is practiced in this area. The fertile soils support the cultivation of various crops, including fruits such as bananas,

mangoes, avocados, papayas, and tomatoes. Cereals like maize, vegetables such as cabbage and peppers, and tuber and root crops like cassava, onions, and carrots are also grown. Additionally, cotton cultivation takes place in this region. These agricultural practices contribute to the local economy and food production in the area (Gelaw, 2019; Kebede, 2012).

Figure 38 the field photo shows the current status of Abaya and Hawassa lakes (a). Shows the use of Abaya wetlands (b). Shows the coverage of Abaya areas agro-forestry (c). The sediment coverage around Hawassa Lake (d). The irrigation around Hawassa Lake

Bekele, (2001) stated the rapid land use land cover change around Abaya and Chamo areas due to urbanization and spread of cultivated land this are resulted from the degradation of forest and shrubland. According to Gelaw (2019), a significant portion of the area west of Lake Abaya was cleared during the 1960s and 1970s to accommodate the expansion of large-scale farms. These farms were primarily established for cultivating crops such as cotton, bananas, and other agricultural commodities. This expansion of agricultural activities in the region had a substantial impact on land use and land cover, contributing to changes in the natural landscape.

According to Gelaw (2007, 2019), the alluvial plain on the western shores of the lakes is primarily used for agroforestry practices. Both rain-fed and irrigation methods are employed in this area. Various crops are cultivated on the fertile soils adjacent to the wetland, including fruits like bananas, mangoes, avocados, papayas, and tomatoes, cereals such as maize, vegetables like cabbage and peppers, and tuber and root crops including cassava, onions, and carrots. Additionally, cotton cultivation is also practiced in this region. These agricultural activities reflect the diverse range of crops grown in the alluvial plain, contributing to the local economy and food production. The spread of agroforestry led to the forest cover increasing around the Abaya and Chamo wetlands. Similarly, the Land use land cover map of this study shows the increment of Forest cover from 2000-2020. Generally in this study, the reduction of bare land is highly recognized due to the spreading of cropland and urbanization.

Factors for the change of surface water availability

The one factor that can cause the fluctuation of surface water in rift valley lakes basin that is going to be detected in this study is temperature. The result of temperature data shows almost similar results from year to year. It shows some fluctuation for basins of western ziway and eastern ziway sub basin for the year 2010 and 2020 except that it is similar almost all year intervals.

The other factor that influences the surface water availability is precipitation. The spatiotemporal rainfall distribution for the years 1990, 2000, 2010 and 2020 shows that the rainfall amount increased from the initial years to the last except for the year 2000. The maximum and minimum rainfall for 1990 is 1099 mm and 801 mm respectively, for year 2000 the maximum rainfall record is 1091 mm and the minimum is 698 mm, for year 2010 the maximum rainfall record is 1332 mm

and the minimum rainfall record is 948 and for year 2020 the maximum rainfall is 1342 mm and the minimum rainfall is 987.

The additional factor is LULC change. River basins are intricate and dynamic systems that encompass a multitude of natural and anthropogenic physical processes operating at different spatial and temporal scales. These processes include hydrological phenomena such as precipitation, evaporation, runoff, groundwater flow, and river channel dynamics. Additionally, human activities such as water abstraction, dam construction, land use changes, and pollution can significantly influence the behavior of river basins. Understanding the complexities and interactions of these processes is crucial for effective water resource management, flood control, and environmental sustainability within river basin systems (Deshmukh et al., 2013).

Natural and anthropogenic activities can have adverse effects on basin hydrology. For instance, agricultural expansion and intensification, urban growth, and changes in economic patterns can lead to LULC changes within river basins. These changes are often driven by the need to meet the demands of a growing population. However, these alterations to the landscape can impact the hydrological processes within the basin. They can affect water availability, alter surface runoff patterns, increase soil erosion, and impact the quality of water resources. It is important to carefully manage and monitor these activities to ensure sustainable water resource management and mitigate potential adverse effects on basin hydrology.

Likewise, this study extracted the Land use land cover by using Landsat imageries to evaluate its influence on surface water availability. The Land use land cover change of the study area as shown from the land use land cover map above the forest cover increased except of the year 2000. This increment in forest cover can lead to the appearance of new surface water bodies. Similarly the precipitation of the study area increases for years 1990-2020 except for year 2000. This increment increases the seasonal water emergence from year to year especially for the year 2010 and 2020 as shown on surface water availability map above.

CHAPTER SIX

CONCLUSIONS AND RECOMMENDATIONS

6.1 Conclusions

GEE is the platform that can execute and process a large amount of remote sensing data. From the remote sensing dataset, the one is satellite images of Landsat data can widely be executed in a GEE. The results that are shown in this study are the surface availability map and the extracted Spatio temporal fluctuation of Ziway, Abijata, Langano, Shala, Abaya, Chamo, and Hawassa lakes of RVLB of years 1984, 2000, 2010 and 2020, the Land use land cover map of years 1990, 2000, 2010 and 2020 as well the temperature and rainfall spatiotemporal change of years 1990, 2000, 2010 and 2020.

The results of the study shows that the spatio-temporal surface water availability fluctuates from time to time. The No observation increased by 40 km^2, decreased by 56 $km^{2,}$ and decreased by 569 km^2 for year intervals 1984-2000, 2000-2010, and 2010-2020 respectively as well the no water decreased by 60 km^2, increased by 63 km^2 and decreased by 41 km^2 for the above intervals respectively. The seasonal water increased by 10 km^2, increased by 48 km^2, and increased by 577 km^2 for the above intervals respectively. Lastly, permanent water is increased by 10 km^2, decreased by 56 km^2 and it increased by 34 km^2 for three intervals respectively.

The temperature spatiotemporal change result shows that almost the temperatures of all year intervals are similar except for Western Ziway and Eastern Ziway sub-basins this shows that the temperature has no effect on the surface water availability. The rainfall spatiotemporal distribution shows that the lowest annual rainfall record is in the year 2000 and for the rest of the years 1990, 2010, and 2020 it shows increments respectively.

The LULC spatiotemporal change shows that from 1990-2000 the forest cover decreased and then increased for the next years respectively. And the Farmland increased from 1990-2020 as well the bare land decreased from 1990-2020 and the water bodies fluctuates from year to year. Therefore this study shows, the surface water fluctuation is caused by the Rainfall and the land use land cover change.

6.2 Recommendations

The surface water availability and individual lakes of the rift valley lakes basin shows that fluctuation from time to time. By using the result data and the applicability of GEE platform for surface water availability mapping the next researchers can generate another ideas of research additionally,

- ✓ They can further expand the remote sensing application for extraction and mapping surface water availability.
- ✓ They can explore other additional factors for the fluctuation of surface water availability.
- ✓ They can use the GEE for computing a large data size, especially Satellite data, they can save the computer space and time of processing.
- ✓ They can have data of the Lakes of Rift Valley spatiotemporal change data for further study.
- ✓ The concerned body should take action in order to stabilize the fluctuation of surface water availability spatiotemporally.

References

Abburu, S., & Golla, S. B. (2015). Satellite image classification methods and techniques: A review. *International journal of computer applications*, *119*(8).

Acharya, T. D., Lee, D. H., Yang, I. T., & Lee, J. K. (2016). Identification of water bodies in a Landsat 8 OLI image using a J48 decision tree. *Sensors*, *16*(7), 1075.

Aires, F., Venot, J.-P., Massuel, S., Gratiot, N., Pham-Duc, B., & Prigent, C. (2020). Surface water evolution (2001–2017) at the Cambodia/Vietnam border in the upper mekong delta using satellite MODIS observations. *Remote Sensing*, *12*(5), 800.

Alemayehu, T., Ayenew, T., & Kebede, S. (2006). Hydrogeochemical and lake level changes in the Ethiopian Rift. *Journal of hydrology*, *316*(1-4), 290-300.

Alesheikh, A. A., Ghorbanali, A., & Nouri, N. (2007). Coastline change detection using remote sensing. *International Journal of Environmental Science & Technology*, *4*, 61-66.

Alpaydin, E. (2020). *Introduction to machine learning*. MIT press.

Arvor, D., Daher, F. R., Briand, D., Dufour, S., Rollet, A.-J., Simoes, M., & Ferraz, R. P. (2018). Monitoring thirty years of small water reservoirs proliferation in the southern Brazilian Amazon with Landsat time series. *ISPRS Journal of Photogrammetry and Remote Sensing*, *145*, 225-237.

Averyt, K., Meldrum, J., Caldwell, P., Sun, G., McNulty, S., Huber-Lee, A., & Madden, N. (2013). Sectoral contributions to surface water stress in the coterminous United States. *Environmental Research Letters*, *8*(3), 035046.

Balling, R. C., & Goodrich, G. B. (2011). Spatial analysis of variations in precipitation intensity in the USA. *Theoretical and Applied Climatology*, *104*, 415-421.

Barton, I. J., & Bathols, J. M. (1989). Monitoring floods with AVHRR. *Remote Sensing of Environment*, *30*(1), 89-94.

Brakenridge, R., & Anderson, E. (2006). MODIS-based flood detection, mapping and measurement: the potential for operational hydrological applications. Transboundary floods: reducing risks through flood management,

Brisco, B. (2015). Mapping and monitoring surface water and wetlands with synthetic aperture radar. *Remote Sensing of Wetlands: Applications and Advances*, 119-136.

Brown, T. C., Mahat, V., & Ramirez, J. A. (2019). Adaptation to future water shortages in the United States caused by population growth and climate change. *Earth's Future*, *7*(3), 219-234.

Cai, X., Feng, L., Hou, X., & Chen, X. (2016). Remote sensing of the water storage dynamics of large lakes and reservoirs in the Yangtze River Basin from 2000 to 2014. *Scientific reports*, *6*(1), 36405.

Ceola, S., Laio, F., & Montanari, A. (2019). Global-scale human pressure evolution imprints on sustainability of river systems. *Hydrology and Earth System Sciences*, *23*(9), 3933-3944.

Chen, B., Xiao, X., Li, X., Pan, L., Doughty, R., Ma, J., Dong, J., Qin, Y., Zhao, B., & Wu, Z. (2017). A mangrove forest map of China in 2015: Analysis of time series Landsat 7/8 and Sentinel-1A imagery in Google Earth Engine cloud computing platform. *ISPRS Journal of Photogrammetry and Remote Sensing*, *131*, 104-120.

Chen, Y., Huang, C., Ticehurst, C., Merrin, L., & Thew, P. (2013). An evaluation of MODIS daily and 8-day composite products for floodplain and wetland inundation mapping. *Wetlands*, *33*, 823-835.

Chen, Y., Wang, B., Pollino, C. A., Cuddy, S. M., Merrin, L. E., & Huang, C. (2014). Estimate of flood inundation and retention on wetlands using remote sensing and GIS. *Ecohydrology*, *7*(5), 1412-1420.

Cooley, S. W., Ryan, J. C., & Smith, L. C. (2021). Human alteration of global surface water storage variability. *nature*, *591*(7848), 78-81.

Davranche, A., Lefebvre, G., & Poulin, B. (2010). Wetland monitoring using classification trees and SPOT-5 seasonal time series. *Remote Sensing of Environment*, *114*(3), 552-562.

Deshmukh, D. S., Chaube, U. C., Hailu, A. E., Gudeta, D. A., & Kassa, M. T. (2013). Estimation and comparision of curve numbers based on dynamic land use land cover change, observed rainfall-runoff data and land slope. *Journal of hydrology*, *492*, 89-101.

Deutsch, M., & Ruggles, F. (1974). Optical data processing and projected applications of the erts-1 imagery covering the 1973 mississippi river valley floods 1. *Jawra journal of the american water resources association*, *10*(5), 1023-1039.

Dewan, A. M., & Yamaguchi, Y. (2009a). Land use and land cover change in Greater Dhaka, Bangladesh: Using remote sensing to promote sustainable urbanization. *Applied Geography*, *29*(3), 390-401.

Dewan, A. M., & Yamaguchi, Y. (2009b). Using remote sensing and GIS to detect and monitor land use and land cover change in Dhaka Metropolitan of Bangladesh during 1960–2005. *Environmental Monitoring and Assessment*, *150*, 237-249.

Domenikiotis, C., Loukas, A., & Dalezios, N. (2003). The use of NOAA/AVHRR satellite data for monitoring and assessment of forest fires and floods. *Natural Hazards and Earth System Sciences*, *3*(1/2), 115-128.

Donchyts, G., Baart, F., Winsemius, H., Gorelick, N., Kwadijk, J., & Van De Giesen, N. (2016). Earth's surface water change over the past 30 years. *Nature Climate Change*, *6*(9), 810-813.

Du, Z., Li, W., Zhou, D., Tian, L., Ling, F., Wang, H., Gui, Y., & Sun, B. (2014). Analysis of Landsat-8 OLI imagery for land surface water mapping. *Remote sensing letters*, *5*(7), 672-681.

Du, Z., Linghu, B., Ling, F., Li, W., Tian, W., Wang, H., Gui, Y., Sun, B., & Zhang, X. (2012). Estimating surface water area changes using time-series Landsat data in the Qingjiang River Basin, China. *Journal of Applied Remote Sensing*, *6*(1), 063609-063609.

Duan, K., Caldwell, P. V., Sun, G., McNulty, S. G., Zhang, Y., Shuster, E., Liu, B., & Bolstad, P. V. (2019). Understanding the role of regional water connectivity in mitigating climate change impacts on surface water supply stress in the United States. *Journal of hydrology*, *570*, 80-95.

Duan, Q., Tan, M., Guo, Y., Wang, X., & Xin, L. (2019). Understanding the spatial distribution of urban forests in China using Sentinel-2 images with Google Earth Engine. *Forests*, *10*(9), 729.

Dwivedi, R., Sreenivas, K., & Ramana, K. (2005). Cover: Land-use/land-cover change analysis in part of Ethiopia using Landsat Thematic Mapper data. *International Journal of Remote Sensing*, *26*(7), 1285-1287.

El-Asmar, H., & Hereher, M. (2011). Change detection of the coastal zone east of the Nile Delta using remote sensing. *Environmental Earth Sciences*, *62*, 769-777.

Erler, A. R., Frey, S. K., Khader, O., d'Orgeville, M., Park, Y. J., Hwang, H. T., Lapen, D. R., Richard Peltier, W., & Sudicky, E. A. (2019). Simulating climate change impacts on surface water resources within a lake-affected region using regional climate projections. *Water Resources Research*, *55*(1), 130-155.

Feng, D. (2012). A new method for fast information extraction of water bodies using remotely sensed data. *Remote Sensing Technology and Application*, *24*(2), 167-171.

Feyisa, G. L., Meilby, H., Fensholt, R., & Proud, S. R. (2014). Automated Water Extraction Index: A new technique for surface water mapping using Landsat imagery. *Remote Sensing of Environment*, *140*, 23-35.

Fisher, A., & Danaher, T. (2013). A water index for SPOT5 HRG satellite imagery, New South Wales, Australia, determined by linear discriminant analysis. *Remote Sensing, 5*(11), 5907-5925.

Fisher, A., Flood, N., & Danaher, T. (2016). Comparing Landsat water index methods for automated water classification in eastern Australia. *Remote Sensing of Environment, 175*, 167-182.

Flörke, M., Kynast, E., Bärlund, I., Eisner, S., Wimmer, F., & Alcamo, J. (2013). Domestic and industrial water uses of the past 60 years as a mirror of socio-economic development: A global simulation study. *Global Environmental Change, 23*(1), 144-156.

Gao, H., Wang, L., Jing, L., & Xu, J. (2016). An effective modified water extraction method for Landsat-8 OLI imagery of mountainous plateau regions. IOP conference series: earth and environmental science,

Gelaw, A. (2019). Analysis of the Values and Impacts of Ecosystem Services Dynamics, and Valuation of Selected Provisioning Services in Hare River Catchment, Southern Ethiopia. *A PhD Dissertation, Addis Ababa: Addis Ababa University, Ethiopia*.

Godwin, P. M., Pan, Y., Xiao, H., & Afzal, M. T. (2019). Progress in preparation and application of modified biochar for improving heavy metal ion removal from wastewater. *Journal of Bioresources and Bioproducts, 4*(1), 31-42.

Grizzetti, B., Pistocchi, A., Liquete, C., Udias, A., Bouraoui, F., & Van De Bund, W. (2017). Human pressures and ecological status of European rivers. *Scientific reports, 7*(1), 205.

Guo, Y., Xia, H., Zhao, X., Qiao, L., Du, Q., & Qin, Y. (2022). Early-season mapping of winter wheat and garlic in Huaihe basin using Sentinel-1/2 and Landsat-7/8 imagery. *IEEE Journal of Selected Topics in Applied Earth Observations and Remote Sensing*.

Gupta, B., Bhardwaj, S., Lamba, J. K., & Singh, A. (2022). Dark Side of Industrialization on Environmental Sustainability and Climate Change: A Case-based Approach.

Gürsoy, Ö., & Atun, R. (2019). Investigating surface water pollution by integrated remotely sensed and field spectral measurement data: A case study. *Polish Journal of Environmental Studies, 28*(4).

Gürsoy, Ö., Birdal, A., Özyonar, F., & Kasaka, E. (2015). Determining and monitoring the water quality of Kizilirmak River of Turkey: First results. *The International Archives of the Photogrammetry, Remote Sensing and Spatial Information Sciences, 40*, 1469-1474.

Haghighi, A. T., & Kløve, B. (2015). A sensitivity analysis of lake water level response to changes in climate and river regimes. *Limnologica, 51*, 118-130.

Hamunyela, E., Hipondoka, M., Persendt, F., Nghiyalwa, H. S., Thomas, C., & Matengu, K. (2022). Spatio-temporal characterization of surface water dynamics with Landsat in endorheic Cuvelai-Etosha Basin (1990–2021). *ISPRS Journal of Photogrammetry and Remote Sensing*, *191*, 68-84.

Hao, B., Ma, M., Li, S., Li, Q., Hao, D., Huang, J., Ge, Z., Yang, H., & Han, X. (2019). Land use change and climate variation in the three gorges reservoir catchment from 2000 to 2015 based on the Google Earth Engine. *Sensors*, *19*(9), 2118.

Hasan, M., Hassan, L., Al, M. A., Abualreesh, M. H., Idris, M. H., & Kamal, A. H. M. (2022). Urban green space mediates spatiotemporal variation in land surface temperature: a case study of an urbanized city, Bangladesh. *Environmental Science and Pollution Research*, *29*(24), 36376-36391.

Hong, Y., Tang, G., Ma, Y., Huang, Q., Han, Z., Zeng, Z., Yang, Y., Wang, C., & Guo, X. (2019). Remote sensing precipitation: Sensors, retrievals, validations, and applications. *Observation and measurement of ecohydrological processes*, 107-128.

Huang, C., Chen, Y., Zhang, S., & Wu, J. (2018). Detecting, extracting, and monitoring surface water from space using optical sensors: A review. *Reviews of Geophysics*, *56*(2), 333-360.

Huiping, Z., Hong, J., & Qinghua, H. (2011). Landscape and water quality change detection in urban wetland: A post-classification comparison method with IKONOS data. *Procedia Environmental Sciences*, *10*, 1726-1731.

Islam, M. M., & Sado, K. (2000). Development of flood hazard maps of Bangladesh using NOAA-AVHRR images with GIS. *Hydrological Sciences Journal*, *45*(3), 337-355.

Ji, L., Zhang, L., & Wylie, B. (2009). Analysis of dynamic thresholds for the normalized difference water index. *Photogrammetric Engineering & Remote Sensing*, *75*(11), 1307-1317.

Kandekar, V. U., Pande, C. B., Rajesh, J., Atre, A., Gorantiwar, S., Kadam, S., & Gavit, B. (2021). Surface water dynamics analysis based on sentinel imagery and Google Earth Engine Platform: a case study of Jayakwadi dam. *Sustainable Water Resources Management*, *7*(3), 44.

Kassawmar, N. T., Rao, K. R. M., & Abraha, G. L. (2011). An integrated approach for spatio-temporal variability analysis of wetlands: a case study of Abaya and Chamo lakes, Ethiopia. *Environmental Monitoring and Assessment*, *180*(1-4), 313.

Kebede, Y. (2012). Land Use/Cover Dynamics, Environmental Degradation and Management Practices in Hare River Catchment, Abaya-Chamo Basin, Ethiopia, Using Geo-Spatial Technology. *D Thesis, Andhra: Department of Env'tal Sciences (Andhra University), India*, *2*.

KEDİRKAN, N. (2019). Water surface Changes of Lakes in the Central Rift Valley of Ethiopia. *International Journal of Environment and Geoinformatics*, *6*(3), 264-267.

Khan, M. S., & Coulibaly, P. (2006). Application of support vector machine in lake water level prediction. *Journal of Hydrologic Engineering*, *11*(3), 199-205.

Ko, B. C., Kim, H. H., & Nam, J. Y. (2015). Classification of potential water bodies using Landsat 8 OLI and a combination of two boosted random forest classifiers. *Sensors*, *15*(6), 13763-13777.

Kundzewicz, Z. W. (2008). Climate change impacts on the hydrological cycle. *Ecohydrology & Hydrobiology*, *8*(2-4), 195-203.

Legesse, D., Vallet-Coulomb, C., & Gasse, F. (2004). Analysis of the hydrological response of a tropical terminal lake, Lake Abiyata (Main Ethiopian Rift Valley) to changes in climate and human activities. *Hydrological processes*, *18*(3), 487-504.

Liu, D., Chen, N., Zhang, X., Wang, C., & Du, W. (2020). Annual large-scale urban land mapping based on Landsat time series in Google Earth Engine and OpenStreetMap data: A case study in the middle Yangtze River basin. *ISPRS Journal of Photogrammetry and Remote Sensing*, *159*, 337-351.

Liu, Z., Yao, Z., & Wang, R. (2016). Assessing methods of identifying open water bodies using Landsat 8 OLI imagery. *Environmental Earth Sciences*, *75*, 1-13.

Ma, S., Zhou, Y., Gowda, P. H., Dong, J., Zhang, G., Kakani, V. G., Wagle, P., Chen, L., Flynn, K. C., & Jiang, W. (2019). Application of the water-related spectral reflectance indices: A review. *Ecological indicators*, *98*, 68-79.

Mahmon, N. A., Ya'acob, N., & Yusof, A. L. (2015). Differences of image classification techniques for land use and land cover classification. 2015 IEEE 11th International Colloquium on Signal Processing & Its Applications (CSPA),

Maru, H., Haileslassie, A., Zeleke, T., & Teferi, E. (2023). Analysis of the impacts of land use land cover change on streamflow and surface water availability in Awash Basin, Ethiopia. *Geomatics, Natural Hazards and Risk*, *14*(1), 1-25.

McGinnis, D., & Rango, A. (1975). Earth resources satellite systems for flood monitoring. *Geophysical Research Letters*, *2*(4), 132-135.

Miao, Z., Fu, K., Sun, H., Sun, X., & Yan, M. (2018). Automatic water-body segmentation from high-resolution satellite images via deep networks. *IEEE geoscience and remote sensing letters*, *15*(4), 602-606.

Mueller, N., Lewis, A., Roberts, D., Ring, S., Melrose, R., Sixsmith, J., Lymburner, L., McIntyre, A., Tan, P., & Curnow, S. (2016). Water observations from space: Mapping

surface water from 25 years of Landsat imagery across Australia. *Remote Sensing of Environment*, *174*, 341-352.

Munyaneza, O., Mukubwa, A., Maskey, S., Uhlenbrook, S., & Wenninger, J. (2014). Assessment of surface water resources availability using catchment modelling and the results of tracer studies in the mesoscale Migina Catchment, Rwanda. *Hydrology and Earth System Sciences*, *18*(12), 5289-5301.

Muttitanon, W., & Tripathi, N. K. (2005). Land use/land cover changes in the coastal zone of Ban Don Bay, Thailand using Landsat 5 TM data. *International Journal of Remote Sensing*, *26*(11), 2311-2323.

Oliphant, A. J., Thenkabail, P. S., Teluguntla, P., Xiong, J., Gumma, M. K., Congalton, R. G., & Yadav, K. (2019). Mapping cropland extent of Southeast and Northeast Asia using multi-year time-series Landsat 30-m data using a random forest classifier on the Google Earth Engine Cloud. *International Journal of Applied Earth Observation and Geoinformation*, *81*, 110-124.

Olthof, I., & Rainville, T. (2022). Dynamic surface water maps of Canada from 1984 to 2019 Landsat satellite imagery. *Remote Sensing of Environment*, *279*, 113121.

Otsu, N. (1979). A threshold selection method from gray-level histograms. *IEEE transactions on systems, man, and cybernetics*, *9*(1), 62-66.

Palazzoli, I., Montanari, A., & Ceola, S. (2023). Contribution of anthropogenic and hydroclimatic factors on the variation of surface water extent across the contiguous United States. *Environmental Research Communications*, *5*(5), 051006.

Pan, L., Xia, H., Zhao, X., Guo, Y., & Qin, Y. (2021). Mapping winter crops using a phenology algorithm, time-series Sentinel-2 and Landsat-7/8 images, and Google Earth Engine. *Remote Sensing*, *13*(13), 2510.

Pande, C. B. (2022). Land use/land cover and change detection mapping in Rahuri watershed area (MS), India using the google earth engine and machine learning approach. *Geocarto International*, *37*(26), 13860-13880.

Pardo-Pascual, J. E., Almonacid-Caballer, J., Ruiz, L. A., & Palomar-Vázquez, J. (2012). Automatic extraction of shorelines from Landsat TM and ETM+ multi-temporal images with subpixel precision. *Remote Sensing of Environment*, *123*, 1-11.

Parry, M., Arnell, N., Berry, P., Dodman, D., Fankhauser, S., Hope, C., Kovats, S., Nicholls, R., Satterthwaite, D., & Tiffin, R. (2009). Adaptation to climate change: assessing the costs. *Environment*, *51*(6), 29-36.

Paterson, W., Rushforth, R., Ruddell, B. L., Konar, M., Ahams, I. C., Gironás, J., Mijic, A., & Mejia, A. (2015). Water footprint of cities: A review and suggestions for future research. *Sustainability*, *7*(7), 8461-8490.

Pekel, J.-F., Cottam, A., Gorelick, N., & Belward, A. S. (2016). High-resolution mapping of global surface water and its long-term changes. *nature*, *540*(7633), 418-422.

Phalke, A., Ozdogan, M., Thenkabail, P., Erickson, T., & Gorelick, N. (2020). Mapping croplands of Europe, Middle East, Russia, and Central Asia using Landsat 30-m data, machine learning algorithms and Google Earth Engine. *ISPRS Journal of Photogrammetry and Remote Sensing*, *167*, 104-122.

Pickens, A. H., Hansen, M. C., Hancher, M., Stehman, S. V., Tyukavina, A., Potapov, P., Marroquin, B., & Sherani, Z. (2020). Mapping and sampling to characterize global inland water dynamics from 1999 to 2018 with full Landsat time-series. *Remote Sensing of Environment*, *243*, 111792.

Polimeni, J. M., & Polimeni, R. I. (2006). Jevons' Paradox and the myth of technological liberation. *Ecological Complexity*, *3*(4), 344-353.

Prakasam, C. (2010). Land use and land cover change detection through remote sensing approach: A case study of Kodaikanal taluk, Tamil nadu. *International journal of Geomatics and Geosciences*, *1*(2), 150.

Ramachandran, R. M., & Reddy, C. S. (2017). Monitoring of deforestation and land use changes (1925–2012) in Idukki district, Kerala, India using remote sensing and GIS. *Journal of the Indian Society of Remote Sensing*, *45*, 163-170.

Ranjan, S. P., Kazama, S., & Sawamoto, M. (2006). Effects of climate and land use changes on groundwater resources in coastal aquifers. *Journal of Environmental Management*, *80*(1), 25-35.

Rawat, J., & Kumar, M. (2015). Monitoring land use/cover change using remote sensing and GIS techniques: A case study of Hawalbagh block, district Almora, Uttarakhand, India. *The Egyptian Journal of Remote Sensing and Space Science*, *18*(1), 77-84.

Reis, S. (2008). Analyzing land use/land cover changes using remote sensing and GIS in Rize, North-East Turkey. *Sensors*, *8*(10), 6188-6202.

Ruan, K., Zha, Y., Zhou, Z., & Yang, P. (2016). A modified GAC model for extracting waterline from remotely sensed imagery. *International Journal of Remote Sensing*, *37*(17), 3961-3973.

Satterthwaite, D., McGranahan, G., & Tacoli, C. (2010). Urbanization and its implications for food and farming. *Philosophical transactions of the royal society B: biological sciences*, *365*(1554), 2809-2820.

Sawaya, K. E., Olmanson, L. G., Heinert, N. J., Brezonik, P. L., & Bauer, M. E. (2003). Extending satellite remote sensing to local scales: land and water resource monitoring using high-resolution imagery. *Remote Sensing of Environment*, *88*(1-2), 144-156.

Schaffer-Smith, D., Swenson, J. J., Barbaree, B., & Reiter, M. E. (2017). Three decades of Landsat-derived spring surface water dynamics in an agricultural wetland mosaic; Implications for migratory shorebirds. *Remote Sensing of Environment*, *193*, 180-192.

Schleich, J., & Hillenbrand, T. (2009). Determinants of residential water demand in Germany. *Ecological Economics*, *68*(6), 1756-1769.

Shapla, T., Park, J., Hongo, C., & Kuze, H. (2015). Agricultural land cover change in Gazipur, Bangladesh, in relation to local economy studied using Landsat images. *Advances in Remote Sensing*, *4*(03), 214.

Srinivasan, V., Seto, K. C., Emerson, R., & Gorelick, S. M. (2013). The impact of urbanization on water vulnerability: A coupled human–environment system approach for Chennai, India. *Global Environmental Change*, *23*(1), 229-239.

Stamps, D. S., Calais, E., Saria, E., Hartnady, C., Nocquet, J. M., Ebinger, C. J., & Fernandes, R. M. (2008). A kinematic model for the East African Rift. *Geophysical Research Letters*, *35*(5).

Sun, Y., Tong, S. T., Fang, M., & Yang, Y. J. (2013). Exploring the effects of population growth on future land use change in the Las Vegas Wash watershed: an integrated approach of geospatial modeling and analytics. *Environment, development and sustainability*, *15*, 1495-1515.

Tulbure, M. G., Broich, M., Stehman, S. V., & Kommareddy, A. (2016). Surface water extent dynamics from three decades of seasonally continuous Landsat time series at subcontinental scale in a semi-arid region. *Remote Sensing of Environment*, *178*, 142-157.

USGS. (2023). *Understanding Water Availability*.

Vivekananda, G., Swathi, R., & Sujith, A. (2021). Multi-temporal image analysis for LULC classification and change detection. *European journal of remote sensing*, *54*(sup2), 189-199.

Vörösmarty, C. J., McIntyre, P. B., Gessner, M. O., Dudgeon, D., Prusevich, A., Green, P., Glidden, S., Bunn, S. E., Sullivan, C. A., & Liermann, C. R. (2010). Global threats to human water security and river biodiversity. *nature*, *467*(7315), 555-561.

Wang, C., Jia, M., Chen, N., & Wang, W. (2018). Long-term surface water dynamics analysis based on Landsat imagery and the Google Earth Engine platform: A case study in the middle Yangtze River Basin. *Remote Sensing*, *10*(10), 1635.

Wang, X., Xiao, X., Zou, Z., Dong, J., Qin, Y., Doughty, R. B., Menarguez, M. A., Chen, B., Wang, J., & Ye, H. (2020). Gainers and losers of surface and terrestrial water resources in China during 1989–2016. *Nature communications*, *11*(1), 3471.

Wang, Y., Li, Z., Zeng, C., Xia, G.-S., & Shen, H. (2020). An urban water extraction method combining deep learning and Google Earth engine. *IEEE Journal of Selected Topics in Applied Earth Observations and Remote Sensing*, *13*, 769-782.

Wang, Y., Ma, J., Xiao, X., Wang, X., Dai, S., & Zhao, B. (2019). Long-term dynamic of Poyang Lake surface water: A mapping work based on the Google Earth Engine cloud platform. *Remote Sensing*, *11*(3), 313.

Woldegabriel, G., Aronson, J. L., & Walter, R. C. (1990). Geology, geochronology, and rift basin development in the central sector of the Main Ethiopia Rift. *Geological Society of America Bulletin*, *102*(4), 439-458.

WoldeGabriel, G., Heiken, G., White, T. D., Asfaw, B., Hart, W. K., & Renne, P. R. (2000). Volcanism, tectonism, sedimentation, and the paleoanthropological record in the Ethiopian Rift System. *Special papers-geological society of america*, 83-99.

Woodcock, C. E., Allen, R., Anderson, M., Belward, A., Bindschadler, R., Cohen, W., Gao, F., Goward, S. N., Helder, D., & Helmer, E. (2008). Free access to Landsat imagery. *SCIENCE VOL 320: 1011*.

Worden, J., & de Beurs, K. M. (2020). Surface water detection in the Caucasus. *International Journal of Applied Earth Observation and Geoinformation*, *91*, 102159.

Wu, P., Shen, H., Cai, N., Zeng, C., Wu, Y., Wang, B., & Wang, Y. (2016). Spatiotemporal analysis of water area annual variations using a Landsat time series: A case study of nine plateau lakes in Yunnan province, China. *International Journal of Remote Sensing*, *37*(24), 5826-5842.

Wulder, M. A., Masek, J. G., Cohen, W. B., Loveland, T. R., & Woodcock, C. E. (2012). Opening the archive: How free data has enabled the science and monitoring promise of Landsat. *Remote Sensing of Environment*, *122*, 2-10.

Xia, H., Bian, X., Pan, L., & Li, R. (2023). Mapping tea plantation area using phenology algorithm, time-series Sentinel-2 and Landsat images. *International Journal of Remote Sensing*, *44*(9), 2826-2846.

Xia, H., Zhao, J., Qin, Y., Yang, J., Cui, Y., Song, H., Ma, L., Jin, N., & Meng, Q. (2019). Changes in water surface area during 1989–2017 in the Huai River Basin using Landsat data and Google earth engine. *Remote Sensing*, *11*(15), 1824.

Xiong, L., Deng, R., Li, J., Liu, X., Qin, Y., Liang, Y., & Liu, Y. (2018). Subpixel surface water extraction (SSWE) using Landsat 8 OLI data. *Water*, *10*(5), 653.

Xu, H. (2006). Modification of normalised difference water index (NDWI) to enhance open water features in remotely sensed imagery. *International Journal of Remote Sensing*, *27*(14), 3025-3033.

Yamazaki, D., Trigg, M. A., & Ikeshima, D. (2015). Development of a global~ 90 m water body map using multi-temporal Landsat images. *Remote Sensing of Environment*, *171*, 337-351.

Yang, Y., Liu, Y., Zhou, M., Zhang, S., Zhan, W., Sun, C., & Duan, Y. (2015). Landsat 8 OLI image based terrestrial water extraction from heterogeneous backgrounds using a reflectance homogenization approach. *Remote Sensing of Environment*, *171*, 14-32.

Yigzaw, W., & Hossain, F. (2016). Water sustainability of large cities in the United States from the perspectives of population increase, anthropogenic activities, and climate change. *Earth's Future*, *4*(12), 603-617.

Yuan, T., Lee, H., & Jung, H. C. (2015). Toward estimating wetland water level changes based on hydrological sensitivity analysis of PALSAR backscattering coefficients over different vegetation fields. *Remote Sensing*, *7*(3), 3153-3183.

Zekarias, T., Govindu, V., Kebede, Y., & Gelaw, A. (2021). Geospatial Analysis of Land Use/Land Cover Dynamics on Lake Abaya-Chamo Wetland in Southern Rift-Valley of Ethiopia.

Zhang, Z., Wang, X., Zhao, X., Liu, B., Yi, L., Zuo, L., Wen, Q., Liu, F., Xu, J., & Hu, S. (2014). A 2010 update of National Land Use/Cover Database of China at 1: 100000 scale using medium spatial resolution satellite images. *Remote Sensing of Environment*, *149*, 142-154.

Zhou, Y., Dong, J., Xiao, X., Liu, R., Zou, Z., Zhao, G., & Ge, Q. (2019). Continuous monitoring of lake dynamics on the Mongolian Plateau using all available Landsat imagery and Google Earth Engine. *Science of the Total Environment*, *689*, 366-380.

Zhuang, X., Li, Y., Nie, S., Fan, Y., & Huang, G. (2018). Analyzing climate change impacts on water resources under uncertainty using an integrated simulation-optimization approach. *Journal of hydrology*, *556*, 523-538.

Zurqani, H. A., Post, C. J., Mikhailova, E. A., Schlautman, M. A., & Sharp, J. L. (2018). Geospatial analysis of land use change in the Savannah River Basin using Google Earth Engine. *International Journal of Applied Earth Observation and Geoinformation*, *69*, 175-185.

Gálvez, J. C. (2023, April 5). GIS ONLINE COURSES | 【TYC GIS Group】. GIS Course | TYC GIS Training - Courses & Training - arcgis 10, arcgis PRO, QGIS, Python, JS, Development. Https://www.giscourse.com/

Frazier, P. S., & Page, K. J. (2000). Water body detection and delineation with Landsat TM data. *Photogrammetric engineering and remote sensing*, *66*(12), 1461-1468.

Jia, K., Jiang, W., Li, J., & Tang, Z. (2018). Spectral matching based on discrete particle swarm optimization: A new method for terrestrial water body extraction using multi-temporal Landsat 8 images. *Remote Sensing of Environment*, *209*, 1-18.

Lan, J., Zhang, L., & Guo, Y. (2022). Spectral index-spatially correlated water extraction method based on GF-5 hyperspectral satellite images. 2022 3rd International Conference on Geology, Mapping and Remote Sensing (ICGMRS),